Elektrische Energietechnik an der TU Berlin Band 5

Simon Michael Schneider

Test Bench Design for Power Measurement of Inverter-Operated Machines in the Medium Voltage Range

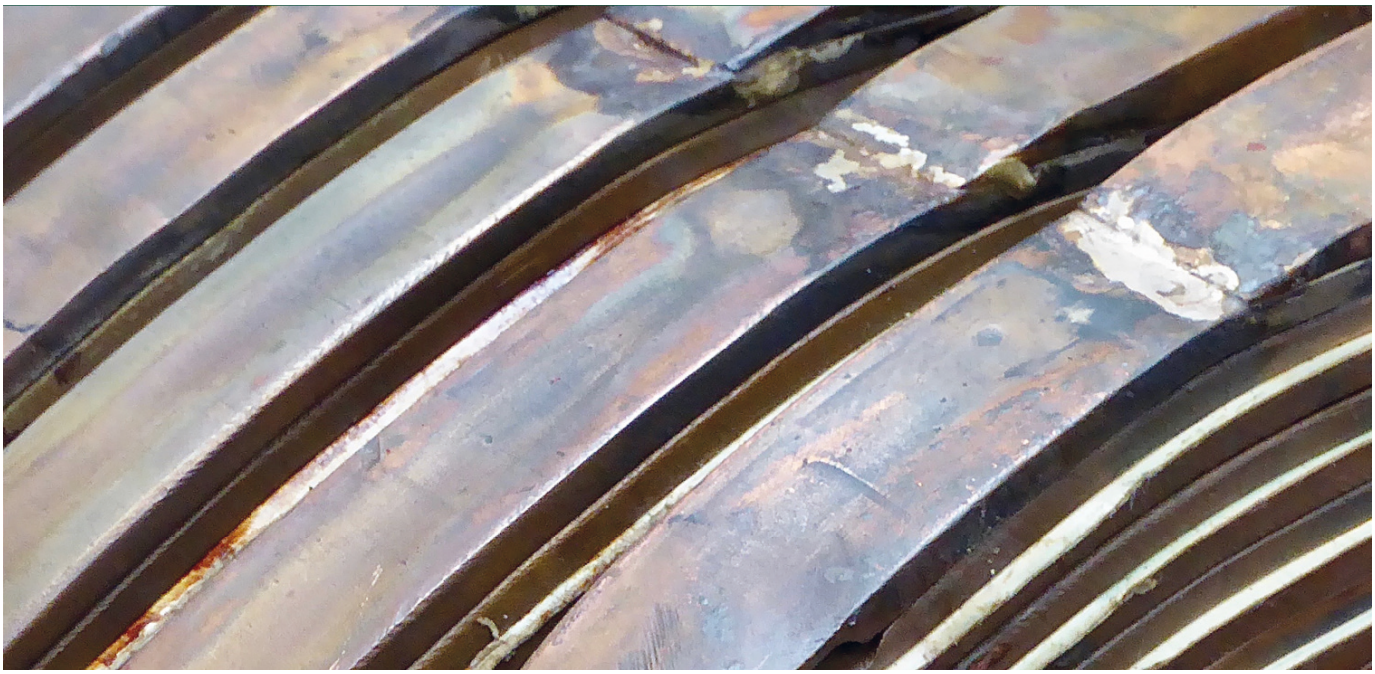

Universitätsverlag der TU Berlin

Technische Universität Berlin

Simon Michael Schneider

Test Bench Design for Power Measurement of Inverter-Operated Machines in the Medium Voltage Range

The scientific series Elektrische Energietechnik an der TU Berlin is edited by:
Prof. Dr. Sibylle Dieckerhoff,
Prof. Dr. Julia Kowal,
Prof. Dr. Ronald Plath,
Prof. Dr. Uwe Schäfer.

Elektrische Energietechnik an der TU Berlin | 5

Simon Michael Schneider

Test Bench Design for Power Measurement of Inverter-Operated Machines in the Medium Voltage Range

Universitätsverlag der TU Berlin

Bibliographic information published by the Deutsche Nationalbibliothek
The Deutsche Nationalbibliothek lists this publication in the Deutsche Nationalbibliografie; detailed bibliographic data are available on the Internet at http://dnb.dnb.de.

Universitätsverlag der TU Berlin, 2018
http://verlag.tu-berlin.de

Fasanenstr. 88, 10623 Berlin
Tel.: +49 (0)30 314 76131 / Fax: -76133
E-Mail: publikationen@ub.tu-berlin.de

Zugl.: Berlin, Techn. Univ., Diss., 2018
Gutachter: Prof. Dr.-Ing. Uwe Schäfer
Gutachter: Prof. Dr.-Ing. Ronald Plath
Gutachter: Prof. Dr.-Ing. Martin Doppelbauer (KIT, Karlsruhe)
Die Arbeit wurde am 24. Oktober 2018 an der Fakultät IV unter Vorsitz von Prof. Dr.-Ing. Clemens Gühmann erfolgreich verteidigt.

Print: Meta Systems Publishing- und Printservices GmbH
Layout/Typesetting: Simon Schneider

ISBN 978-3-7983-3024-5 (print)
ISBN 978-3-7983-3025-2 (online)

ISSN 2367-3761 (print)
ISSN 2367-377X (online)

Published online on the institutional repository of the Technische Universität Berlin:
DOI 10.14279/depositonce-7222
http://dx.doi.org/10.14279/depositonce-7222

Vorwort

Die vorliegende Arbeit entstand während meiner Tätigkeit als Wissenschaftlicher Mitarbeiter an den Fachgebieten Elektrische Antriebstechnik und Hochspannungstechnik des Institutes für Energie- und Automatisierungstechnik an der Technischen Universität Berlin.

Besonders danke ich Herrn Prof. Dr.-Ing. Uwe Schäfer und Herrn Prof. Dr.-Ing. Ronald Plath für die Betreuung meiner Arbeit und die bereichernden Fachgespräche in den letzten Jahren. Mein Dank gilt auch Herrn Prof Dr.-Ing. Martin Doppelbauer für die Anfertigung des universitätsexternen Gutachtens sowie Herrn Prof. Dr.-Ing. Clemens Gühmann für den Vorsitz des Promotionsausschusses.

Die vorliegende Doktorarbeit entstand in Kooperation mit dem Dynamowerk der Siemens AG. In diesem Zusammenhang möchte ich mich bei Herrn Dr.-Ing. Matthias Centner bedanken, der durch unzählige fachliche Diskussionen die Arbeit maßgeblich begleitet hat. Des Weiteren danke ich den Prüfingenieuren und Mitarbeitern im Prüffeld, stellvertretend Herrn Stefan Kender und Herrn Dr.-Ing. José Sayago für die ausgezeichnete technische Zusammenarbeit und dafür, dass sie mir die messtechnischen Untersuchungen ermöglicht haben. In diesem Zusammenhang möchte ich mich bei meinem jetzigen Kollegen Herrn Rüdiger Holle vom IPH Berlin bedanken.

Bei allen Kollegen der beiden Fachgebiete möchte ich mich ganz ausdrücklich für das angenehme Arbeitsumfeld bedanken, in dem es mir eine Freude war, tätig zu sein. Darüber hinaus möchte ich mich bei meinen studentischen Mitarbeitern bedanken, welche ich bei der Erstellung ihrer Abschlussarbeiten betreuen durfte.

Meiner Familie und meinen Freunde, die mich begleitet haben, mich immer wieder mit Energie und Motivation versorgten, diesen Weg zu gehen gilt mein besonderer Dank. Den vielen Unterstützern, die ich hier nicht alle namentlich erwähnen konnte, möchte ich ebenfalls meinen tiefen Dank aussprechen.

Contents

Nomenclature

Greek

η	Efficiency, %
φ, φ_{h}	Phase difference between voltage and current, °
δ	Measurement uncertainty
$\delta_{95\%}$	Expanded measurement uncertainty with $k = 2$
σ	Standard deviation
$\varphi_{\mathsf{u},h}$	Phase harmonic component voltage, °
$\varphi_{\mathsf{i},h}$	Phase harmonic component current, °
δ_u	Measurement uncertainty voltage sample, V
δ_i	Measurement uncertainty current sample, A
δ_{AP}	Relative Uncertainty of Active Power, %
$\delta_{\mathsf{P_{DI,3}}}$	Uncertainty of three phase active power, discrete integration method, W
$\delta_{\mathsf{P_H}}$	Uncertainty of active power, harmonic method, W
μ	Expected measured value
δ_{g}	Relative uncertainties, %

Latin

$\underline{A}_h$	Harmonic component
c_{I}	Sensitivity coefficient voltage
c_φ	Sensitivity coefficient phase difference
$\underline{C}_h$	Complex fourier coefficient
c	Sensitivity coefficient
$ENOB$	Effective number of bits
f_{IGBT}	Switching frequency, Hz
f_{S}	Sample frequency, Hz
f_{max}	Maximum analysable or expected frequency, Hz
f_{0}	Base frequency, Hz

Latin

h	Harmonic order
I_1	Phase current , A
I_3	Phase current , A
I	Current RMS , A
$\hat{I}_h$	Peak value harmonic component current, A
i_{n}	Current sample, A
k	Coverage factor
l	Converter level
L_{Load}	Load-Inductance, H
c_{U}	Sensitivity coefficient voltage
m	Modulation depth
N	Number of samples
P	Active power, W
P_h	Active Power - harmonic component, W
P_{0}	DC component of harmonic active power, W
P_{1MS}	Active power sampled with $f_S = 1\,MS$, W
P_1	Input Power, W
P_2	Output Power, W
P_{1E}	Input power of the excitation systems, W
$P_{\mathsf{1E,M}}$	Input power of the motor excitation systems, W
$P_{\mathsf{1E,G}}$	Input power of the generator excitation systems, W
P_{Aron}	Active power, Aron Method, W
P_{Cu2}	Rotor copper losses, W
P_{Cu1}	Stator copper losses, W
P_{C}	Constant losses, W
$P_{\mathsf{C,H}}$	Constant additional harmonic losses , W
P_{DI}	Active power, discrete integration method, W
$P_{\mathsf{DI,3}}$	Three phase active power, discrete integration method, W
P_{E}	Excitation losses, W
P_{FW}	Windage losses, W
P_{FE}	Iron losses, W
P_{H}	Active power, harmonic method one phase, W
$P_{\mathsf{H,3}}$	Three phase active power, harmonic method, W
P_{L}	Total losses, W

P_{LL}	Stray load losses, W
$P_{\mathsf{LL,H}}$	Load-dependent additional harmonic losses, W
$P_{\mathsf{L,SM}}$	Total losses of synchronous machine, W
P_{N}	Rated power, W
P_{Total}	Total active power, W
P_{V}	Power losses, W
R_{Load}	Load-Resistance, Ω
SF	Scale factor
t_{S}	Sample time, s
t_{jit}	Jitter time, s
T_{cycle}	Cycle time, s
t_{0}	Period time of base frequency, s
T_{Rise}	Divider time constant, s
U_{12}	Line voltage , V
U_{32}	Line voltage , V
U	Voltage RMS , V
U_{LSB}	Last significant-bit voltage, V
$\hat{U}_h$	Peak value harmonic component voltage, V
u_{n}	Voltage sample, V

Acronyms

2L-VSI	2-Level Voltage Source Inverter
ADC	Analog Digital Converter
CCV	Cycloconverter
CDSM	Clamp Double Submodule
CHB VSC	Cascaded H-Bridge Voltage Source Converter
CMR	Common Mode Rejection
DAQ	Data Acquisition
DFT	Discrete Fourier Transform
DUT	Device Under Test
EMC	Electromagnetic Compatibility
FBSM	Full-Bridge Submodule
FFT	Fast Fourier Transform

FLC VSC	Flying Capacitor Voltage Source Converter
FOCS	Fiber-Optic Current Sensor
GUM	Guide to the Expression of Uncertainty in Measurement
HB	H-Bridge
HBSM	Half-Bridge Submodule
HVDC	High Voltage Direct Current
IE	International Efficiency
IEC	International Electrotechnical Commission
IEEE	Institute of Electrical and Electronics Engineers
IGBTs	Insulated-Gate Bipolar Transistors
IGCT	Insulated-Gate Commutated Transistors
LCI	Load Commutated Inverter
LED	Light-Emitting Diode
M2C	Modular Multi-Point Converter
MV	Medium Voltage
MXC	Matrix Converter
NPC VSC	Neutral-Point Clamped Voltage Source Converter
PC	Personal Computer
PCB	Printed Circuit Boards
PTB	Physikalisch-Technische Bundesanstalt
PWM	Pulse Width Modulated
PWM-CSI	Pulse Width Modulated Current Source Inverter
SF	Scale Factor
SM	Submodule
TS	Technical Specification
TS1	Test Setup 1
TS2	Test Setup 2
VSC	Voltage Source Converter

1 Introduction

The efficiency of electrical drives is a key issue in reducing the energy consumption of industrialised countries in the world. Since three-phase AC induction motors consume about 35 % to 40 % of the generated electrical power [1], these countries make an effort in reducing energy use and harmful emissions. Further, electric-motor systems convert nearly half of the worldwide electric energy into the mechanical energy ultimately used in the final application or process [2].

Energy efficiency classes are definitions for motors with voltages below 1 kV and a rated power up to 1 MW. The International Electrotechnical Commission (IEC) as standards organisation for all electronic and related technologies, defined procedures for determining the motor losses and their efficiency classes. The IEC 600034-30-1 and IEC 60034-30-2 defines the energy efficiency classes for sinusoidal and converter supply [3, 4]. The latter one is currently published as a Technical Specification (TS). The basic determination of motor efficiency with a sinusoidal supply is described IEC 60034-2-1 [5], in IEEE standards the test methods are seperated for induction and synchronous machines [6, 7]. Further, there is a TS 60034-2-3 [8] which defines the determination of additional harmonic losses for converter fed induction machines. Another group of standards for motors and drive systems are the European standards – EN 50598-1, EN 50598-2, EN 50598-3 [9–11] – which define procedures for determining the motor losses and the whole drive system losses with the converters included. The standards also define their efficiency classes. More information on the actual standard EN 50598-2 for determination of motors and converters efficiency is given in [12]. The IEC 61800-4 gives ratings for the efficiency determination of Medium Voltage (MV) drive applications [13]. The Technical Specification and standards for drives have long been in discussion [14–20]. Since the introduction of energy efficiency classes, the uncertainty for the determination of efficiency and the necessary electrical power measurement are an emerging issue [21–25].

Currently, energy efficiency classes are not considered for drives above 1 MW. However, they are practical as the combined losses can be a three-figure kilowatt range dependent on the machine dimensions and make massive reductions in the consumption of electrical energy possible. The change of losses and electrical energy consumption per year due to different efficiencies of a few tenth percent is shown in Table 1.1 for a MV motor.

This thesis gives an overview of sources of uncertainty during the power measurement on MV drives. The influence of measurement transducers, voltage dividers, power meters and data acquisition boards are considered. Special methods are shown to assess the measurement setup uncertainty. Further, a possibility is shown to do quantitative uncertainty estimations which are verified with measurements through different measurement setups.

Tab. 1.1: Medium Voltage Machine with Different Efficiency

Rated Power P_N	Efficiency η	Losses P_V	Energy Consumption per year in MWh
12.5 MW	97.9 %	262.5 kW	2299 MWh
12.5 MW	97.6 %	300.0 kW	2628 MWh
Difference	0.3 %	37.5 kW	329 MWh

1.1 Research Review

The influence of uncertainty on drives above 1 MW is analysed with a compressor drive in [26]. The power measurement is analysed dependent on the influence of voltage and currents effective values. The relationship between uncertainty due to deviation of harmonic frequencies up to 300 Hz and the influence of the phase angle between voltage and current was also analysed. The measurement transducers show the major contribution of uncertainty on the active power measurements.

The defined efficiency classes International Efficiency (IE)1-4 in IEC 600034-30-1 are a challenge for motor manufacturers and suppliers. The German national institute of metrology Physikalisch-Technische Bundesanstalt (PTB) indicates the influence of the measurement uncertainty on the determination of efficiency and their methods for small machines below 375 kW. The identification of the uncertainty shows the impact on the classification in the IE-classes [27] [25]. In a further publication of Aarniovuori the uncertainty of efficiency measurements according 60034-2-1 of five different small machines [23] is shown. The increase of accuracy of instrumentation is discussed as well the correct use of multifunctional power analyser devices. Calorimetric systems used for loss determination of electric motors and drives are often discussed [28, 29]. There are four categories of calorimetric systems, which can have different measurement uncertainties.

The results in [22, 30] indicate that the uncertainty of the direct test method for the determination of efficiency is in general higher than that of the indirect test method. The analysis in [23] concludes direct testing method is not recommended for the determination of induction motors efficiency. The article [20] has discussed the importance of the power measurement uncertainty for the additional load losses determination. Especially the direct test method is emphasised as unusable for the determination of high power motors efficiency.

Since the beginning of the electrical energy use from generation, transmission to consumption, the measurement transducers are proven power flow measurement devices. They are designed for the operation with grid frequency 50/60 Hz. The transfer behaviour of the commonly used measurement devices is the topic for research and investigations since the power quality is an upcoming discussion [31–35]. The modelling and measurement of the voltage transformers frequency response are discussed in several publications [36–42]. Further, there are investigations to increase the linearity of

voltage transformers with the focus using them as the essential instrument for harmonic measurement in the grid [43–47]. The calibration of transformers, the used calibration methods and test voltage generation for calibration are the main topics concerning the harmonic voltages in the grid [48–51]. The investigations on alternative measurement devices regarding the potential separation are discussed when dividers are used [52–54]. Since the presence of harmonics in the grid, the current measurement devices and their performance are discussed [55–61]. The topics are the possibilities to improve the transfer behaviour of the measurement devices considering a defined frequency range and used measurement setup. Investigation on the design of voltage dividers is done concerning shielding and SF6 composed [62]. Further, the usability of upcoming electronic current measurement devices is proven for their use in medium and high voltage applications [63–65]. The research fields of harmonic measurement devices in the scope of distorted waveforms is an ongoing discussion[66–70]. Especially the calibration in a defined frequency range or adjustments in uncertainty limits of new measurement devices are the main topics in the working groups of standards. The latest investigations show a combination of two current measurement principles: The combination of high accuracies with the ability to measure currents in the kiloampere range in one measurement device [71].

The data acquisition and processing of a measurement system is a major part used in the digital era. Different sampling methods, real-time algorithms, filters and windowing are commonly used and discussed in the field on the measurement of electrical quantities [72, 73]. There are several articles, books and publications on the correct use of Fourier Analysis or determination of quantities from sampled data. A few papers are named here which relate to the relevant topics utilised in this section.

A general question is the signal bandwidth of the used measurement devices or electronics for the measurement of converter signals. The articles [74, 75] have shown a relation between required analog bandwidth to reach a specified relative uncertainty. Further, three active power calculation methods with different sampling methods in three different scenarios of a measurement setup is analysed [76]. The article showed the simple power calculation, which means the used discrete integration method in this work, is the best solution if synchronised sampling is applied.

A systematical approach has been proposed by Avallone [77] for uncertainty evaluation in active power measurements under highly distorted conditions, including transducer errors. The article showed the influence of angle and amplitude errors by a fixed sample frequency and amount samples, as well the variation of phase angle of the base frequency. The analytical expression of the discrete integration method is advised to be used for the power measurement on high-efficiency variable speed drives. There are further publications relating to the uncertainty of samples on the power measurement using real-time algorithms [78]. However, uncertainties due to different signal processing algorithms used for the analysis of periodic signals are described by Betta [79, 80]. For example, the quantisation errors are analysed which can influence the determination of harmonics. The effect of an integration interval selection is shown by Langella [81, 82]. The results give information about the number of samples to use for the determination of a root mean square value with high probability.

The power measurement and the uncertainty of measurement transducers are primarily discussed in the low voltage range [83]. Also there are discussion on physical definition of power measurement [84]. Since the upcoming feeding of renewable energy into the grid the topic has been discussed in the MV range due to the increased harmonic content of the grid voltages [85]. More and more applications are occurring where power are fed through converter, e.g. solar inverters [86]. The harmonic content in the grid is important for grid operators. The limitation in exact measurements of harmonics, when using transducers was analysed by Cataliotti [85, 87]. The experimental analysis of the effects of current transformer in the measurement of harmonic active power identified the phase shift between harmonic voltage and harmonic current can be responsible for large errors, especially if the phase shift is getting close to $\pm 90°$.

There are typical measuring systems available especially designed for the high voltage range by the company Highvolt. The system is used for the losses measurement on power transformers. The frequency range is specified up to 200 Hz, which is sufficient for the losses measurement of power transformers with a specified uncertainty of 0.08 % and 0.1 %.

The uncertainty of the determination of losses on converter operated drives with regard on the measurement equipment is discussed in the articles for the low voltage range [88–90]. The major speed variable MV drives uses multilevel converters [91–95], which requires a discussion about uncertainty requirements for the harmonic active power measurement of these drives.

1.2 Outline of the Thesis

The focus of this work is the measurement uncertainty of the active power measurement to be used for the determination of efficiency of MV motors. Since the development of multilevel converters with high power ratings, the power measurement is becoming an important issue to investigate, with their application with MV motors. Due to the high voltages and currents, the use of dividers or measurement transformers is necessary, which introduces additional uncertainty.

First, the typical test bench for MV motors is described, and an overview of conventional multilevel converters is given in chapter 2. The consideration of uncertainty in measurements is described in chapter 3, which is used for the whole uncertainty investigations in this thesis.

The focus of chapter 4 is the data acquisition and processing. The digital signal processing is analysed and the possibilities to reduce its uncertainty contribution on an active power measurement. Further, a sensitisation on influence factors of the active power measurement is made, which is necessary for the design of a measurement setup.

In chapter 5 analysis is made of the conventional measurement transducers and devices in the MV-range. The transfer behaviour of the devices is investigated with measurements and their uncertainty characteristics.

Chapter 6 shows with measurement on typical medium voltage drives and an uncertainty analysis, the essential aspects of an active power measurement. The results show the importance of the performance of a used measurement setup. The results of the investigations on the drives are used to indicate the impact on the determination of efficiency in chapter 7.

1.3 Research Concept

The starting point of this thesis is the significance of the measurement uncertainty for active power measurements of inverter supplied MV drives. A better understanding is desired of influences on several measurement components in a measurement chain.

The first investigations are realised in the a voltage laboratory with the investigation of the transfer behaviour of the voltage and current transformers. An important issue is to analyse the properties of the most used measurement devices for 50/60 Hz applications in the medium and high voltage range. Further, the measurement of electrical power due to a data acquisition and calculation unit is analysed with analysis of uncertainty.

After the above mentioned investigations a classification of measurement devices is possible and a basis for the influence of uncertainty for the whole measurement system is realised.

The most important task is the investigation of a complete drive application. The modulation of converter applications has been used to obtain an estimation of the expected voltage and current forms. Measurements are applied to different test benches to investigate several issues necessary for the active power measurement. The investigations lead to a better understanding of power measurement for MV converter drives.

The work gives a significant input for further standardisation processes. The handling of measurement uncertainties for the active power measurement of drives is shown with regard to the permanent topic of energy saving and its efficient use. The work shows a way to handle the categorisation of electrical drives in energy efficiency classes and to make their determination comparable.

2 Medium Voltage Drives

In this chapter the considerations are made for the electrical power measurement and their corresponding devices generally used in motor test benches. Important issues like the monitoring of vibrations or temperatures are not part of this thesis. Measurement of torque and speed to get the output power of a machine under test is only considered for an investigation on the efficiency in section 7.1. These investigations are part of this work as the considerations of the uncertainty in determination of efficiency is treated. There are torque transducers applicable for drives with a high power density, which normally are represented by medium voltage drives, but for this power category and high efficient motors the use of testing methods with less uncertainty is preferred. The determination of efficiency by the direct method which needs a torque measurement is associated with a higher degree of uncertainty for high-efficiency drives [22]. Due to the verification of a high efficiency with a full-load test requires a torque transducer for a high power and a low uncertainty, which become more difficult the more efficient the motors are.

The measurement system used for the active power measurement of inverter supplied motors requires careful consideration. Great care must be taken to ensure that the measurement uncertainty is kept to a minimum. To determine the active power, values collected from a defined number of discrete measurements and the calculated RMS values, a more complex analysis of the drive system would require to know the harmonic content of the measured values. Especially for inverter supplied drives a detailed analysis allows design for minor losses or rather a different distribution of losses between motor and inverter [12, 96].

In the field of low voltage drives with a rated voltage up to 1 kV many manufacturers offer power meters. These devices include signal conditioning, analog to digital conversion and a calculation unit based on microprocessors or computers. In principle, any of the currently used measurement systems can be used for three phase power measurement providing a minimum of four analog signals are available.

The three phase power measurement requires all three phase voltages and currents to record, however the Aron circuit needs two line voltages and two phase currents for the active power determination of a three phase system, see figure 2.1 and the following equation P_{Aron}:

$$P_{\mathrm{Aron}} = U_{12} \cdot I_1 + U_{32} \cdot I_3 \tag{2.1}$$

The features of the Aron circuit and its use are described in detail in section 6.2. In general, the buildup of a test bench for an active power measurement and a further determination of efficiency is a question of user-defined requirements. Here the following aspects are named:

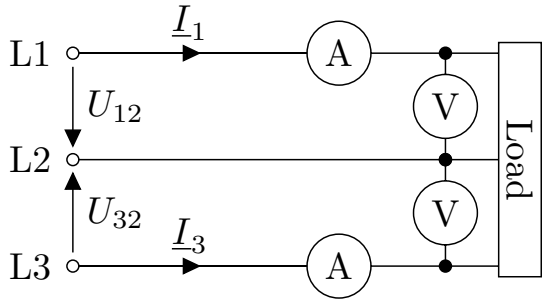

Fig. 2.1: Aron Circuit

Low Measurement Uncertainty Measurement system with low uncertainty for the use in the laboratory and for the approval of new constructed machines

On-Site Measurements Portable system taking on-site measurements and commissioning of drives. The measurement devices are simple to install.

Cost-Effective System Measurement system getting a valuable result with less measurement devices and satisfactory result for a measurement question.

The selection of a measurement system is often a compromise between a system with low measurement uncertainty and low costs. In the following section the requirements for active power measurements on drives in the medium voltage range are described.

2.1 Test Bench Requirements for Medium Voltage Drives

Typical medium voltage drives can have rated line voltages up to 11 kV and currents up to 4 kA. It is essential to have measurement transformers or voltage dividers for the recording of signals with a PC equipped with a data acquisition card or a conventional power meter. More and more medium voltage drives are supplied by multilevel converters, which produce pulsed non-sinusoidal voltages and currents against the relating ground potential, see also in [97, 98]. A typical voltage form of a commonly used converter is depicted in figure 2.2. These waveforms show an application for a 60 Hz machine, what infers from the period time of 16.7 ms.

There are several voltage peaks visible due to the switching of the power semiconductors, which result in oscillations. These unintentional oscillations are caused by long cables between the converter and the machine. Parasitic capacitances, the inductances of the motor cables as well the impedance of the motor create an oscillatory circuit. A harmonic active power can be only produced by harmonics in voltage and current with the same order. The shown voltage forms are extremely challenging conditions for an accurate active power measurement. The measurement devices need an expanded frequency range compared to usual sinusoidally supplied drives, but especially a zero-crossing detection is needed to detect the base frequency.

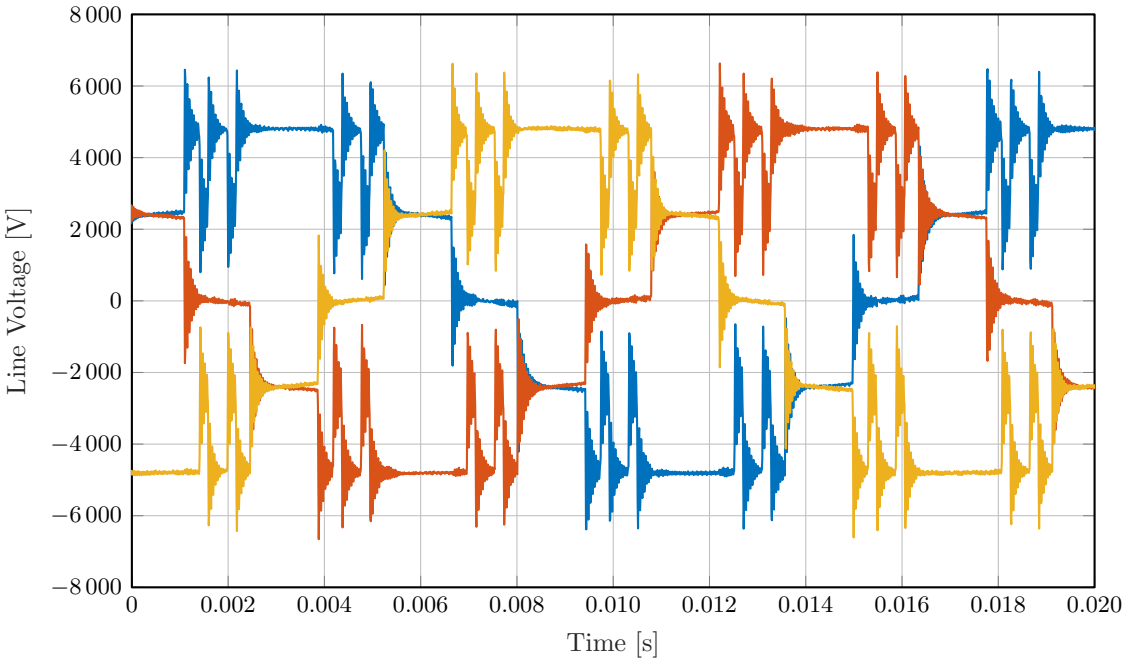

Fig. 2.2: Line Voltages of a Multilevel-Converter

A measurement system has to fulfil the following requirements necessary for the determination of harmonics and active power [99, 100]:

- Usable for the highest expected frequency of the signals contributing electrical power,
- insulation resistance against expected voltage peaks,
- a sufficient common mode rejection [101–103],
- a sufficient sample time and recording time of the signal processing,
- a galvanic isolation against high voltages for the protection of the measurement devices and the operating personnel,
- correct evaluation of the sampled signal and zero-crossing detection, especially for a Fast Fourier Transform (FFT) analysis.

2.2 Measurement System Setup

The named requirements in 2.1 have to be considered if a low measurement uncertainty is desired, which is also the focus of the further investigations in this thesis. In figure 2.3 a principle setup of a measurement system for medium voltage drives is shown.

The machine under test (MUT) is supplied by a multilevel converter with a nonsinusoidal waveform. The performing of a load test requires a mechanically connected load machine. The measurement setup consists of voltage and current transformers, nevertheless voltage

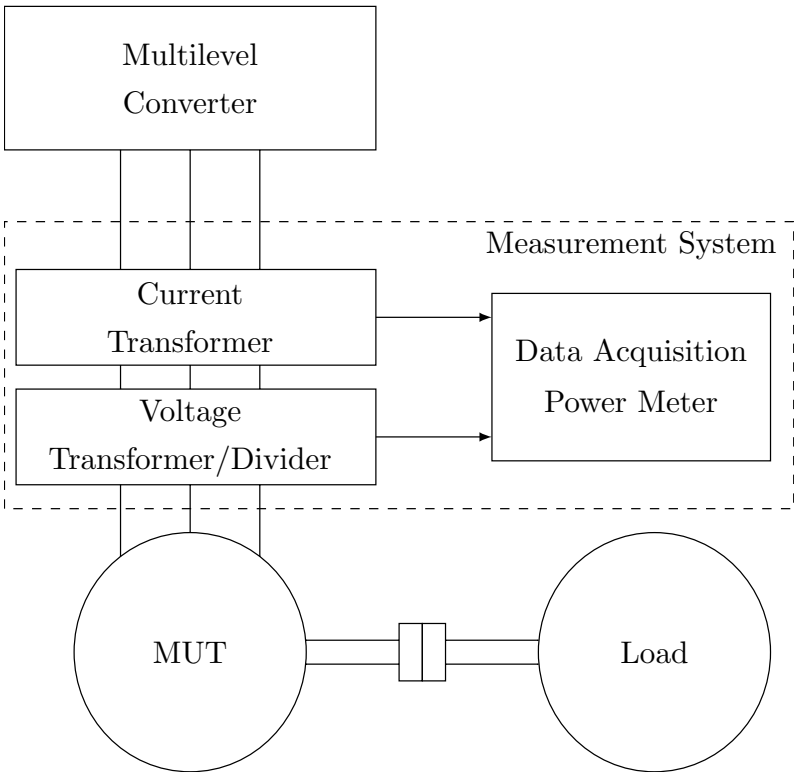

Fig. 2.3: Active Power Measurement System

dividers can be used to transform the medium voltage into low voltage levels. The recording of the signals is usually realised with a data acquisition unit which can be a power analyser or measuring cards with analog to digital converters. In principle the choice of these individual components is dependent on the measuring requirements. The use of a non-sinusoidal power supply required different measurement devices than those typically used for 60/50 Hz testing. Transformers with a frequency independent transfer behaviour is necessary. The sample frequency and resolution of the data acquisition unit have to be sufficient to record the expected frequencies: The voltages and currents which produce active power.

Further, the instrumentation of the whole test bench has an essential influence on the accuracy and repeatability of the taken measurement. The control of the motor and load can induce additional variations of speed, torque or active power, see section 3.1.

The choice of a measurement setup and its components is a compromise of different requirements which have to be respected. The performance testing of an inverter supplied motor needs a consideration of basic aspects, which are partly discussed in [88, 89]. There are different tests used to categorise the drive performance like the indirect methods. The short circuit and no load test of a synchronous machine can both be done with current transformers able to record the rated current. However it is possible to use a smaller current transformer with a few percentage of the rated current for the no load test to get a better uncertainty. The measurement analysis in chapter 3 is a guidance on the handling of uncertainties to configure a measurement system.

2.3 Multilevel Converters

Converters are used in several industrial processes. At the beginning of the semiconductor development, applications for low voltage drives have been build, but within the further development process more and more for medium voltage drives. There is a wide variety of converter types which is a result of specially developed applications with their individual requirements. A few authors have summarised the different converter applications [104–108] used in the medium voltage range. A classification according to [106, 107] is shown and summarised in figure 2.4.

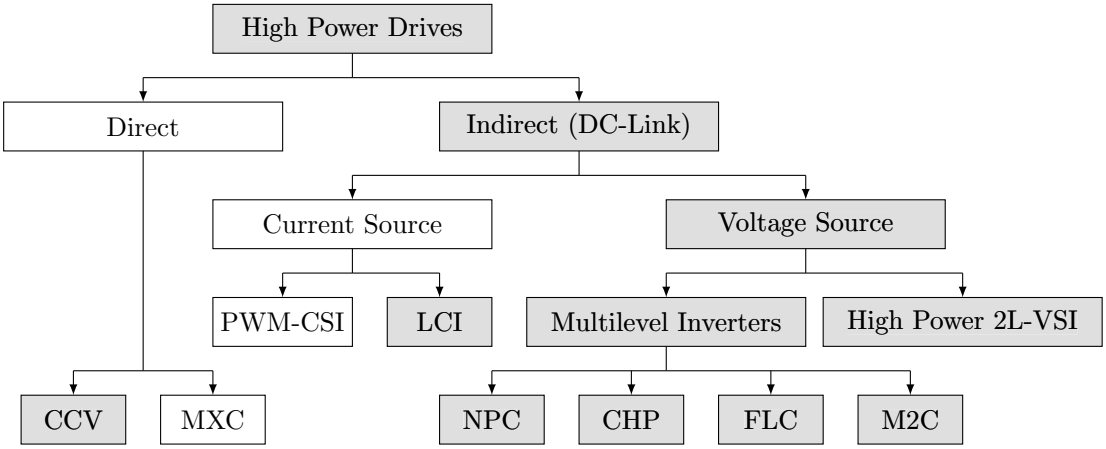

Fig. 2.4: Classification of Converter Topologies [106, 107]

Multilevel converters are used in industry as one of the preferred choices for electronic power conversion. Medium or high power application like the high power AC motor drives shown in figure 2.4 exist in the apparent power range of 0.3 kV A and 72 MV A.

A distinction is made between direct and indirect topologies. The grey blocks in figure 2.4 characterise the inverter topologies that are most used in the market of high power drives. Direct converters connect the electrical network and the electric machine without using an additional energy storage device such as an inductance or a capacitor. Indirect converters have an additional energy storage to decouple the grid and the machine. The basic arrangement is a rectifier connected to the dc-link which is connected through an inverter with the motor, see section 2.3.1.

The most used direct topology, also named direct converter, is the Cycloconverter (CCV) which is a line-commutated thyristor converter. The converter connects a three-phase grid with a three-phase machine. The Matrix Converter (MXC) is a self-commutated converter, which can connect all three phases of the grid with each of the three motor phases [109–111].

Indirect topologies, respectively indirect converters, have a dc-link with a capacitor or an inductance as energy storage. The latter one is a current source converter where a current supplies the load causing the energy flow. The converters with a capacitive dc-link are voltage source converters. The voltage supplies the load which influences the energy flow.

There are two current source converters which are used for a high power drive application. A Load Commutated Inverter (LCI) is used for synchronous machines as pumps, compressors or fans. The LCI is a network controlled or load commutated thyristor converter, in which the grid or the machine voltages cause the commutation of the currents. The Pulse Width Modulated Current Source Inverter (PWM-CSI) uses switches which can be actively switched on and off instead of the passive switching off of thyristors [112].

Indirect converters with a capacitor as a decoupling energy storage device are divided into two-level and multilevel converters. The 2-Level Voltage Source Inverter (2L-VSI) consists of three half-bridges, each consisting of two active switches. The switches are usually Insulated-Gate Bipolar Transistors (IGBTs) or Insulated-Gate Commutated Transistors (IGCT) each of them can have an inverse diode added.

The 2L-VSI is common used converter topology for drive applications in industry or for traction drives[113]. Due to series connected IGBTs the voltage can be increased which makes high power and high voltage applications possible. The latest research has even shown a medium voltage high frequency two-level converter design realised with 10 kV SiC MOSFETs [114].

The multilevel converters are categorised in four different topologies:

- the Neutral-Point Clamped Voltage Source Converter (NPC VSC)
- the Cascaded H-Bridge Voltage Source Converter (CHB VSC)
- the Flying Capacitor Voltage Source Converter (FLC VSC)
- the Modular Multi-Point Converter (M2C)

The topologies are commonly used for high power drives. The M2C is a new converter which has some advantages compared to the first three listed topologies[115]. The M2C has several voltage levels realised with semiconductors and components typical in the serial production industry. The properties of a M2C allows an almost sinusoidal voltage form compared to the other multilevel topologies. The investigations of the M2C topology are used and further made in the low voltage range [116]. The converter topology is described in section 2.3.2.

The main reason of using multilevel converters is to eliminate cost intensive transformers in high power applications. The use of multilevel converters has advantages due to nearly sinusoidal current waveforms, lower common mode voltage, lower voltage peaks and low additional losses compared to a 2L-VSI. This turns into reduced stress on motor bearings and windings. More detailed description of these power converters, their advantages and disadvantages are given in [104, 106, 107, 117–120].

Special applications exist for motors which are supplied with a number of converters to reach high power ratings[92]. The motors have several winding systems forming independent three-phase systems. There are various applications and converter topologies, respectively. The important issue for a power measurement system is the voltage and current waveform with their harmonic content. The following two section describe the converter topology used in this thesis for to show the typical waveforms.

2.3.1 Converter Topology and Waveform

The figure 2.5 shows a converter topology used for high power drives with a dc-link. Depending on the requirements for a high power drive the individual components are used, e.g. the Line- or Motor-Filter to smooth the waveforms. A transformer with multiple secondary windings is often used, as the following described five-level cascaded H-Bridge (HB) converter shows. The Voltage Source Converter (VSC) consists of a rectifier, a dc-link and an inverter. The rectifier converts the ac supply voltage to a dc voltage, which is commonly realised with multipulse diodes, thyristor rectifiers or Pulse Width Modulated (PWM) rectifiers. The dc link has a capacitor, as depicted in figure 2.5, providing a voltage for a drive. Current source converters have an inductance placed as dc-link.

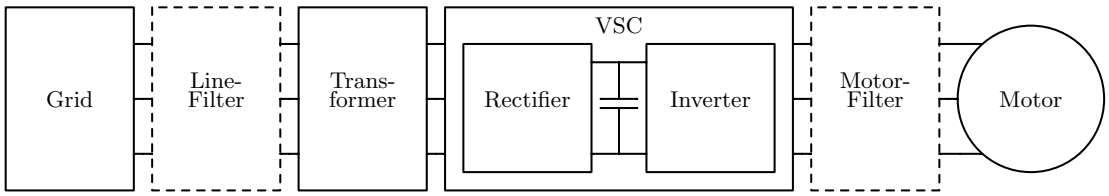

Fig. 2.5: Indirect Converter Topology with DC-Link

This section describes the 5 Level Cascaded H-Bridge Voltage Source Converter (5L-CHB VSC) to give a comprehension of the voltage and current waveform. The increasing of the voltage level is realised with a combination of several VSC. The 5L-CHB VSC contains two HB for each phase, see figure 2.6.

The dashed lines mark the modular expandability. Each HB-cell has its own dc-link which is supplied from a rectifier, depicted in figure 2.6. The rectifiers can be energy recoverable if the appropriate semiconductor switches are selected. All converters consist of a rectifier and are potential separated to each other. The converter level l of the CHB VSC corresponds to the amount of HB-cells necessary for each motor phase m, see table 2.1.

The shown converter topology is implemented in a PLECS model[121], which is an additional tool of Matlab Simulink. The model is used to simulate an expected waveform

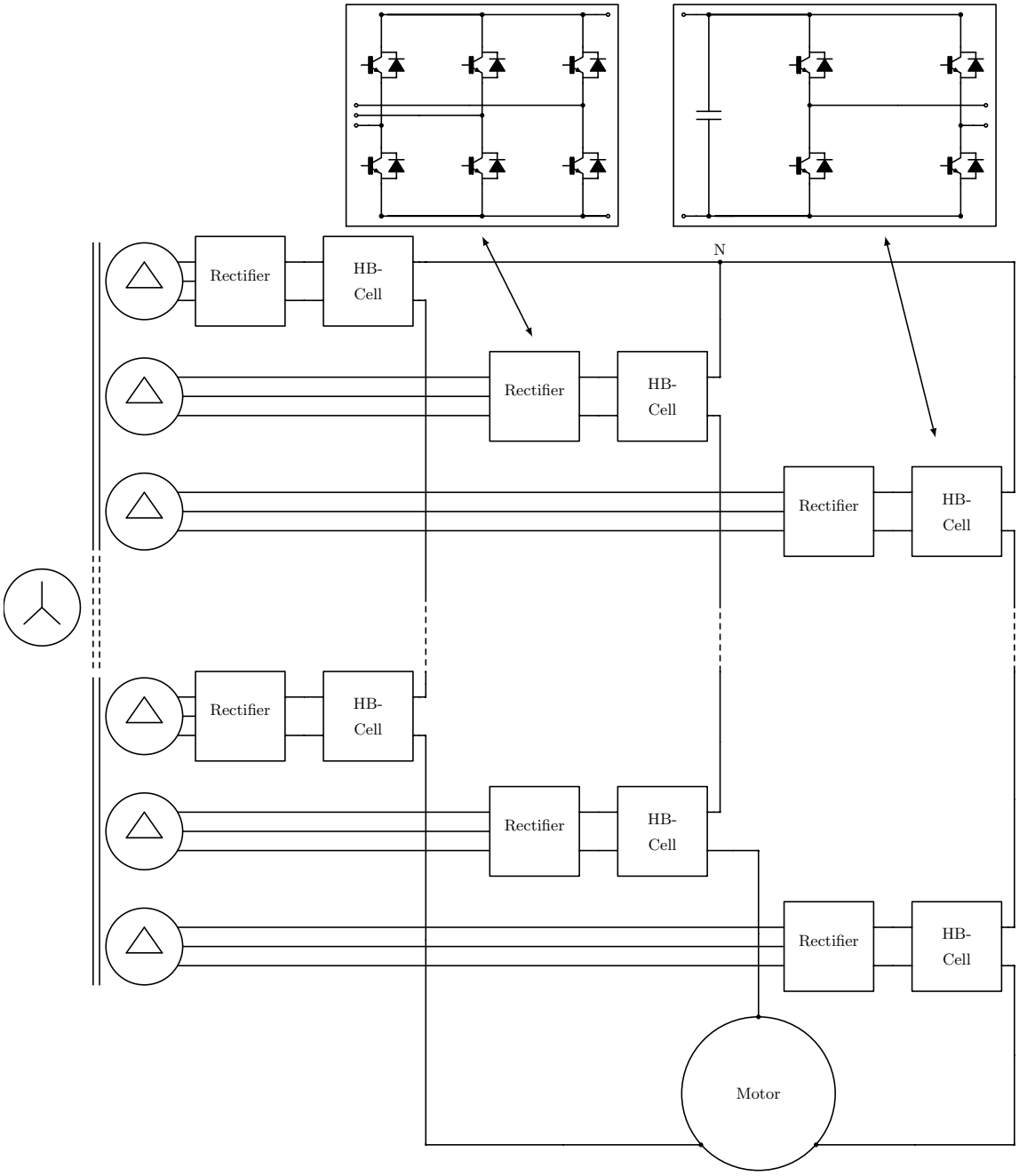

Fig. 2.6: 5 Level-Cascaded H-Bridge Voltage Source Converter

Tab. 2.1: The CHB VSC with l-Level

Level	Levels of Phase Voltage	Levels of Line Voltage	HB-cells per Phase
3	3	5	1
5	5	9	2
7	7	13	3
l	l	$2l-1$	$m=\frac{l-1}{2}$

of voltage and current to analyse the harmonic content. The model includes the 5L-CHB VSC connected to inductive load which is a typical motor, see table 2.2.

Tab. 2.2: Data of the Motor and Converter used for the PLECS Simulation Model

	Symbol	Value
Load-Resistance	R_{Load}	$5\,\Omega$
Load-Inductance	L_{Load}	$9\,\text{mH}$
Switching Frequency	f_{IGBT}	$375\,\text{Hz}$

A specific chain conductor model, described in [122, 123] , for a precise prediction of harmonic active power is not implemented due to the focus on the measurement setup. Therefore the harmonic content of the voltage and current waveform is essential and shown in this chapter. The waveform of the phase voltages are shown in the figure 2.7 with the reference signals $u_{UVW,Soll}$. The five voltage levels are visible as well as the PWM modulated signal.

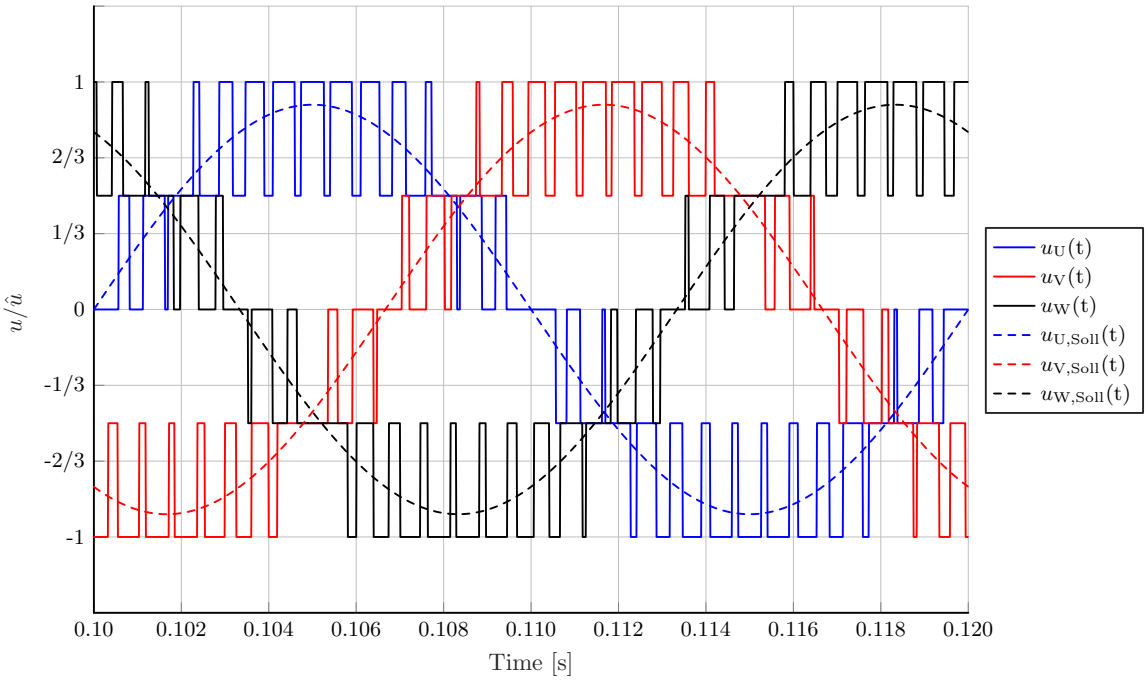

Fig. 2.7: 5 Level Cascaded H-Bridge Voltage Source Converter (5L-CHB VSC)- Phase Voltage

A FFT analysis delivers the harmonic content of the signal, see figure 2.8 with the harmonic order h. The PLECS model has ideal switches implemented, which means no switching edge modulation and current dependent transfer behaviour is included. Some harmonics have an amplitude of 10% referred to the base frequency. The PLECS

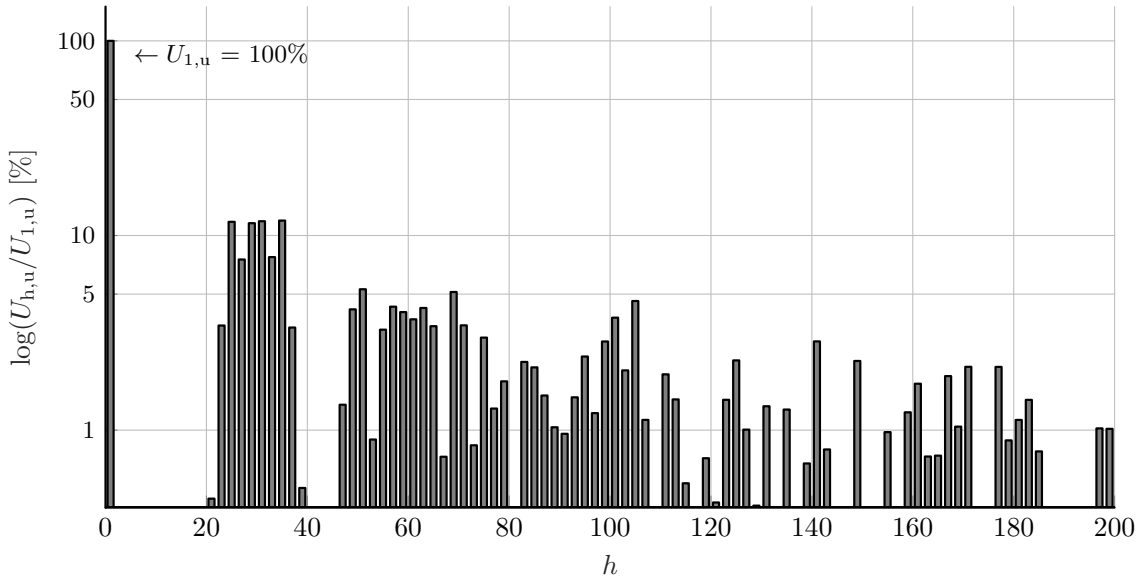

Fig. 2.8: 5L-CHB VSC - Phase Voltage - Harmonics

simulation with the load data gives corresponding harmonics in the current, see figure 2.9. The harmonic amplitudes are almost up to 1% referred to the base frequency of the current. Whether these harmonics result in harmonic active power is dependent on the phase angle between each harmonic in current and voltage, which means a detailed model as described in [122, 123]. Significant for the further investigation on uncertainty determination is the expected value of harmonics in voltage and current.

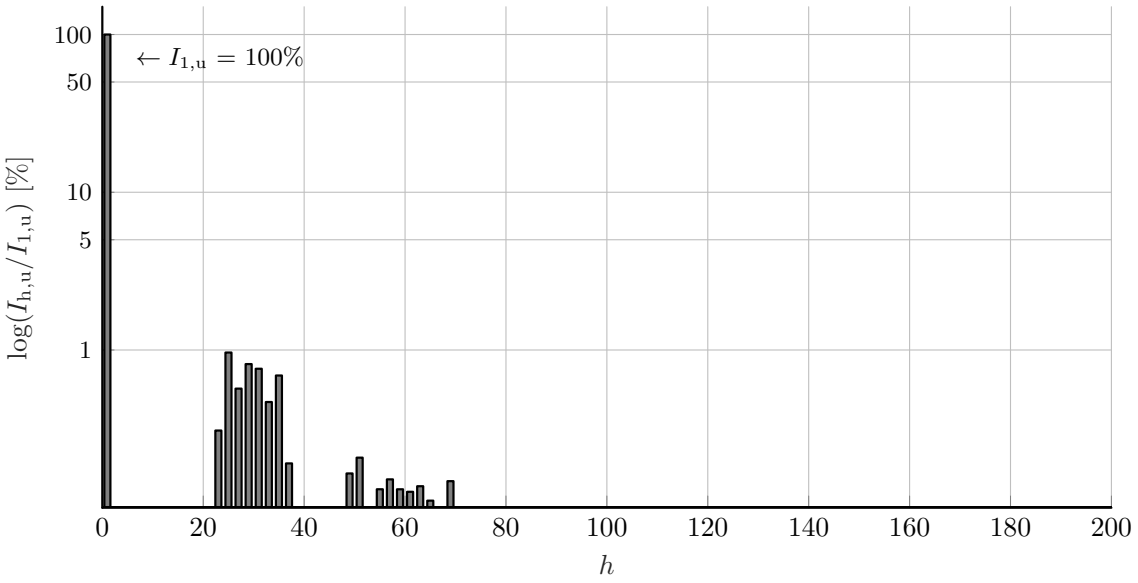

Fig. 2.9: 5L-CHB VSC - Phase Current - Harmonics

It is necessary to do investigations on the active power measurement uncertainty dependent on the sample rate of measurement devices. The generated waveforms with PLECS are used for further considerations in section 4.3.

2.3.2 Converter Topology of Modular Multi-Point Converter

The Modular Multi-Point Converter (M2C) is a multilevel converter with several converter cells connected in series in each leg. The figure 2.10 shows the topology of the converter, which has several Submodules (SMs). A Half-Bridge Submodule (HBSM) is shown in figure 2.10 which is a typical used SM for an M2C [107]. There are modules with Bypass-Thyristor, Full-Bridge Submodule (FBSM) or Clamp Double Submodules (CDSMs), which are also used for M2C converters [124].

Each SM and their functionality in an M2C converter is summarised in [125]. The disadvantages of a converter with one dc link are listed below, e.g. Voltage Source Converters (VSCs):

- Short circuits of the dc link due to faulty switching commands that lead to the failure of the IGBTs.
- The steep switching edges of the output voltage and long cables can lead to resonances, which can lead to failures in the stator windings.
- The common mode voltage usually has high frequencies can cause bearing damage.
- The effort of filtering on the grid side.

All the listed disadvantages are avoided with the use of an M2C.

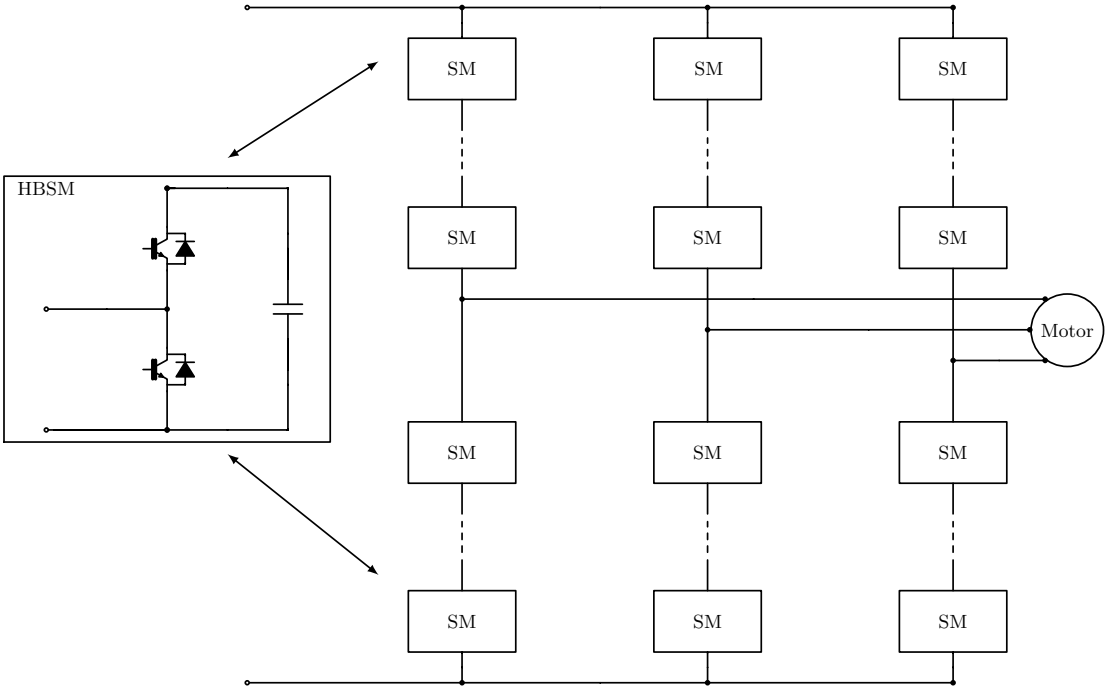

Fig. 2.10: Modular Multi-Point Converter with HBSM

The Figure 2.10 shows the several installed submodules. The dashed lines mark the modular expandability. The medium voltage motor in chapter 6 is fed with an M2C, which has 48 SMs installed[1]. The measured voltage and current wave form are shown in the appendix 9.4.1.

The output voltage is divided into several SMs in one phase, which allows the use of low-priced standard IGBTs with 1.7 kV blocking voltage. Due to the distribution of the output voltage on several SMs the steep voltage edges are low in amplitude, so the problem of resonance with long motor cables is reduced.

The typical problem of a VSC with one dc link is the current change between different circuits. Due to parasitic inductances, the current change is more difficult. This problem of current change does not exist for the M2C, and parasitic inductances have do not affect.

The recharging of the capacitors voltages in the SMs is achieved by internal circular currents, which realises the required energy exchange. The switching procedure and control methods are also described for applications in [115, 116].

[1]This means 16 submodules in one phase

3 Consideration on the Uncertainty in Measurement

The Guide to the Expression of Uncertainty in Measurement (GUM) [126] is a compendium for the determination and declaration of measurement uncertainties to get international comparable measurement results. GUM is used in this thesis for the theoretical uncertainty determination of measurement systems. Further, the guide is used to characterise measurement devices and compare results of different power measurement setups.

The general proceeding is separated in the following steps:

a) Creation of a model of the measurement setup,

b) Determination of uncertainties of the input quantity,

c) Determination of the measurement uncertainty for the output quantity,

d) Providing the measurement uncertainty.

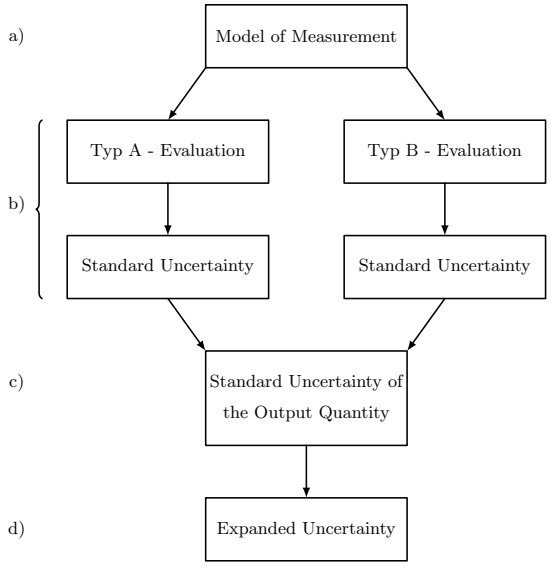

Fig. 3.1: Uncertainty Determination According to GUM

The general concept of GUM is shown in figure 3.1, which is based on modelling the measurement with a mathematical function. The function has input quantities with corresponding standard uncertainties, which can be evaluated by statistical analysis (Type A) or the use of reliable data (Type B). All uncertainties are combined by an error propagation and given with probability distribution. The next sections describe the individual steps of an uncertainty determination for the active power measurement using GUM.

3.1 Model of the Measurement

Input quantities that influence the measurement are necessary to create a mathematical model of the measurement. Therefore the input quantities have to be structured and assessed. An Ishikawa-Diagram is a proven method to show all possible influences on a measurement. As an example the figure 3.2 shows a diagram for active power measurement on medium voltage drives, which represents the output quantity.

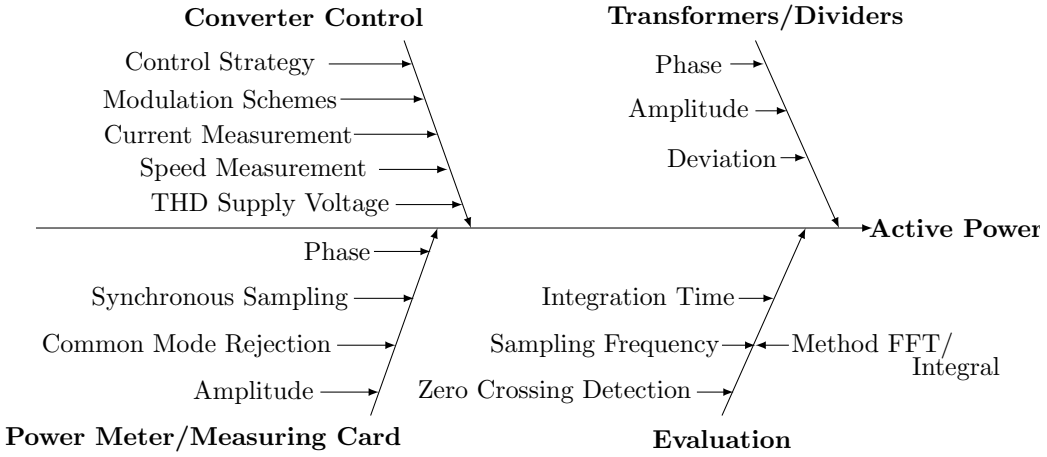

Fig. 3.2: Ishikawa-Diagram for the Input Quantities Influencing the Active Power Measurement

The influence of the converter control is difficult to quantify and can only be analysed by viewing the results of the measurement in figure 3.3. Dependent on the control procedure, the output quantity, respectively the active power, can have an enormous variation[127]. To characterise the uncertainty of the active power consumption of a motor a constant operation point is assumed. Therefore often a speed and current measurement is necessary which can provide a further uncertainty to the control loop. Hence the considered output quantity is affected with that uncertainty.

The figure 3.3 shows the determined active power of a motor driven with a multilevel converter. There are 1000 cycles recorded in which the active power values are calculated

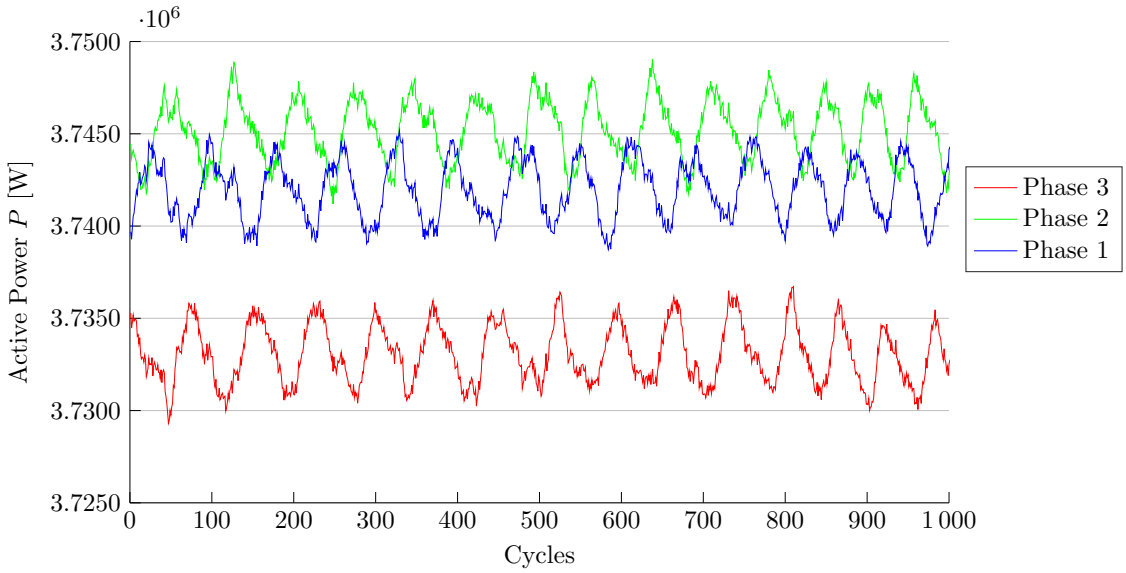

Fig. 3.3: Influence of Converter Control on the Active Power Measurement

from 10 periods of the motor base frequency - which corresponds to a record window of 200ms per cycle. The influence of the converter control is visible as oscillation of the active power P values between a maximum and minimum value. In all three phases the values are in a range of 5kW, which is 1 ‰ of the mean value, see in figure 3.3.

The sum of all phases, the total active power P_{Total}, is depicted in figure 3.4, where a periodic oscillation is difficult to identify. However an oscillation of the determined active power values is still visible and even larger in amplitude compared to the power values of the individual phases, but in relation to the mean value still 1 ‰.

The measurement system uses the voltages and currents of the motor supplying converter to determine the active power. If a comparison between two measurement systems is focused, an uncertainty contribution of the converter is not respected with the model equation, but is included in the measurements.

However a quantification of uncertainties is a complex task by the means of recorded currents and voltages evaluation. In principle it is possible to reduce the influence of uncertainty on a measurement if known principles of the signal processing are observed. A sufficient sample and integration time must be selected to get sufficient information of the recorded signals. The integration time defines the amount of base frequency periods whereof an average value is calculated. The sample frequency choice f_{S} defines the maximum analysable frequency f_{max}, which is given through the Nyquist-Shannon-Criterion.

$$f_{\text{S}} = 2 \cdot f_{\text{max}} \tag{3.1}$$

A further aspect is the synchronisation to the base frequency in order to detect the signal zero-crossings correctly. The synchronisation allows an accurate determination of the phase shift and the integration interval for the active power determination. In a channel which is independent of the measuring channels, the basic frequency is determined from

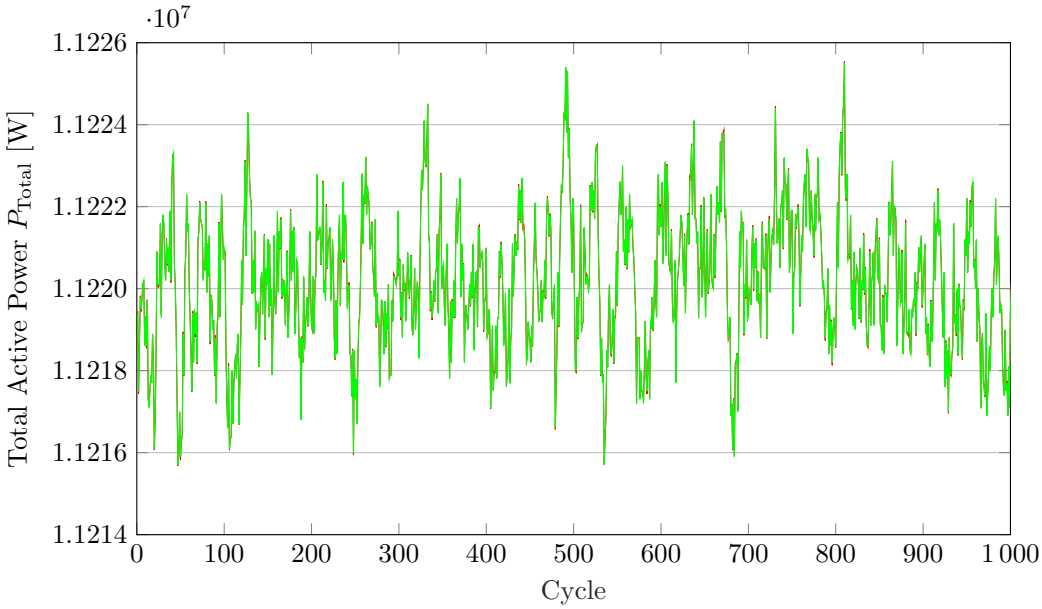

Fig. 3.4: Influence of Converter Control on the Total Active Power Measurement

several zero crossings. For this purpose filters and phase lock techniques are frequently used in power analysers, which allow an accurate zero-crossing detection in the case of non-sinusoidal input quantities [128, 129].

The used transformers or dividers are calibrated, whereby measurement deviations and uncertainties are quantified, respectively can be derived from the protocols. For example, according to IEC 60044-8 [130] uncertainties for electronic current transformers are given with amplitude and phase in the certificates. These figures can be used for an uncertainty consideration and combined with the uncertainty of other uncertainty sources.

The measurement board or power meter uncertainty is defined differently.Values of uncertainty are given for amplitude or phase depending on the measured value and the measuring range. A power meter or a measurement board must digitise the signals synchronously. A time offset between current and voltage would cause a phase error, which in turn influences the determination of the active power.

The mathematical model for the measurement of an average active power P over a period sinusoidal signal result from the root mean square values of voltage U, current I and the phase angle φ, φ_{h}.[1] The model is only valid for one harmonic or rather one frequency component of all input quantities, e.g. the base frequency.

$$P = f\left(U, I, \varphi\right) = U \cdot I \cdot \cos(\varphi) \tag{3.2}$$

The model in equation 3.2 considers the determined active power for one phase.

[1]Phase angle between voltage and current $\varphi = \varphi_{\text{U}} - \varphi_{\text{I}}$

3.2 Determination of Measurement Uncertainty

The equation 3.2 is now used to determine the measurement uncertainty of P by error propagation. A combined standard measurement uncertainty results from the uncertainties of the input variables $\delta(U)$, $\delta(I)$ und $\delta(\varphi)$.

$$\delta(P)^2 = \Big(c_{\mathrm{U}} \cdot \delta(U)\Big)^2 + \Big(c_{\mathrm{I}} \cdot \delta(I)\Big)^2 + \Big(c_{\varphi} \cdot \delta(\varphi)\Big)^2 \tag{3.3}$$

The uncertainties are multiplied by sensitivity coefficients c_{U}, c_{I} and c_{φ}, which results from the partial derivations of the model equation 3.2.

$$c_{\mathrm{U}} = \frac{\partial P}{\partial U} = I \cdot \cos(\varphi) \tag{3.4}$$

$$c_{\mathrm{I}} = \frac{\partial P}{\partial I} = U \cdot \cos(\varphi) \tag{3.5}$$

$$c_{\varphi} = \frac{\partial P}{\partial \varphi} = -U \cdot I \cdot \sin(\varphi) \tag{3.6}$$

The uncertainty of the input variables can be determined by repeated measurements according to GUM Type A, see in figure 3.1. This corresponds to the empirical standard mean value deviation out of several measurements. The principle for Type A evaluation of standard uncertainty is shown in section 3.4. In this work an uncertainty analysis according to GUM Type B is applied in which quantified data is used. This data is taken from protocols of calibration or measurement uncertainty provided by the manufacturer. This is the usual procedure for an uncertainty analysis in order to determine the accuracy of a measuring system. The GUM Type B is usually used for the worst case evaluation before measurements are done.

The uncertainties of the input variables usually consist of several components of the measuring chain. In this example the uncertainties have to be derived from a current transformer $\delta(I_{\mathrm{CT}})$, a voltage divider $\delta(U_{\mathrm{VD}})$ and a power measurement device $\delta(U_{\mathrm{PM}})$. According to GUM, several uncertainties of an input variable are combined by means of a sub-model. Using the active power measurement as an example, voltage, current and phase have the following equations for their uncertainty contribution.

$$\delta(U) = \sqrt{\delta(U_{\mathrm{PM}})^2 + \delta(U_{\mathrm{VD}})^2} \tag{3.7}$$

$$\delta(I) = \sqrt{\delta(I_{\mathrm{PM}})^2 + \delta(I_{\mathrm{CT}})^2} \tag{3.8}$$

$$\delta(\varphi) = \sqrt{\delta(\varphi_{\mathrm{PM}})^2 + \delta(\varphi_{\mathrm{VD}})^2 + \delta(\varphi_{\mathrm{CT}})^2} \tag{3.9}$$

Usually the data in calibration protocols are given with a probability density distribution. If this information is not available, a rectangular distribution is assumed for these uncertainties, which represents the worst case distribution.

3.3 Specification of Measurement Uncertainty

The expanded measurement uncertainty $\delta_{95\%}$ can be obtained by multiplication of the combined standard uncertainty $\delta(P)$ with the coverage factor k. For a coverage probability of 95.45 %, according the Gaussian distribution, the value $k = 2$ is chosen. The coverage probability of a measurement uncertainty specification indicates the probability in which the measurement uncertainty range contains the true measurement value.

$$\delta_{95\%} = 2 \cdot \delta(P) \tag{3.10}$$

The expanded measurement uncertainty $\delta_{95\%}$ is given with the assigned coverage factor or the coverage probability, as shown in table 3.1. The example uncertainty calculation of active power determination is examined for the base frequency since all uncertainty contributions of higher harmonic components are expected according to their amount lower than the contribution of the base frequency. The harmonic components of a drive application fed by a multilevel converter are low compared to the base frequency component, which the uncertainty components are also applied to. However, a measurement uncertainty analysis is helpful for determining individual harmonics of a power oscillation. There are known loss calculation models using a voltage spectrum to calculate additional losses by harmonics [131, 132]. An uncertainty analysis on such models are an useful method to evaluate these calculations.

Tab. 3.1: Example for a Measurement Uncertainty Budget - one Phase

Quantity	Value	$\delta(U,I,\varphi)$	Probability distribution	$c(U,I,\varphi)$	Contribution of uncertainty	Total MU
U	2190 V	4.471 V	Rectangle	214.5 A	553.7 W	73.07 %
I	280 A	0.3185 A	Rectangle	1677.6 V	308.49 W	22.68 %
φ	40°	0.0336°	Rectangle	394 kW	133.45 W	4.25 %

Measured Quantity	P
Value	469 kW
Expanded Measurement Uncertainty $\delta_{95\%}$	± 1.3 kW
Coverage factor k	2

The measurement uncertainty budget in the table 3.1 summarizes the elements of the measurement uncertainty determination. It contains the measurement uncertainty contributions of the input variables and the effect on the output variable. The budget clearly demonstrates the individual influence of the uncertainty contributions and can be used to evaluate them. Individual measuring devices can be analysed in different

operating points and be replaced as required. The uncertainty of the overall active power is calculated by the following equation:

$$\delta_{95\%,\mathrm{3Phase}} = \sqrt{(\delta_{95\%,\mathrm{PhaseU}})^2 + (\delta_{95\%,\mathrm{PhaseV}})^2 + (\delta_{95\%,\mathrm{PhaseW}})^2} \tag{3.11}$$

3.4 Statistical Analysis of Measurement Series

A correct statement on the measurement uncertainty of measurement setups and measurement devices needs an accurate consideration of errors, which in turn gives the possibility to minimise these errors. In the section before GUM Type A is named as a method to determine the measured quantity standard uncertainty. The method is based on a statistical analysis of a measurement series, which is commonly used for the characterisations of a measurement.

In measurements, differentiation between systematic measuring errors and random measuring errors is required. The systematic errors are predictable and therefore correctable. The random errors can only be quantified with probability distributions.

A further classification in measurements is done between static and dynamic errors. While the static errors refer only to the static properties of the measuring device, the dynamic measurement errors are the deviations resulting from the non-ideal transmission characteristics of the measuring system, which results in a deviation of the true time dependent measurement quantity[133]. The analysis on the transfer behaviour of measurement devices in section 5.1.2 shows the determination of static and dynamic errors.

The described method in GUM does not distinguish between systematic and random uncertainty components. If possible, the elimination or correction of systematic errors is assumed, otherwise this error is added to the whole uncertainty. The expected value of a quantity to be measured corresponds to the arithmetic mean value of a number of repeated measurements.

$$\bar{x} = \frac{x(1) + x(2) + \cdots + x(n)}{n}$$

$$\begin{aligned} \bar{x} &: \text{Mean value} \\ x(1), x(2), ..., x(n) &: \text{Observed measurement values} \\ n &: \text{Number of repeated measurements} \end{aligned}$$

The standard uncertainty is the empirical standard deviation of the mean value determined with a number of n observations. The number of observations n should be large enough to ensure that mean value $\bar{x}$ is a reliable estimate of the expected value [126].

$$\sigma = \sqrt{\frac{\left(x(1) - \bar{x}\right)^2 + \left(x(2) - \bar{x}\right)^2 + \cdots + \left(x(n) - \bar{x}\right)^2}{n-1}} \tag{3.12}$$

The variation of the measured values should be determined and covers the random variable errors with the calculated standard uncertainty. If only random errors are present in a measurement, the mean value is equal to the true value of the measured quantity. In practice often only a limited repetition of the measurement is possible and a certain variation of the mean values exists. The methods of GUM, especially the Type B estimation, shows the determination of a measurement uncertainty which still covers a variation of the mean value. The GUM Type B is an efficient and less time consuming method to characterise an measurement setup uncertainty. The methods of GUM were used and compared in this thesis with the results of the determined standard uncertainties of active power measurements.

4 Data Acquisition and Processing

This chapter is divided into four sections, which are necessary for the determination of active power values with the measured signals. The Data Acquisition and Signal Conditioning are essential to prepare the signals for the digital signal processing.

4.1 Data Acquisition and Signal Conditioning

The data acquisition requires basically a signal conditioning in power technology applications. Signal conditioning is necessary to convert all measurable signals to a recordable format for an Analog Digital Converter (ADC). Using the active power measurement on electrical drives, the following aspects of signal conditioning are important:

Amplification/Attenuation
A shunt used for the measuring of a current provides a voltage signal in the range of 0 to 10 mV. This signal has to be amplified to a voltage matching the range of the used ADC, e.g. 0 to 10 V. The opposite is the attenuation of a signal with hundreds of volts adapted to the ADC input range.

Electrical Isolation
Electrical isolation usually called galvanic isolation is an important issue in power technologies. It isolates the signal input to the output by an optical or magnetic coupling. A differential measurement is possible if a line voltage measurement is focused on. Additionally undesired ground loops are avoided which can influence the measurement of a signal by a voltage drop between ground and reference of the input channel.

Common Mode Rejection
Common Mode Rejection (CMR) is essential for the power measurement of converter applications, otherwise the measured voltage or current can be incorrect. Converters have steep voltage edges in the output signal, which can result in common mode voltages. Due to parasitic capacitances of the parallel motor lines, capacitive interference currents can occur and lead to signal distortions at the input resistor of a measurement device. Power meters use differential amplifiers or instrumentation amplifiers to realise a CMR. Common mode voltages can reach maximum a third of the dc-link voltage and have often steep switching edges, so they occur at high frequencies [103, 125, 134].

Filtering
Filters in power measurement are often used to prevent aliasing effects caused by the influence of high frequency signals. Anti aliasing filters cut off the frequency components above the Nyquist-Shannon frequency which is specified by the sample frequency of the ADC, see equation 3.1. Filtering and keeping the Nyquist-Shannon criterion is essential for the correct harmonic power analysis. Filtering should not influence the active power measurement, which means the active power components in the signals should not be limited due to a low cutoff frequency of the filter. In general, it is possible as the active power components of medium voltage motors are below 1 kHz, see the measurements in chapter 6.

Sampling
It is not unusual to use a multiplexer to enable one single ADC to digitise two or more signals. However, for an active power measurement, a simultaneous sampling is recommended to determine the exact phase angle between voltage and current signal. If they are not simultaneously sampled, additional uncertainty to the active power measurement can be induced.

Excitation
Some current sensors require an excitation voltage to operate. Especially flux compensated current transducers are often used in measurements with non-sinusoidal currents in power technologies. If the voltage supply is reliable, there should be no influence on the active power measurement.

4.1.1 Analog Digital Converter

Digital computers are used for processing the voltage and current signals. The analog signals have to be digitised with an ADC into amplitude and time discrete signals. The significant quantities are given below:

Sampling The sample frequency f_S is defined as inverse of the sampling time t_S, which is the time between two samples.

Number of samples N
The number of samples in one sequence or a defined time.

Resolution
The number of bits gives information about the resolution of an ADC input range.

The selection of the sampling frequency is important for digital signal processing due to the described aliasing effects in section 4.1. If the Nyquist-Shannon theorem of equation 3.1 is not respected, aliasing occurs which means overlaps in the frequency spectrum of the sampled signal. The following sections give an overview on the ADC uncertainty of the amplitude and phase.

4.1.2 Measurement Uncertainty of ADC

The evaluation on uncertainty of an ADC and its testing is described in a standard [135]. This standard is a guideline to identify the error sources which are influencing the conversion of an analog signal to digital one. Some manufacturers of ADCs give a maximum uncertainty for an error source. This allows a quantification of a standard measurement uncertainty for an operation point of an ADC. Power meters have uncertainties defined for the determined power quantities where the ADC errors are already included. However, the section here will summarise these errors to give an overview of the influence on measuring quantities. According to several articles [136–140] five parameters are sufficient to calculate the total uncertainty:

- Offset,
- Gain,
- Total Harmonic Distortion (THD),
- Total Spurious Distortion (TSD),
- Noise Floor (SNR).

These parameters have been analysed with measurements and compared to an uncertainty modelling by a Monte Carlo approach [141]. A Monte Carlo approach is used to evaluate a probability density of uncertainty for a quantity with the random combination of several uncertainty sources. However it is possible to model all the relevant parameters with the proposed guideline of GUM to get uncertainty for a quantity.

The uncertainty of the phase depends on the duration of the ADC conversion process. The conversion time causes a phase delay between the input and output signals. The maximum sample frequency can be calculated from the acquisition time T_{aq}, which is the sum of the aperture time, the settling time and the conversion time. In [133] the conditions for a minimum acquisition time and the basic evaluation of ADC requirements are given. The requirements are dependent on the effective number of bits ($ENOB$) and the maximum frequency expected $f_{\max}$ in the signal, with the condition of minimum error of a half significant-bit voltage U_{LSB}.

The aperture time is also named as jitter time t_{jit} and is defined with the equation:

$$t_{\mathrm{jit}} = \frac{1}{(2^{ENOB} - 1) \cdot 2 \cdot \pi \cdot f_{\max}} \tag{4.1}$$

The jitter time defines the maximum sample frequency and can used to assume the phase uncertainty for an ADC. An uncertainty for the phase can be assumed with:

$$\delta_{\varphi} = t_{\mathrm{jit}} \cdot 360° \cdot f_{\max} \tag{4.2}$$

In the case power measurement devices or oscilloscopes, there are one or more ADC modules installed to measure several signals. Time delay between these channels result in a measurement uncertainty for the phase, which can be dominating dependent on

the measurement device and its ADC's [142]. Manufacturers indicate these uncertainty and define a sum of all measurement uncertainties in their device specifications. The equation 4.1 and 4.2 can be used to estimate the phase measurement uncertainty.

4.2 Data Processing

The sample frequency influences the active power determination and the corresponding measurement uncertainty, which is summarised in the research review section 1.1. The two well-known determination methods for active power in section 4.2.1 and 4.2.2 are analysed on the uncertainty with the methods of GUM. Data processing is not expected as an uncertainty source if the algorithm and the calculations are implemented correctly. However, there are conditions to respect to have no uncertainty contribution for a measurement quantity. This section describes the different processing method to get correct active power quantities from sampled voltage and current signals with high probability. A general overview and comparisons of the existing Power Definitions are given in the book of Emanuel [143].

4.2.1 Discrete Integration Method and its Uncertainty

The discrete integration method is the simplest method to implement for the active power determination since the sampled voltage and current signals are multiplied to get the instantaneous power. The sum of the instantaneous power values over a defined averaging time gives the mean value of the active power. The defined averaging time is known as cycle time or cycle period in measurements. The active power mean value P is defined for continuous signals:

$$P = \frac{1}{T} \int_0^T u(t) \cdot i(t) \cdot dt \tag{4.3}$$

There are different discretisation methods [73], here the forward Euler method is used, the active power P_{DI} is determined from the sampled values of the voltage and the current with the amount of samples N. The amount of samples is defined depending on the highest frequency to measure and the amount of base frequency periods to record. The more samples per base frequency period the higher is the probability of a determined value P_{DI}, see figure 4.2 in section 4.3.

$$P_{\mathrm{DI}} \approx \frac{1}{N} \sum_{n=1}^{N} u_n \cdot i_n \tag{4.4}$$

In three phase systems the active power of all phases has to be summarized.

$$P_{\mathrm{DI,3}} \approx \frac{1}{N}\sum_{n=1}^{N}\left(u_{U,n}\cdot i_{U,n} + u_{V,n}\cdot i_{V,n} + u_{W,n}\cdot i_{W,n}\right) \tag{4.5}$$

The three phase power measurement with the use of the discrete integration method is also be done with different configurations, e.g. measure the line voltages instead of the phase voltages using a delta-wye conversion. Further, the Aron circuit can be used with the discrete integration method, which needs two line voltages and two phase currents for the active power determination, see section 2.

Uncertainty of Discrete Integration Method The uncertainty analysis starts building a mathematical model of the focused measurement. The equation for active power 4.4 is the model equation:

$$P_{\mathrm{DI}} = \frac{1}{N}\sum_{n=1}^{N} u_n \cdot i_n =: f(u_n,i_n,N) \tag{4.6}$$

The following equation is used to determine the uncertainty of the active power.

$$\delta^2_{\mathrm{P_{DI}}} = \sum_{n=1}^{N}\Big((c_{\mathrm{u},n}\cdot\delta_{\mathrm{u},n})^2 + (c_{\mathrm{i},n}\cdot\delta_{\mathrm{i},n})^2 \Big) + (c_N\cdot\delta_N)^2 \tag{4.7}$$

The sensitive coefficients $c_{\mathrm{u},n}$, $c_{\mathrm{i},n}$ and c_N are given with the partial derivation of the model equation:

$$c_{\mathrm{u},n} = \frac{\partial P_{\mathrm{DI}}}{\partial u_n} = \frac{1}{N}\cdot i_n \qquad\qquad c_{\mathrm{i},n} = \frac{\partial P_{\mathrm{DI}}}{\partial i_n} = \frac{1}{N}\cdot u_n$$

$$c_N = \frac{\partial P_{\mathrm{DI}}}{\partial N} = -\frac{1}{N^2}\sum_{n=1}^{N} u_n\cdot i_n + \frac{u_N\cdot i_N}{N} = -\frac{P_{DI}}{N} + \frac{u_N\cdot i_N}{N} \tag{4.8}$$

The derivation of the model equation according to the number of samples is calculated with the product rule and the parameter integral. [1]

The sensitive coefficients can be set into the equation 4.7. The measurement uncertainty for a voltage sample $\delta_{u,n}$ is assumed as the same for all samples δ_u, corresponding to all current samples δ_i. The measurement uncertainty for the determined active power results from the standard measurement uncertainty of every individual sampled point.

[1] $\frac{\partial}{\partial X}\int_a^X f(t)\,dt = \frac{\partial}{\partial X}(F(X)-F(a)) = f(X)$

The uncertainty dependent on the sample frequency decreases with a higher number of samples. The uncertainty contribution of δ_N is decreasing significantly compared to the voltage and current part, see equations 4.9 and 4.8. In the article of Betta [79] the uncertainty is analysed with different signal processing algorithms used for the measurement of periodic signals. The uncertainty of the algorithms are analysed on quantisation errors and methods of undersampling of signals. The focus of this thesis is to find the lowest uncertainty for the active power dependent on the dominating uncertainty sources. The uncertainty of the algorithms are not investigated and the quantisation error is negligible, which leads to an uncertainty equation in a reduced form without the uncertainty δ_N.

$$\delta^2_{\mathrm{P_{DI}}} = \sum_{n=1}^{N} \left(\left(\frac{1}{N} \cdot i_n \cdot \delta_{u,n} \right)^2 + \left(\frac{1}{N} \cdot u_n \cdot \delta_{i,n} \right)^2 \right) + \left(-\frac{P}{N} + \frac{u_N \cdot i_N}{N} \right)^2 \cdot \delta^2_N \quad (4.9)$$

$$\delta_{\mathrm{P_{DI}}} = \frac{1}{N} \cdot \sqrt{\delta^2_u \cdot \sum_{n=1}^{N} i^2_n + \delta^2_i \cdot \sum_{n=1}^{N} u^2_n} \quad (4.10)$$

The uncertainty for the three phase active power is given as the geometric sum.

$$\delta_{\mathrm{P_{DI,3}}} = \sqrt{3} \cdot \delta_{\mathrm{P_{DI}}} \quad (4.11)$$

4.2.2 Harmonic Active Power Determination and its Uncertainty

The active power can be determined from its harmonic components. The sampled voltage and current signals are transformed from the time domain with a Discrete Fourier Transform (DFT) or Fast Fourier Transform (FFT) to get the frequency components of the signals.[2] The methods of Fourier Transform and the derivations are many times described in the literature e.g. [144]. First, the section here describes the basic equation for the Fourier Transform to show the dependency on the harmonic active power determination from a sampled signal. The complex Fourier coefficient $\underline{C}_h$ is expressed as:

$$\underline{C}_h = \frac{1}{T_0} \int_0^{T_0} f(t) \cdot e^{-j \cdot 2\pi \cdot h \cdot f_0 \cdot t} dt \quad (4.12)$$

The time T_0 is defined as the length of the recorded signal which has to be a multiple integer of the base frequency period. The harmonic order is given by h, the base

[2] The FFT efforts $N = 2^m$ samples in a signal to analyse and has the advantage of a shorter calculation time compared to the DFT

frequency with f_0 and the given signal to analyse $f(t)$. With the use of the forward Euler method, the complex Fourier coefficient is determined from the sampled values with a number of samples N.

$$\underline{C}_h = \frac{1}{N} \sum_{n=1}^{N} f_n \cdot e^{-j \cdot \frac{2\pi}{N} \cdot h \cdot (n-1)} \tag{4.13}$$

The phase angle of the signal equates the one of the Fourier coefficient.

The lowest frequency f_{min} to analyse, which is the frequency resolution Δf of the frequency spectrum, is given by the reciprocal of the record length with the sample time t_S and the number of samples N. The maximum frequency to determine is provided by the half of the samples $\frac{N}{2}$.

$$f_{min} = \Delta f = \frac{1}{N \cdot t_s} \qquad\qquad f_{max} = \frac{N}{2}$$

The result of a FFT or DFT will be a mirrored frequency spectrum and needs a multiplication with the factor two to calculate the correct value of the harmonic components. The harmonic component $\underline{A}_h$ is a peak value, respectively the peak value of the voltage $\hat{U}_h$ and the current $\hat{I}_h$. The active power of a harmonic with the order h is calculated with the determined coefficients and following equation for one phase.

$$\underline{A}_h = 2 \cdot \underline{C}_h \tag{4.14}$$

$$P_h = \frac{\hat{U}_h \cdot \hat{I}_h}{2} \cdot \cos(\varphi_h) \tag{4.15}$$

Only components of voltage and current of the same order h contribute to active power. The phase φ_h is the phase shift between the voltage and current harmonics.

$$\varphi_h = \varphi_{\mathrm{u},h} - \varphi_{\mathrm{i},h} \tag{4.16}$$

The harmonic components are calculated with the equation 4.13 and 4.14 dependent on the samples with the following equations.

$$\hat{U}_h = \frac{2}{N} \cdot \left| \sum_{n=1}^{N} u_n \cdot e^{-j \cdot \frac{2\pi}{N} \cdot h \cdot (n-1)} \right| \tag{4.17}$$

$$\hat{I}_h = \frac{2}{N} \cdot \left| \sum_{n=1}^{N} i_n \cdot e^{-j \cdot \frac{2\pi}{N} \cdot h \cdot (n-1)} \right| \tag{4.18}$$

The harmonic components have to be summarized to get the active power P_H of one phase.

$$P_\mathrm{H} = P_0 + \sum_{h=1}^{\frac{N}{2}} P_h \tag{4.19}$$

The dc component P_0 is included setting $h = 0$ and is given with the following equation:

$$P_0 = U_0 \cdot I_0 \tag{4.20}$$

with

$$U_0 = \frac{1}{N}\sum_{n=1}^{N} u_\mathrm{n} \qquad\qquad I_0 = \frac{1}{N}\sum_{n=1}^{N} i_\mathrm{n} \tag{4.21}$$

The determination of the whole active power of a three phase system $P_{\mathrm{H,3}}$ is given with the sum of all phases.

$$P_{\mathrm{H,3}} = P_{\mathrm{H,U}} + P_{\mathrm{H,V}} + P_{\mathrm{H,W}} \tag{4.22}$$

Starting from these, the corresponding measurement uncertainties were determined using the methods of GUM. The harmonic active power determination is often implemented in power meters and makes a quick analysis of the harmonic power content possible.

Uncertainty of Harmonic Method The DFT method is used to determine the active power of its several harmonic components.The harmonic components of voltages and currents are given with amplitude and phase. In this section, the uncertainty due to the harmonic active power determination is determined with the equation 4.15, which is the model equation:

$$P_h = \frac{\hat{U}_h \cdot \hat{I}_h}{2} \cdot \cos(\varphi_h) := f\left(\hat{U}_h, \hat{I}_h, \varphi_h\right) \tag{4.23}$$

$$\varphi_h = \varphi_{U_h} - \varphi_{I_h} \tag{4.24}$$

The uncertainty of the harmonic active power components is given with:

$$\delta_{P_{a,h}} = \sqrt{\left(c_{\hat{u},h} \cdot \delta_{\hat{U}_{a,h}}\right)^2 + \left(c_{\hat{i},h} \cdot \delta_{\hat{I}_{a,h}}\right)^2 + \left(c_{\varphi,h} \cdot \delta_{\varphi_{a,h}}\right)^2} \tag{4.25}$$

The sensitivity coefficients are given with the derivation of the individual input quantity.

$$c_{\hat{u},h} = \frac{\partial P_h}{\partial \hat{U}_h} = \frac{\hat{I}_h \cdot \cos(\varphi_h)}{2} = \frac{P_h}{\hat{U}_h} \tag{4.26}$$

$$c_{\hat{i},h} = \frac{\partial P_h}{\partial \hat{I}_h} = \frac{\hat{U}_h \cdot \cos(\varphi_h)}{2} = \frac{P_h}{\hat{I}_h} \tag{4.27}$$

$$c_{\varphi,h} = \frac{\partial P_h}{\partial \varphi_h} = \frac{-\hat{U}_h \cdot \hat{I}_h \cdot \sin(\varphi_h)}{2} = -\frac{P_h}{\cos(\varphi_h)} \cdot \sin(\varphi_h) \tag{4.28}$$

Inserting the coefficients $c_{\hat{u},h}$,$c_{\hat{i},h}$ and $c_{\varphi,h}$ into the equation 4.25 leads to the sum of relative uncertainties.

$$\delta_{P_h} = |P_h| \cdot \sqrt{\left(\frac{\delta_{\hat{U}_h}}{\hat{U}_h}\right)^2 + \left(\frac{\delta_{\hat{I}_h}}{\hat{I}_h}\right)^2 + (\tan(\varphi_h) \cdot \delta_{\varphi_h})^2} \tag{4.29}$$

The equation 4.29 describes an uncertainty when a harmonic active power is available. In the appendix 9.1 the equations 4.17 and 4.18 are used to determine the uncertainties of the harmonic components of voltage and current. In a further article of Betta [80] the uncertainty reasoned by quantisation errors and signal processing components is analysed. There are conditions for a Fourier analysis like the Nyquist-Shannon criteria and the complete recording of periods, which is described in [144] with further background knowledge of Fourier analysis. The effects of aliasing and leakage are well known for an incorrect determination of frequency components. For further investigation, the uncertainty due to the number of samples is not taken into account.

The derivation in the appendix 9.1 lead to an uncertainty for the voltage harmonic $\delta_{\hat{U}_h}$ and the current harmonic $\delta_{\hat{I}_h}$.

$$\delta_{\hat{U}_h} = \sqrt{\frac{2 \cdot \delta_u^2}{N}} \qquad \delta_{\hat{I}_h} = \sqrt{\frac{2 \cdot \delta_i^2}{N}} \tag{4.30}$$

$$\delta_{\varphi_h} = \sqrt{\frac{2}{N} \cdot \left(\delta_{\mathrm{u}}^2 \cdot \sum_{m=1}^{N} \frac{1}{\hat{U}_h^2} + \delta_{\mathrm{i}}^2 \cdot \sum_{m=1}^{N} \frac{1}{\hat{I}_h^2}\right)} \tag{4.31}$$

The uncertainty for the voltage samples δ_u, the current samples δ_i and the number of samples N is used. The mean value active power is determined by the sum of all harmonics and the dc component, see equation 4.19. The uncertainty of the dc component is given as relative uncertainties with equation 4.20.

$$\delta_{P_0} = |P_0| \cdot \sqrt{\left(\frac{\delta_{U_0}}{U_0}\right)^2 + \left(\frac{\delta_{I_0}}{I_0}\right)^2} \tag{4.32}$$

with

$$\delta_{U_0} = \sqrt{\frac{\delta_u^2}{N}} \qquad \delta_{I_0} = \sqrt{\frac{\delta_i^2}{N}}$$

The uncertainty of the active power determined with the harmonic method is the sum of the uncertainties of all components.

$$\delta_{\mathrm{P_H}} = \sqrt{\sum_{h=0}^{\frac{N}{2}} \delta_{P_h}^2} \tag{4.33}$$

The uncertainty of the three phase active power is given as the geometric sum.

$$\delta_{\mathrm{P_{H,3}}} = \sqrt{3} \cdot \delta_{\mathrm{P_H}} \tag{4.34}$$

4.3 Active Power Determination and Uncertainty

The simulation model of the drive presented in chapter 2.3.1 is used to analyse the active power determination and the uncertainty in data processing. The two determination methods and their uncertainty estimation are used, which are introduced in the sections 4.2. The model is implemented to vary the sample frequency and the record length. The scenarios with different sampling frequencies in the range of 1 kHz to 1 MHz is shown in table 4.1.

Tab. 4.1: Simulation Scenarios - The Given Sample Frequency f_S, Cycle Time T_{cycle} and Number of Samples N

T_{cycle} [s]	f_S [kHz]	$N = f_S \cdot T_{cycle}$
0.2	1	200
0.2	5	1000
0.2	10	2000
0.2	50	10000
0.2	100	20000
0.2	500	100000
0.2	1000	200000

In figure 4.1 are more than the seven scenarios calculated due to the less computation effort of the used discrete integration method. The cycle time T_{cycle} defines the number of recorded periods of the base frequency, which is kept constant in the scenarios. If the number of samples N matches in the defined recorded periods, a scenario is calculated for a range of sample frequencies f_S.

The more time-consuming simulation whose results are shown in the figures 4.3 to 4.6, only the seven listed scenarios are used. In every scenario, the sampled voltage and current measurement signals are used to determine the active power using equation 4.5 described in section 4.2.1. The values $P_{DI,3}$ in figure 4.1 are normalised to the determined active power value P_{1MS} with the highest sample frequency of 1 MHz. With the increase of the sampling frequency, the active power value reaches the true value. The recorded voltage has frequency components with a minimum of 0.1 % base frequency amplitude up to 40 kHz and in the current up to 3.5 kHz. Base frequency amplitudes below 0.1 % can be neglected due to their neglectable contribution to the whole active power. The active power has doubled frequency components due to the multiplication of voltage and current signals. These frequency components define the possible harmonics

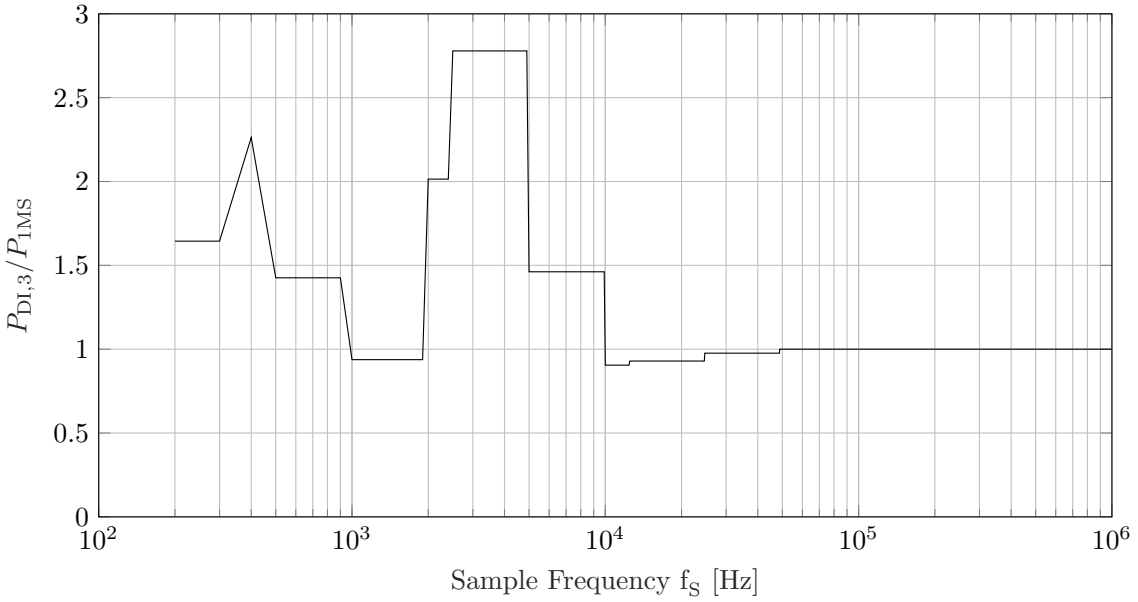

Fig. 4.1: Determination of Active Power with Different f_S

active power to measure. Figure 4.1 shows almost no deviation with a sample frequency f_S above 48.9 kHz. The investigations lead to the derivation of the equation 4.35.

The sample frequency and cycle time influence the determination of active power dependent on the signal to record. An equation can be defined which provides a sample frequency f_S dependent on the focused uncertainty δ_{AP}, the cycle time T_{cycle}, the period time of voltage base frequency t_0 and the maximum frequency expected f_{max} in the power signal.

$$f_S = 2 \cdot f_{max} \cdot 2^{250\,(0{,}01-\delta_{AP})} \cdot (e^{-\frac{T_{cycle}}{t_0}-1} + 1) \tag{4.35}$$

An accuracy of 0.2 % can be realised with a cycle time of 0.2 s, a base frequency period time of 0.02 s and a maximum expected frequency of 14 kHz, when a sample frequency of 112 kHz is chosen. The limit of 0.2 % is chosen due to the defined uncertainty limits for voltage and current measurement devices in the standard IEC 60034-2-1. The scenarios are used to evaluate this equation. Figure 4.2 shows the sample frequency with regard to the uncertatinty δ_{AP}, maximum expected frequency f_{max} and the number of base frequency periods. The latter one is given with the quotient of cycle time T_{cycle} and the base frequency period time t_0, which is only valid with integer values for a power measurement. The sample frequency increases with less recorded base frequency periods and a higher accuracy.

The equation 4.10 is used to calculate the uncertainty as a function of sample frequency f_S and cycle time T_{cycle}. Figure 4.3 shows the uncertainty contribution in percent, where an equivalent behaviour as the active power determination is expected. The uncertainty contribution $\delta_{\mathrm{P_{DI,3}}}$ is normalised on the corresponding active power $P_{\mathrm{DI,3}}$. The uncertainty for the voltage and current ±0.2 % is assumed for a measuring range of ±10 kV and ±500 A. In general, the result shows a decreasing uncertainty with a higher number of samples, which decrease theoretically to zero. The storage and ADC

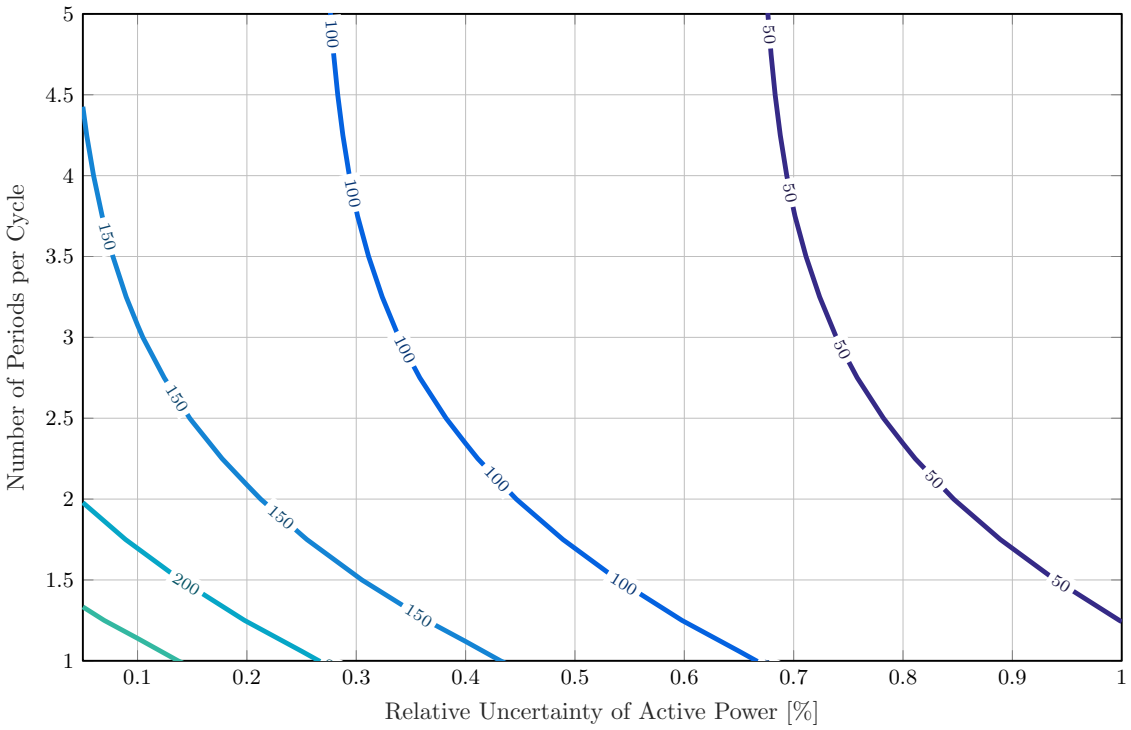

Fig. 4.2: Sample Frequency f_S in kHz for maximum expected frequency f_{max}=14 kHz

speed of measurement devices are limited, which has to be respected with the focus of less uncertainty in a measurement.

The real measurements still have an uncertainty which can not be eliminated by the number of samples as there are still physical components in the measurement chain, e.g., voltage and current transducer. Nevertheless, the probability of a determined value is increasing with the number of samples in a corresponding uncertainty range. The uncertainty determination is examined with the defined measurement setup uncertainty, which applies for a sampling frequency and a cycle time.

The simulation model is used to analyse the active power determination and the measurement uncertainty using the harmonic method. The harmonic active power is less than 0.1 % of the total power P_H, which occurs in the harmonic range between 30 and 40 with a sum of 0.035 741 %. The figure 4.4 shows the the harmonic active power dependent on the harmonic order h.

Hence, the active power of the base frequency component dominates with the largest share of 99.964 % of the total power. In the figure 4.4 relative harmonic amplitudes P_h of the active power are shown with a sample frequencies f_S of 1 MHz. The highest sample frequency is shown due to the standard use in power analysers and the sufficient active power measurement performance. The choice of a chain conductor model would result in a more accurate generation of harmonics[122, 123]. The harmonic active power is desired to be low in a drive application. If a measurement system should measure a low harmonic active power compared to the base frequency components, a wide measuring range with a low measurement uncertainty is necessary. The equation 4.33 is used to show the

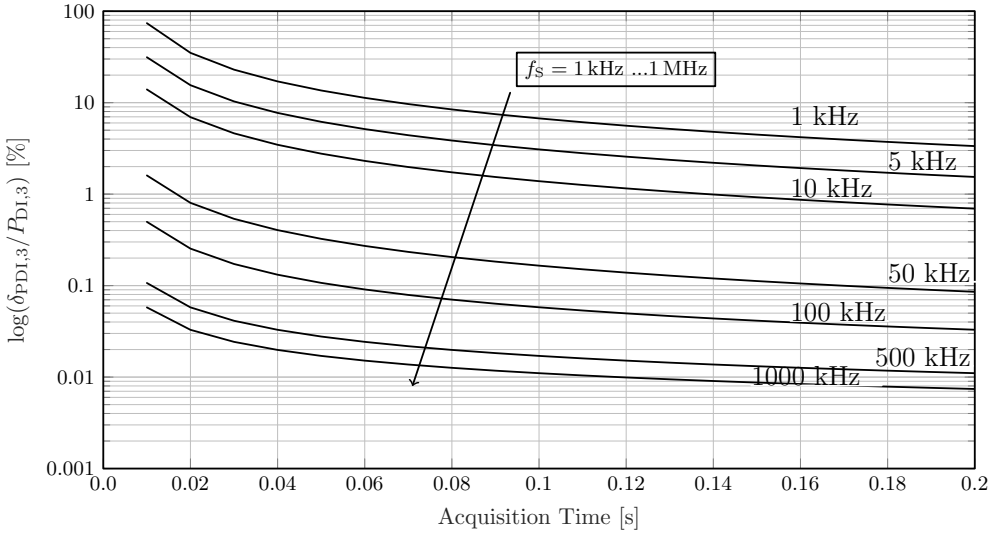

Fig. 4.3: The Relative Measurement Uncertainty with Different Sample Frequencies f_{S} and the Acquisition Time

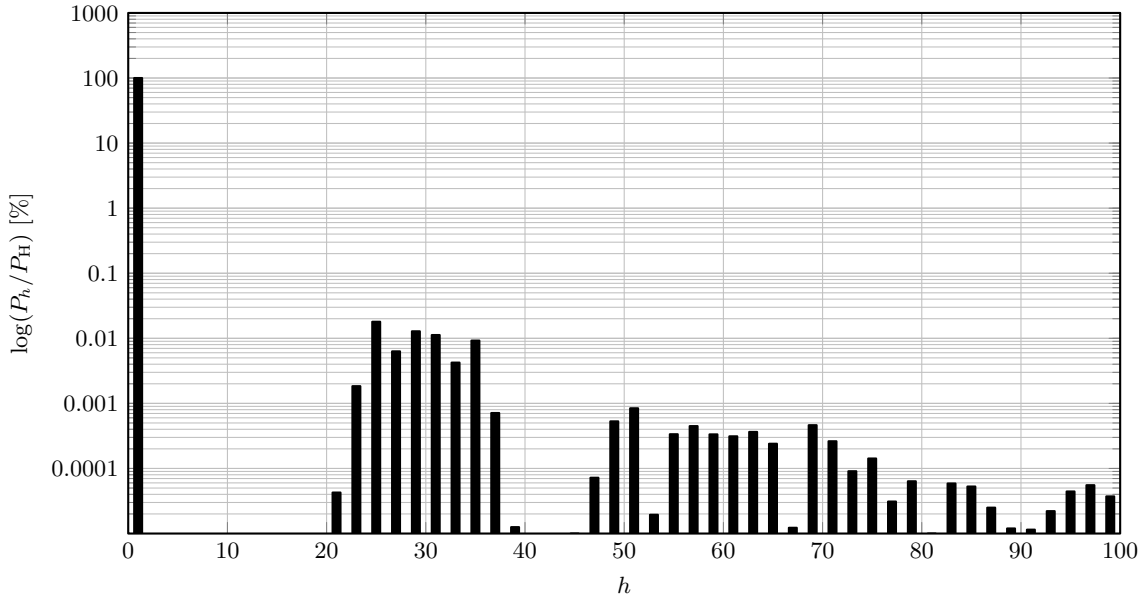

Fig. 4.4: Harmonic Components of Active Power, $f_{\mathrm{S}} = 1\,\mathrm{MHz}$

uncertainty contribution of each harmonic, see figure 4.5. The values are normalised to the total uncertainty of whole the active power $\delta_{\mathrm{P_H}}$, determined with the harmonic method. The measurement uncertainty of the base frequency component contributes 97.5 % of the total uncertainty. The maximum uncertainty of the individual harmonics is less than 10% of the total uncertainty $\delta_{\mathrm{P_H}}$. Due to less harmonic components above the base frequency, less uncertainty contribution can be expected. A analysis of the harmonic active power is given in section 6.5.

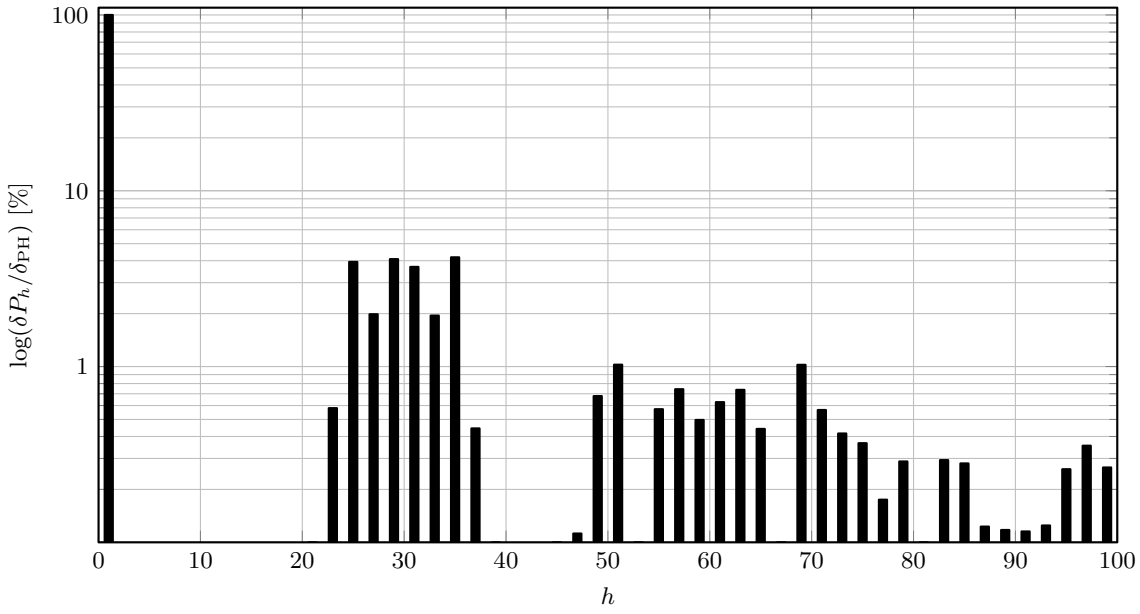

Fig. 4.5: Uncertainty Harmonic Components of Active Power, $f_S = 1\,\mathrm{MHz}$

4.4 Comparison of Active Power Processing Methods

In this section, the two methods for determination of active power and their corresponding uncertainty are compared using the described scenarios, see table 4.1. The figure 4.6 shows the active power and the uncertainty with regard to sampling frequency from 1 kHz to 1 MHz . The increase of the sampling frequency leads to an approach of the calculated active power P and the expected active power value $P_{1\mathrm{MS}}$ for both methods. However with a sample frequency below 50 kHz a deviation between the methods and their determined power values is visible[3]. It results from the standard for the determination of harmonics and instrumentations [145], which is also discussed in the comparative study of various methods of DFT coefficient calculation [146]. The standard describes the correct use of a frequency analysis and a limit of uncertainty for the measurement of harmonics. The harmonics of active power which are lower than the uncertainty limit cannot be summarized to the total active power, which is described in [145]. It results in a difference in the active power between both methods at a low sampling frequency. With a sufficient sampling frequency of 50 kHz the difference between both methods is negligible, see in figure 4.6.

In the same figure 4.6 the measurement uncertainty drawn to the total active power is shown. The determined uncertainty of both modes deviates at the different sampling frequencies. In general, the relative uncertainty of the harmonic method is insignificant higher than for the discrete integration method. The discrete integration method is only influenced by the absolute uncertainty values δ_u and δ_i, which can be seen in equation 4.29. However the harmonic method is more affected due to doubled uncertainties

[3]The base frequency in the simulation is 50 Hz

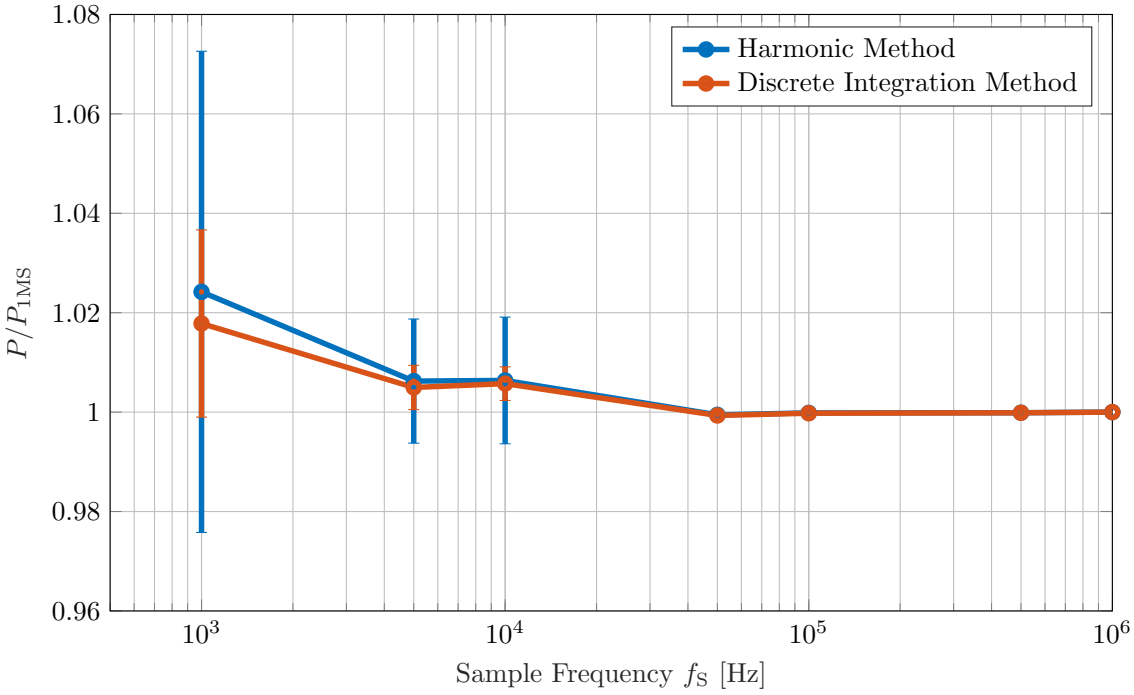

Fig. 4.6: Comparison Discrete Integration and Harmonic Method

of current and voltages, as well the additional phase uncertainty of the phase shift φ between the two signals, see equation 4.33.

5 Power Measurements: Equipment and Characterisation

The used measurement equipment used for the voltage and current measurement in the medium voltage range is presented. The chapter is divided into two parts, where the typical and commonly used measurement devices are summarised.

5.1 Voltage Measurement

The measurement of voltages above one kV has increased requirements for a measurement system and its used devices. The most recording devices, such as the oscilloscope or data acquisition boards, are designed for low voltage. The reduction of high voltages to a value acceptable to the measuring devices is a precondition for the measurement of voltages above one kV. This statement would apply to all measurements beyond the specifications of the measuring equipment, and not just to voltages above one kV. The measured value should not differ from the real value and reproducibility is expected. The transmission characteristics of the measuring device are vital in determining the suitability of the available measuring equipment for medium voltage drives applications. These characteristics have to be taken into account including the proven measurement uncertainty given in a calibration protocol according to the standard IEC 60060-2 [147]. The potential separation is a further aspect of the selection of voltage measurement equipment. Voltage transformers have a magnetic decoupling whereby voltage dividers are connected through the earth potential with the recording device.

5.1.1 Voltage Measuring Devices

An overview of the usually used voltage measurement devices in high voltage and medium voltage applications is shown in figure 5.1.

a) Resistive Divider

b) Resistive Capacitive Divider

c) Capacitive Divider

d) Damped Capacitive Divider

e) Inductive Voltage Transformer

f) Capacitive Voltage Transformer

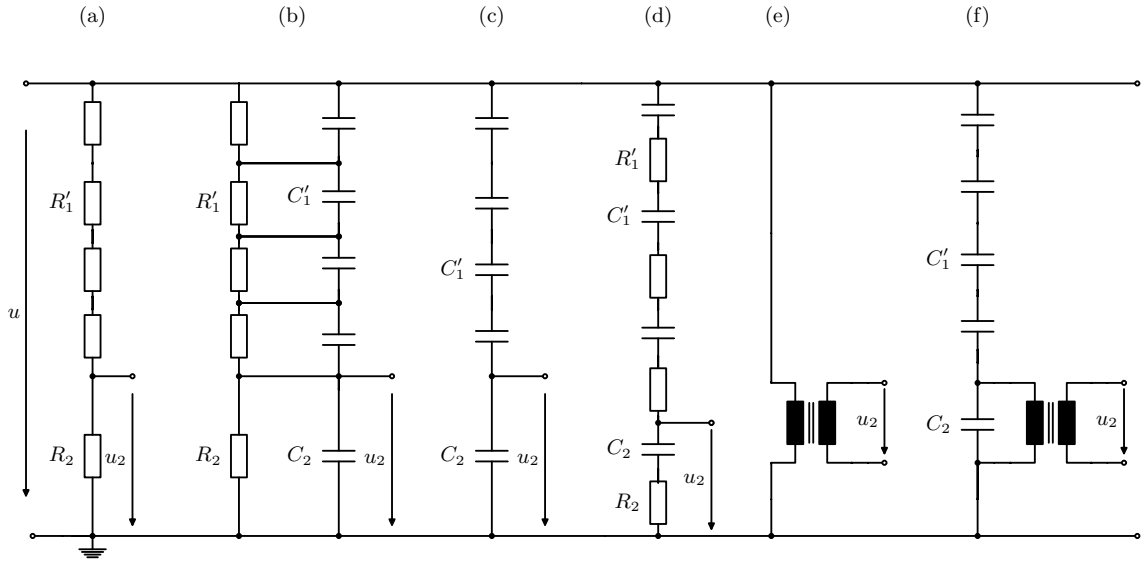

Fig. 5.1: Voltage Measurement Devices

Other Sensor Types: In several publications, field sensors are often used for the measurement of transient high voltages. The sensors use the record of displacement currents on the ground surfaces, generated by the electric and magnetic fields in homogenous or coaxial symmetric environment, to trace the input waveform. Field sensors are very small in their design and have their used frequency range above 1 MHz. Their main use is the detection of partial discharges in monitoring systems or testing of high voltage equipment. The field sensors are not used and are not discussed in this work, as they are not suitable for a conventional voltage measurement due to the effects of magnetic or capacitive couplings[148].

Optical voltage sensors are based on the Pockels effect. The output of the sensor is modulated light of an optoelectronic source such as a Light-Emitting Diode (LED) or a laser passed through a crystal. The crystal acting as a polarization modulator and the resulting light is mathematically linked to the applied voltage or the electric field [149, 150]. The optical sensors are not used in this work due to the effects of vibrations that can influence the measurement device [151] and they are usually used in gas isolated applications. Despite the possibility of compensation methods for the sensors against vibrations, they are designed for permanently installed applications and not for changing test bench setups. Further, the technologies are more expensive than the other introduced measurement devices.The most important voltage measuring equipment and its technical specification are introduced in the following sections as well investigations on the transfer behaviour of some are shown.

Voltage Dividers The essential characteristic of voltage dividers is to reduce voltages from a higher voltage range of up to several MV down to a range of a few volts. With the increasing dimension of dividers, the stray capacitances or inductances show an influence on their transfer behaviour. These influences are frequency dependent and can induce measurement errors. Therefore the effects of such disturbances are important to consider

in a calibration process of these measuring instruments. In high voltage engineering, there are various voltage dividers used depending on the type and characteristic of the signal to be measured, see the summary in [151]. There are ohmic, capacitive, ohmic-capacitive and damped-capacitive voltage dividers and their combinations, and some are shown in figure 5.1.

Resistive Divider A resistive voltage divider is the first choice to measure high DC voltages. Such a voltage divider is designed with series connected resistors. The resistors of the high voltage side have values in the GΩ range. The resistor R_1 should be of sufficient resistive value to ensure that no or minimal additional load is placed on the circuit. The Scale Factor (SF) is given by

$$SF_{\mathrm{RD}} = \frac{u_2}{u} = \frac{R_2}{R_1 + R_2} \tag{5.1}$$

The resistive dividers can have frequency dependent behaviour at measurement of impulse voltages. The high voltage side usually has several resistors thereby forming stray capacitances between the resistors and the ground. These are typically referred as capacities to ground. The high ohmic resistors and the earth capacitances build a chain of resistive and capacitive elements with large time constants, which results in a low pass behaviour with limiting frequencies in the one digit Hz range. Due to the frequency dependency that ohmic dividers exhibit, they are not suitable for alternating voltage measurements and not further investigated in this work.

Resistive Capacitive Divider The resistive capacitive voltage divider is constructed with resistors and capacitors connected in parallel. The connection has to satisfy the compensation condition. The resistive capacitive relation between the high voltage $R_1'C_1'$ and low voltage R_2C_2 side have to be the same.

$$R_1C_1 = R_1'C_1' = R_2C_2 \tag{5.2}$$

This condition results in a frequency independent scale factor.

$$SF_{\mathrm{RCD}} = \frac{u_2}{u} = \frac{R_2}{R_1 + R_2} = \frac{C_1}{C_1 + C_2} \tag{5.3}$$

Thus the divider can be used for all voltage types. If the condition of equation 5.2 is not fulfilled an overcompensation will occur [152]. The divider is of limited value for impulse voltage measurement despite an ideal compensation. The undamped capacitive part builds a resonant circuit with the inductance of the measuring circuit. The measuring circuit inductance is a summarised quantity, which occurs due to the construction of the circuit. This includes lines and wound resistors, which can have an inductive effect. A damping resistor is connected to the high voltage taps for the prevention of oscillation in some applications. However, the frequency independent behaviour of the divider is no

longer available. High voltage probes are designed as ohmic capacitive voltage dividers, where a compensation with the input channel of the recording device is necessary. Their measuring range reaches voltage up to maximum 60 kV. Two voltage probes and their transfer behaviours are analysed in section 5.1.3.

Capacitive Divider Capacitive dividers are often used to detect high AC voltages. These dividers are less suitable for impulse voltages. An undamped divider produces results very similar to that of the resistive capacitive divider. Also travelling waves can be induced along the divider due to fast-rising voltage edges. A damping resistor can reduce these effects. In the case of a capacitive divider, stray capacitances to the ground can occur, which affect only on the magnitude of the scale factor and not on its frequency behaviour.

$$SF_{\mathrm{CD}} = \frac{u_2}{u} = \frac{C_1}{C_1 + C_2} \tag{5.4}$$

When a damping resistor is connected to the divider it reacts as a resistive capacitive component, which should be considered. The rise time can be derived using the following formula [151]:

$$T_{\mathrm{Rise}} = 2.2 \cdot R_{\mathrm{D}} C_1 \tag{5.5}$$

If an impulse voltage is to be measured the time constant T_{Rise} of the divider should be considerably smaller than the rise time of the voltage to be measured. The capacitive divider is not further analysed because of the necessity to measure DC voltages.

Damped Capacitive Divider A damped capacitive divider has resistors and capacitors connected in series. The distributed arrangement of resistors and capacitors has an optimal damping effect for travelling waves. The compensation condition from equation 5.2 as the ohmic capacitive divider is suitable for this divider to guarantee their frequency independence. Damping capacitive dividers are very well suited for AC and impulse voltage measurements, where it is commonly used. The divider has a capacitive behaviour for low frequencies and resistive behaviour for high frequencies. Stray capacitances to the ground can have an effect on the magnitude of the scale factor and its frequency behaviour. The ideal scale factor is the same as for the resistive capacitive divider.

$$SF_{\mathrm{DCD}} = \frac{u_2}{u} = \frac{R_2}{R_1 + R_2} = \frac{C_1}{C_1 + C_2} \tag{5.6}$$

These dividers have an excellent transfer behaviour if they are constructed with low inductive components. They are also reference-dividers when calibrating other divider types [152]. If the damped capacitive divider has resistances connected to the RC elements in parallel, all voltage forms are detectable. This is a combination of a resistive capacitive and a damped capacitive divider. This is often known as a resistive capacitive

composite voltage divider, also known as a universal divider[153]. A universal divider is used as reference for the analysis in section 5.1.3.

Voltage Transformers A commonly used measuring device for high and medium voltages is the inductive voltage transformer, see figure 5.1(e). It is a transformer operated with no load on the secondary side. The most of these measuring devices are cast resin transformers in the medium voltage range. The main advantage of measuring a voltage with voltage transformers is the galvanic isolation. Inductive voltage transformers are often used in the supply grid measuring the voltage for control, protection and monitoring purposes. Depending on the application, the accuracies become essential.

The higher the voltages to be measured, the more extensive the construction of inductive voltage transformers. When the voltage is very high, the windings, the iron core and the insulation construction become very large. The costs rise with the construction size. A more economical alternative for the measurement of higher voltages up to 1 MV is the capacitive voltage transformer, see figure 5.1 (f). In principle, this is a capacitive voltage divider whose low voltage part has an inductive voltage transformer with an inductor connected in between. The advantage is the potential separation compared to a capacitive divider.

The transformers are conventional voltage measurement devices. They exist since the beginning of the electrical energy use and their transmission. Transformers are used in measurement circuits with a higher power - secondary voltage in the range of 0 V to 100 V - than nowadays used digital measurement technique, which has a typical small operation and signal voltages. The transformers are still used in the energy transmission grid and also used for power measurement of medium voltage drives. In section 5.1.3 the transfer behaviour of a typical voltage transformer for medium voltage applications is analysed.

Inductive Voltage Transformer The inductive voltage transformer is often used to measure alternating voltages. Maximum voltages up to 30 kV is the usual measuring range. The energy is transferred from the primary side to the secondary side via the magnetic flux in the core. The output can be influenced by the windings. The ideal scale factor is determined by the SF winding ratio [154].

$$SF_{\mathrm{T}} = \frac{u_2}{u_1} = \frac{w_1}{w_2} \tag{5.7}$$

Normally, the scale factor is set that the rated voltage on the primary side corresponds to a secondary voltage u_2 of 100 V.

There are losses due to resistances and magnetic coupling which cause a voltage drop. In some cases, iron losses are also to be considered. These characteristics influence their transfer behaviour and can be seen in the equivalent circuit in figure 5.2. The stator quantities are based on the quantities of the secondary side with the scale factor. The primary and secondary coil have dependent on the wire characteristic finite resistances $\mathrm{R}_1^{'}$ and R_2. The flux has an stray leakage part $\mathrm{L}_{1\sigma}^{'}$ and $\mathrm{L}_{2\sigma}$, which does not contribute

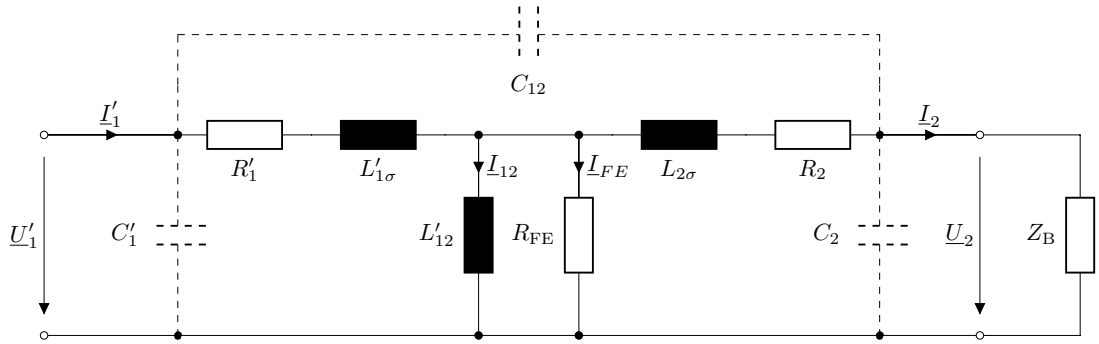

Fig. 5.2: Equivalent Circuit of a Voltage Transformer

to the main flux. Due to the non-ideal characteristic of the iron core, there are eddy currents and hysteresis losses $\mathrm{R_{FE}}$. The main flux in the iron core is described as main inductance $\mathrm{L_{12}}$. Parasitic capacitances, $\mathrm{C_1^{'}}$, $\mathrm{C_2}$ and $\mathrm{C_{12}}$, occur when high frequencies are applied, which can also result in losses. Fast transients can build resonance circuits and result in Ferro resonance, see also [155, 156].

The measuring transformer usually has a load on the low voltage side connected in parallel, which is the burden impedance Z_{B}. The voltage transformer should operate in no load for a voltage measurement, which means $Z_{\mathrm{B}} \rightarrow \infty$. However, a high impedance termination of a few MΩ is sufficient. The burden impedance is usually selected or defined with a power factor and an apparent power in IEC 61869-3 [157].

There are deviations due to voltage drops which can be observed in the measurement, which means

$$\underline{U}_2 - \underline{U}_1^{'} \neq 0 \tag{5.8}$$

with

$$\underline{U}_1^{'} = \underline{U}_1 \cdot \frac{w_2}{w_1} \tag{5.9}$$

and a deviation between the measured $\underline{U}_2$ and the primary voltage $\underline{U}_1^{'}$ occurs. As a result, the voltage transformer has an amplitude error δ_{UVT} as well a phase shift $\delta_{\varphi\mathrm{VT}}$ between primary and secondary side. The figure 5.3 shows a vector diagram based on the equivalent circuit of the voltage transformer 5.2.

$$\delta_{\mathrm{UVT}} = \frac{\underline{U}_2 - \underline{U}_1^{'}}{\underline{U}_1^{'}} \tag{5.10}$$

$$\delta_{\varphi\mathrm{VT}} = \mid \varphi_{\mathrm{U_2}} - \varphi_{\mathrm{U_1^{'}}} \mid \tag{5.11}$$

According to these factors, inductive voltage transformers are classified into accuracy classes. These accuracy classes are defined in the standard IEC 61869-3 [157] dependent on the rated burden and a defined voltage range. An accuracy class of 0.2 defines a

maximum deviation δ_{UVT} of 0.2 % and a limit $\delta_{\varphi\mathrm{VT}}$ of maximum 10 minutes phase deviation. The 10 minutes deviation corresponds to 0.167°, which is valid for the rated frequency of 50 Hz, only. With increasing frequency, the deviation is rising, too. The burden impedance can influence the accuracy of the voltage transformer[158]. The measurements in section 5.1.3 are focused on analysing the deviations for higher frequencies than 50 Hz.

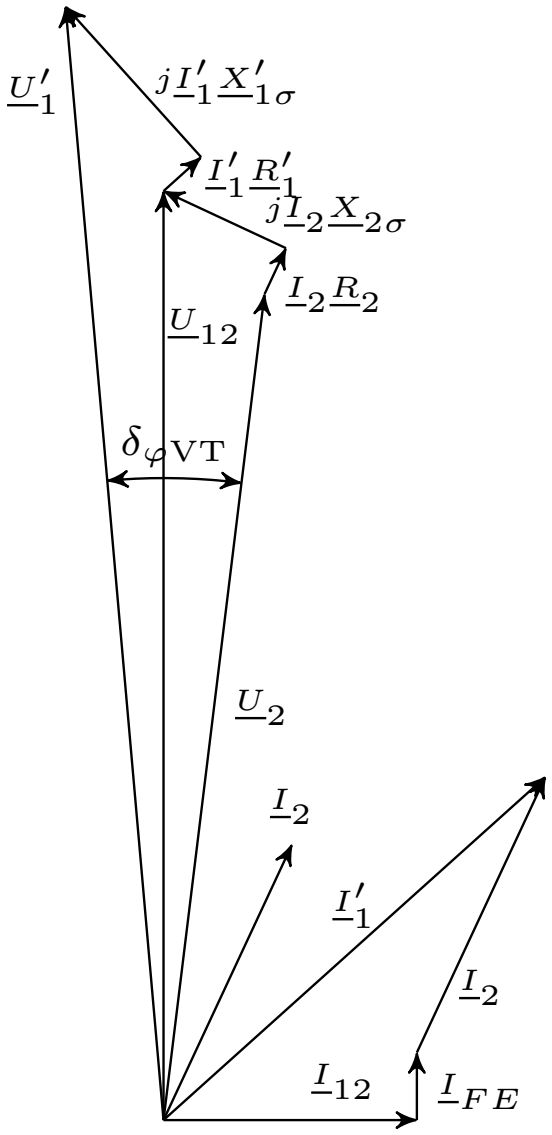

Fig. 5.3: Vector Diagram of Voltage Transformer

Capacitive Voltage Transformers A further application for measuring high voltages are capacitive voltage transformers. They are commonly used in high voltage applications for the measurement of voltages and protection use in the supply grid. This type of transformer is not analysed in this work, as they are more used in high voltage grid applications. But the principle of operation and their characteristic is described here. Capacitive voltage transformers are often used when inductive voltage transformers become uneconomical due to high or extra high voltages, where inductive voltage transformers are becoming extensive constructions, which also means an enormous use of copper for the coil building. The structure is similar to the capacitive voltage divider, see figure 5.1(f).

The difference is an inductive voltage transformer connected due to an inductor on the low voltage side C_2. The capacitive divider reduces the high voltage to a lower value, which can be applied to the inductive voltage transformer. The advantage is a small inductive voltage transformer which are a more cost-effective solution than a larger dimensioned one. The divider is thus dimensioned for voltage drop on C_2 in the range between 10 kV and 30 kV. The capacitive voltage transformer has a small operating frequency range. The transformer has deviations in phase and amplitude if the operating range is left [159]. Further, a variation of insulation characteristics due to construction can have a significant effect on measurement error, shown in [160].

5.1.2 Determination of Transfer Behaviour

The transfer behaviour is the main characteristic of a voltage or current measurement device, which is used for the power measurement of converter driven drives. The section summarises a method to characterise the transfer behaviour of measurement transformers and dividers. This technique is described in the international standard IEC 60060-2 [147], which is used by manufacturer and calibration laboratories. The scale factor determination is used to analyse voltage transformers, dividers, and current transformers over a defined frequency range. An impulse voltage or current is generated to provide a signal with several frequencies at once instead of a sinusoidal calibration at multiple frequencies. A few conventional devices are investigated in this thesis as they were available.

To ensure a suitable comparison of the measuring system to be calibrated several aspects have to be respected, e.g. symmetrical arrangements to minimise electromagnetic influences of the individual measurement setup components against each other. The main steps for a measurement device characterisation and the corresponding uncertainty determination are summarised here. The characterisation is used for comparisons in section 5.1.3, where the uncertainties of the scale factor are necessary.

Scale Factor The scale factor indicates the ratio of the applied voltage to the voltage detected by a measuring device. An applied signal is recorded simultaneously by a reference measurement system and the device under test. The scale factor SF_{M} determination is a mean value of M scale factor determinations.

$$SF_{\mathrm{M}} = \frac{1}{M} \sum_{i=1}^{M} SF_i \tag{5.12}$$

$$\sigma_{\mathrm{SF_M}} = \frac{1}{SF_{\mathrm{M}}} \sqrt{\frac{1}{M-1} \sum_{i=1}^{M} \left(SF_i - SF_{\mathrm{M}}\right)^2} \tag{5.13}$$

$$\delta_{\mathrm{SF_M}} = \frac{\sigma_{\mathrm{SF_M}}}{\sqrt{M}} \tag{5.14}$$

Using the M individual scale factors, the standard deviation $\sigma_{\mathrm{SF_M}}$ and the standard uncertainty δ_{SF} can be calculated. A scale factor with a high probability can be reached with a higher number of taken measurements, but the standard IEC 60060-2 [147] defines a maximum of 10 measurements as sufficient.

Scale Factor over the Measuring Range ($\delta_{\mathrm{B,0}}$ & $\delta_{\mathrm{B,1}}$) The scale factor may dependent on the voltage level. Therefore it is necessary to calibrate the whole measuring range of a measurement device. The scale factors and standard deviations are determined for at least five different voltage levels L. The most used voltage levels are 20 %, 40 %, 60 %, 80 % and 100 % of the maximum voltage to be measured.

$$SF_{\mathrm{MR}} = \frac{1}{L} \sum_{i=1}^{L} SF_{\mathrm{M},i} \tag{5.15}$$

$$\delta_{\mathrm{SF_{MR}}} = \max_{i=1}^{L} (\delta_{\mathrm{SF_{M,i}}}) \tag{5.16}$$

The scale factor $SF_{\mathrm{M},i}$ can be used as scale factor when the uncertainty component $\delta_{\mathrm{B_0}}$ is included in the determined expanded uncertainty, see equation 5.18. The figure 5.4 shows an example for the determined scale factors and uncertainties. The uncertainty of the nonlinearity $\delta_{\mathrm{B,0}}$ of scale factor is given with the following equation:

$$\delta_{\mathrm{B,0}} = \frac{1}{\sqrt{3}} \max_{i=1}^{L} \left| \left(\frac{SF_{\mathrm{M},i}}{SF_{\mathrm{MR}}} - 1 \right) \right| \tag{5.17}$$

The uncertainty $\delta_{\mathrm{B,1}}$ is a component to calculate when a calibration in the whole measurement range of a device under test is impossible. The detailed description is given in IEC 60060-2 [147], which is not used in the analysis and measurements here.

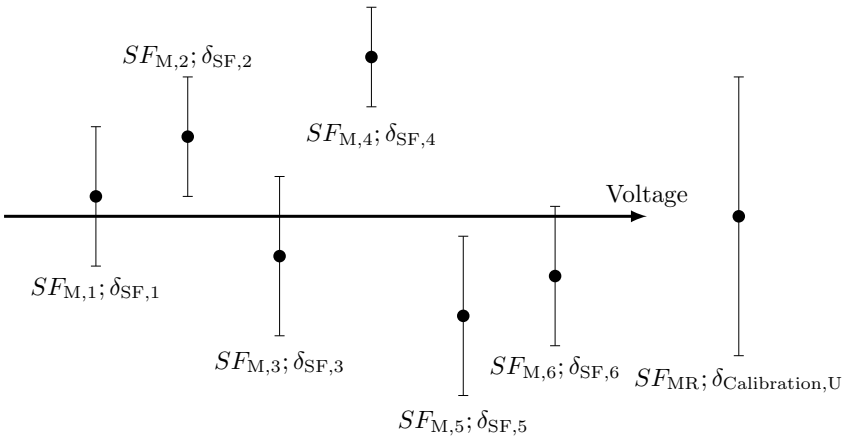

$$\delta_{\text{Calibration,U}} = 2 \cdot \sqrt{\delta^2_{\text{SF}_\text{M}} + \delta^2_{\text{B,0}}} \quad \text{with:}$$

$$\delta_{\text{B}_0} = \frac{1}{\sqrt{3}} \max_{i=1}^{6} \left| \left(\frac{SF_{\text{M},i}}{SF_{\text{MR}}} - 1 \right) \right| = \frac{1}{\sqrt{3}} \left| \left(\frac{SF_{\text{M},3}}{SF_{\text{MR}}} - 1 \right) \right|$$

$$\delta_{\text{SF}_\text{M}} = \max_{i=1}^{6} (\delta_{\text{SF},i}) = \delta_{\text{SF},5}$$

Fig. 5.4: Calibration over a Defined Measurement Range

Dynamic behaviour ($\delta_{\text{B,2}}$) A further important step for the calibration of a measuring device is their dynamic behaviour. The measurement device is expected to have different transfer behaviour at different frequencies. The step response is often used to get the frequency behaviour of the measurement device under test. The used calibration signal is a step voltage and the results represent the dynamic behaviour.

Short- and Long-Term Stability ($\delta_{\text{B,3}}$ & $\delta_{\text{B,4}}$) The short-term behaviour is used to characterise the properties of measuring device in continuous operation. In principle, the measuring device is applied with the maximum voltage for several hours. Afterwards, the scale factor is measured at the voltage maximum or minimum. These measurements also include the self-heating.

The long-term characteristic of a measuring device is to ensure the stability of the scale factor over a long operating time. The scale factor is measured after a defined time, usually one year. However, there are deviations of 1 % possible as the measuring conditions are never identical and random errors cannot be avoided.

Temperature Effect ($\delta_{\text{B,5}}$) A further influence on the scale factor is the temperature. It is possible to use a factor for the temperature compensation. The factor is related to the calibration temperature.

Proximity effects ($\delta_{\mathrm{B},6}$) The influence on the scale factor of measuring devices by the distance to grounded walls or to live parts is characterised by the proximity effect. Leakage currents occur, which flow to grounded parts due to stray capacitances and are not detectable at the measurement output.

Software-Effekt ($\delta_{\mathrm{B},7}$) Various software tools are used to process the recorded measurement data. It can be expected that depending on the software, the effects on the result may differ. This should be included in the protocol when a selection is carried out.

Uncertainty of the calibration The extended uncertainty of the calibration is defined from the previously considered uncertainty sources $\delta_{\mathrm{B},i}$. The individual uncertainties can be determined by several measurements (Type A) or given characteristic values of an used measurement device (Type B), e.g. given in a calibration protocol. The measurement uncertainty of the reference measurement δ_{Ref} system is included and is determined by the following calculation. For a coverage probability of 95.45 %, according the Gaussian distribution, the value $k = 2$ is chosen.

$$\delta_{\mathrm{Calibration}} = k \cdot \sqrt{\delta_{\mathrm{Ref}}^2 + \delta_{\mathrm{SF_M}}^2 + \sum_{i=0}^{N} \delta_{\mathrm{B},i}^2} \tag{5.18}$$

The described uncertainty is important to characterise a measurement device. The figure 5.4 shows the uncertainty factors $\delta_{\mathrm{B},0}$ and $\delta_{\mathrm{SF_M}}$ used for measurement characterisation in the next section 5.1.3. The principle of a scale factor SF_{MR} determination in a defined measurement range is described. Measurements of the transfer behaviour are examined for some typically used measurement devices in the medium voltage range.

5.1.3 Investigations on Transfer Behaviour of Voltage Measurement Devices

The characterisation of a voltage transformer and typical resistive capacitive dividers, dimensioned for the medium voltage range, are realised with a step voltage. The principle of calibration over a defined frequency range using a step signal is described in a research report [161]. The research report is dealing with current measurement devices, but the principle of calibration can also used for voltage measurement devices. The detailed procedure is also used in this work to characterise the frequency behaviour of current measurement devices, see in section 5.2.2. The impulse signal method is an alternative to the commonly used sinusoidal methods [161]. It is a procedure based on step response measurement of the device under test. A FFT is used to investigate the frequency behaviour of the devices, due to a scale factor determination for several frequencies. The measurement setup for the determination of the frequency behaviour is shown in figure 9.2 in the appendix 9.3.

The figure 5.5 shows the step voltage used for the analysis of the transfer behaviour of the measurement devices. The reference divider shows a frequent high oscillation in the

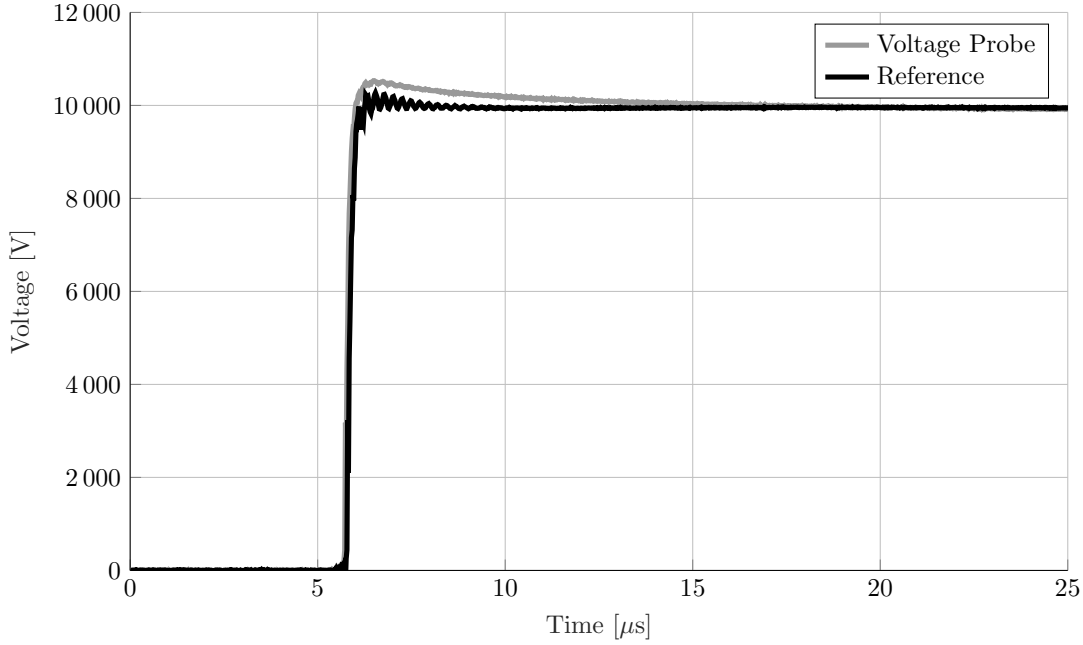

Fig. 5.5: Step Response of Voltage Probe

rising edge, which can be a result of the inductance and capacity of the measurement setup. The oscillation is an effect of travelling waves which is commonly reduced with a damping resistor. The measured signal by the voltage probe shows a deviation to the reference in the rising edge. It is a known effect of voltage probes which is usually minimised by compensation possibilities. If the voltage probe is used with the same recording device for measurements, compensation is only necessary once. If the measurement setup changes, a new compensation is required. The frequency behaviour of the individual measurement devices from DC up to 20 kHz is shown in figure 5.6. The scale factor and deviation in phase of a Voltage Transformer (VT), Resistive Capacitive Divider (RC), Voltage Probe Compensated (VP Comp) and Voltage Probe (VP) are shown. The scale factor of the voltage transformer is expectably changing with deviation to the rated frequency. The same frequency behaviour of voltage transformers is explained in the article [45]. The voltage transformers are suitable for the operation with their rated frequency. It is possible to use a determined scale factor, which can be different for a defined frequency range. These individual scale factor can be used for the variously measured harmonics, which means the use of a FFT with similar programming effort. Of course, a calibration of the application would be necessary.

The determination of the transfer behaviour in the voltage range from 0 V to 20 kV is carried out in this work despite the reference permits a higher rated voltage. The procedure for comparing the scale factor in the entire fixed measuring range of the device under test is sufficient. In the investigations, a maximum voltage of 20 kV is used, with individual measurements at 4 kV, 8 kV, 12 kV and 16 kV. From the individual scale factors at different voltage levels, an overall scale factor SF_{MR} can be calculated, see equation 5.15. The total standard uncertainty $\delta_{\mathrm{SF_M}}$ results from the largest value of the individual standard uncertainties of Type A. The significant magnitude for the influence of nonlinearity in the scale factor SF_{MR} can be described by the standard

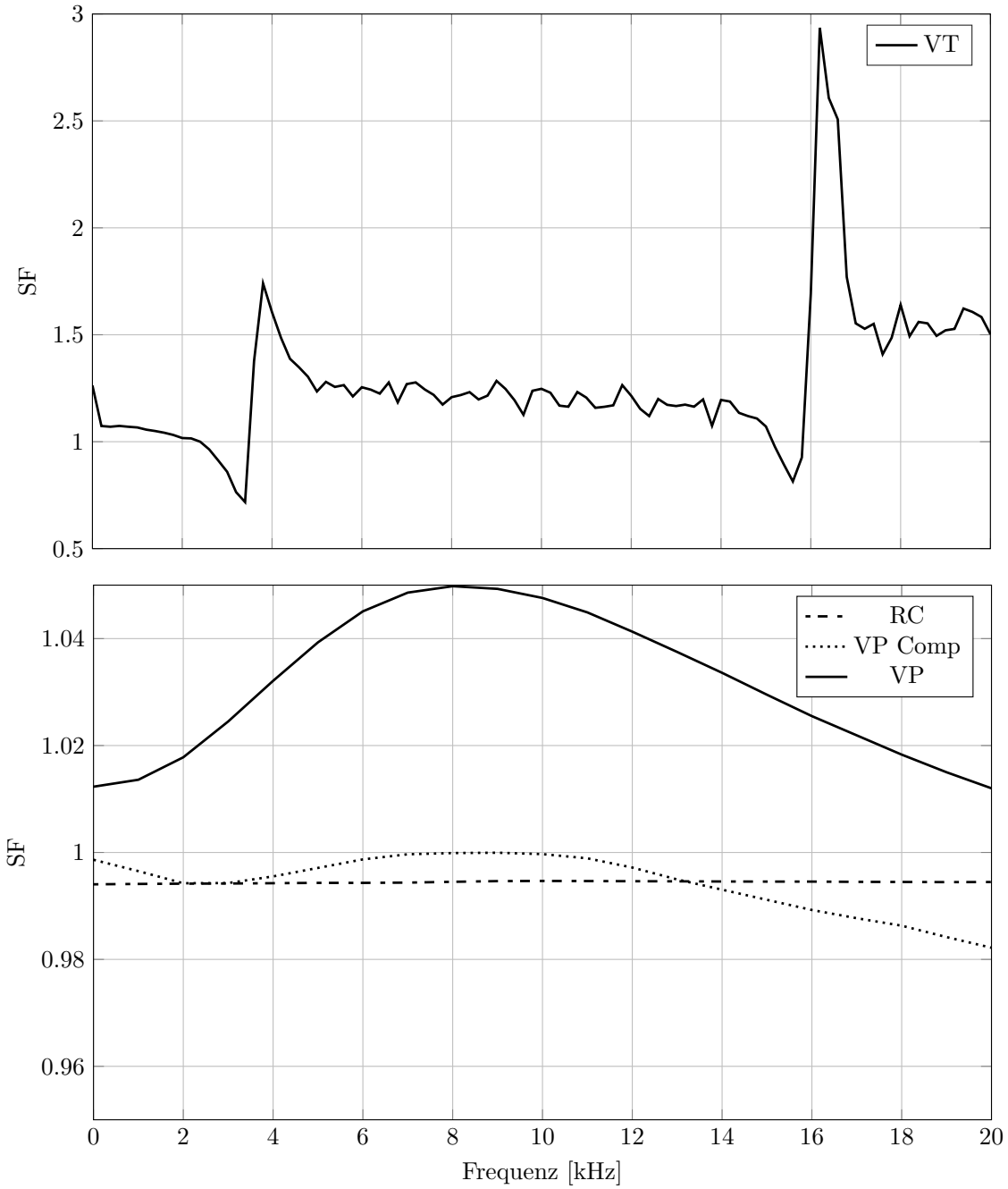

Fig. 5.6: Scale Factor Determination of Voltage Measurement Devices: Voltage Transformer (VT), Resistive Capacitive Divider (RC), Voltage Probe Compensated (VP Comp) and Voltage Probe (VP)

uncertainty of Type B according to equation 5.17. The uncertainties are not focused due to the scale factor in a frequency range is of interest.

The RC-Divider shows an insignificant deviation of the scale factor in the illustrated frequency range. In general, the linear behaviour with the frequency approves the usability as reference dividers.

The deviation with the frequencies is shown by the voltage probes, whereby the compensated probe shows minor influences. A significant phase deviation in phase of the voltage probes is shown in figure 5.7. The phase deviation has essential influence on the active power determination, which is shown in chapter 6.4. The scale factor over the measuring range, see $\delta_{B,0}$ in section 5.1.2, is not focused on the measurements. However, the deviation of the scale factor over the frequency range can be expected as independent of the voltage amplitude to measure. The phase deviation of the voltage transformer is not shown, which is too high for the shown range in figure 5.7.

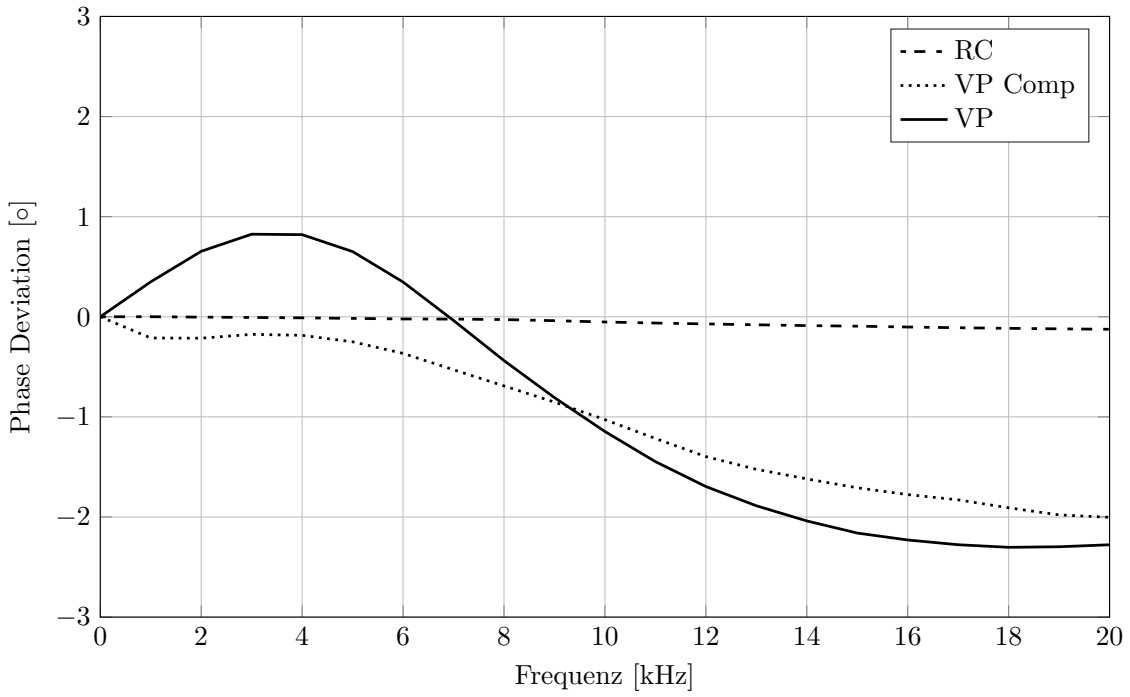

Fig. 5.7: Phase Deviation of Voltage Measurement Devices: Resistive Capacitive Divider (RC), Voltage Probe Compensated (VP Comp) and Voltage Probe (VP)

The scale factor determination of the investigated measurement devices has an uncertainty $\delta_{\text{Calibration}}$ of less than 1 % for each frequency in the considered range from DC to 20 kHz. However if only one scale factor should be given for the entire frequency range, which is usually expected for measurement devices, the deviations of the scale factors have to be added to the uncertainty $\delta_{\text{Calibration}}$. This fact would lead to an uncertainty

higher than 1 % for the voltage probes and the voltage transformer, which can be seen in figure 5.6.

5.1.4 Transfer Behaviour of Voltage Measurement Devices

The frequency ranges of the typically used voltage measurement devices for medium or high voltage are shown in figure 5.8. The figures show a rough overview of the usable frequency range, which is based on the information of the IEC 61869-103 [162] and additional results of the studies examined in this section. The overview takes not the main features of the measurement devices in the account, such as size, material, technical design of the active part or the sensor, temperature and voltage coefficients. However, the figure gives an overview, due to the fact the limit values depend on a variety of parameters, within the same technology of measurement device. These cases are marked as an arrow line without a block. The dividers have the largest frequency range and

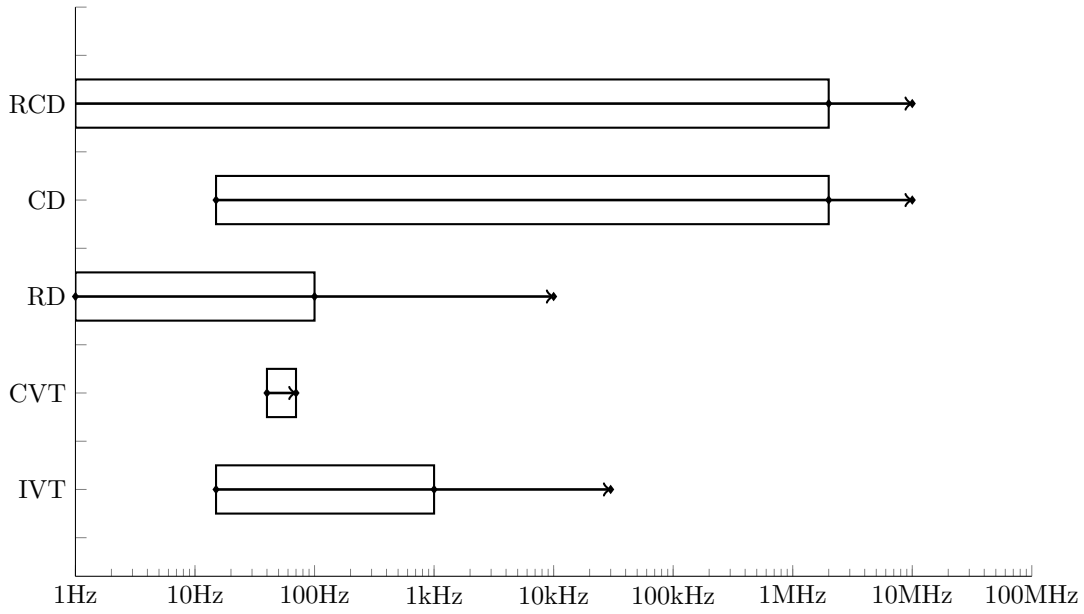

Fig. 5.8: Voltage Measurement Devices - Frequency Range: Resistive Capacitive Divider (RCD), Capacitive Divider (CD), Resistive Divider(RD), Capacitive Voltage Transformer (CVT) and Inductive Voltage Transformer (IVT)

the voltage transformers the smallest. The frequency behaviour of inductive voltage transformers is especially influenced by the design and the selected burden. In general, with the increasing voltage, the maximum frequency range of voltage transformers becomes smaller, see also in the standard IEC 61869-103 [162]. If the voltage is increased, the isolation capability must be enhanced. The whole construction becomes larger, which results in larger stray capacitances tending the whole construction to oscillations.

Additional larger inductances result from the higher number of windings, which reduce the frequency range of the voltage transformers. The limits of evaluable frequencies for medium voltage transformers are about single-digit kHz, which was visible in the scale factor determination see figure 5.6.[1] The capacitive voltage transformer has a small range in which a measurement is still applicable. The dimensioning is the reason for the characteristic of these transformers. The capacitive voltage transformers are dimensioned for a rated operating frequency. Using them for other frequencies can result in resonances and deviations [38].

In principle, the resistive capacitive dividers are the best voltage measurement device as they can measure dc voltages and voltages up to some megahertz, dependent on their fulfilment of the compensation condition, see equation 5.2. Especially the analysed voltage probes have shown with an uncertainty of 1 % the importance of a correct compensation condition.

5.1.5 Comparison of Voltage Measurement Devices

The classification in this section is based on the articles [163, 164] and with additional results of the investigations in this work. In the article [163] a figure with the transfer behaviour and accuracy comparison of voltage transformers or dividers are shown. The comparison of the devices is made with different properties derived for the conditions of a converter operated medium voltage motor.

- The device has a linear scale factor in the expected frequency range. Thus the information of the transient performance is given. The important criteria for medium voltage drives with converters are the frequency range from DC to 20 kHz, see section 4.3.

- The uncertainty is given with the maximum value for 50 Hz and the whole frequency range. The device with the lowest uncertainty for 50 Hz and the higher harmonics have the best usability.

- The weight and size of the measurement device are important for transportability and handling. The voltage transformers have a larger weight due to the amount of copper used for the device compared to the voltage dividers. The dividers can reach a larger height than the voltage transformers, but the newest dividers are constructed in compact systems [165]

- The Electromagnetic Compatibility (EMC) describes the influence due to the environment or influences trough parallel current carrying lines. A shielded construction is withstanding against electromagnetic influences.

- The Ferro Resonances with system or itself are known from switching processes in the grid.

[1] The limit for high voltage transformers is significantly lower compared to medium voltage transformers.

- The galvanic isolation and a possible short circuit secondary are a condition for the protection of the measuring or recoding device which operate with low voltage. Necessary realised with the signal conditioning of DAQ or power measurement device at low voltage side. Transmission systems based on an optical interface can be used to realise galvanic isolation. However, optical transmission systems can reduce the operating frequency range and induces additional uncertainty [54].
- The Electrical Analysis Unit criteria qualify the effort of conditioning the secondary voltage of the measurement device to a low signal level of an ADC.

The above named properties are evaluated with the following gradings:

- Excellent ++
- Satisfactory +
- Poor -
- unsatisfactory - -

Tab. 5.1: Comparison of Voltage Measurement Devices

Properties	Dividers			Transformers	
	Resistive	Capacitive	(Damped) Resistive Capacitive	Inductive	Capacitive
Frequency Range	-	-	++	-	- -
	DC-100 Hz	15 Hz - 2 MHz	DC - 2 MHz	15 Hz - 1 kHz	50 Hz
Uncertainty 50 Hz/> 50 Hz	++/-	++/-	++/++	++/-	++/- -
Weight & Size	+	+	++	- -	- -
Electrical Analysis Unit	+	+	+	+	+
EMC	+	+	+	++	++
Ferro Resonances	++	+	++	- -	- -
Galvanic Isolation	-	-	-	++	++
Sum	7 + & 3 -	6 + & 3 -	12 + & 1 -	7 + & 6 -	7 + & 8 -

5.2 Current Measurement

The measurement of currents in the kA range increases requirements for a measurement system and its devices. The reduction of the high currents to a value suitable for an ADC and a galvanic isolation are the main tasks. The measured value should not differ from the real value and a reproducibility is expected. The sufficient transfer characteristic of the measuring device is essential for the suitability of medium voltage drive applications. These characteristics have to be taken into account including the proven measurement uncertainty given in a calibration protocol according to the standard IEC 60060-2 [147].

5.2.1 Current Measurement Devices

An overview of the usually used current measurement devices in high voltage and medium voltage applications is shown in figure 5.9 and listed below.

a) Shunt

b) Inductive Current Transformer

c) Rogowski Coil

d) Hall Sensor

e) Zero-Flux Transformer

The use of the different devices has advantages and disadvantages. An important decision criterion for their selection is the potential separation between the current conductor and the digital measurement device. Current measuring systems are subjected to electrical and magnetic fields, which can lead to interferences in the measuring signal. Depending on the design of the measurement devices and the arrangement of the measuring circuit, the effect of disturbances can be eliminated.

Other Sensors: A Rogowski coil reduced to a single winding is a suitable device for measuring fast-changing magnetic fields in a defined environment, which is known as a magnetic field sensor. These are usually installed in gas-insulated switchgear and pulse generators with high power[152]. The field sensors principle are not considered further due to their lack of experience in uncertainty stability and their use for non-permanent installation [166].

Magneto-Optical Sensors The magneto-optical sensors or Fiber-Optic Current Sensor (FOCS), which using the Faraday effect, are a known principle to measure the currents in high voltage applications. A magnetic field induces in a transparent material the rotation of the polarization plane of a linearly polarized light wave. The magneto-optical principle is similar to the electrooptic effect in section 5.1.1. Examples of optical current measurement devices and their functionality are shown in [167–170]. The systems are usable for grid applications with a vibration immunity sensing loop. They

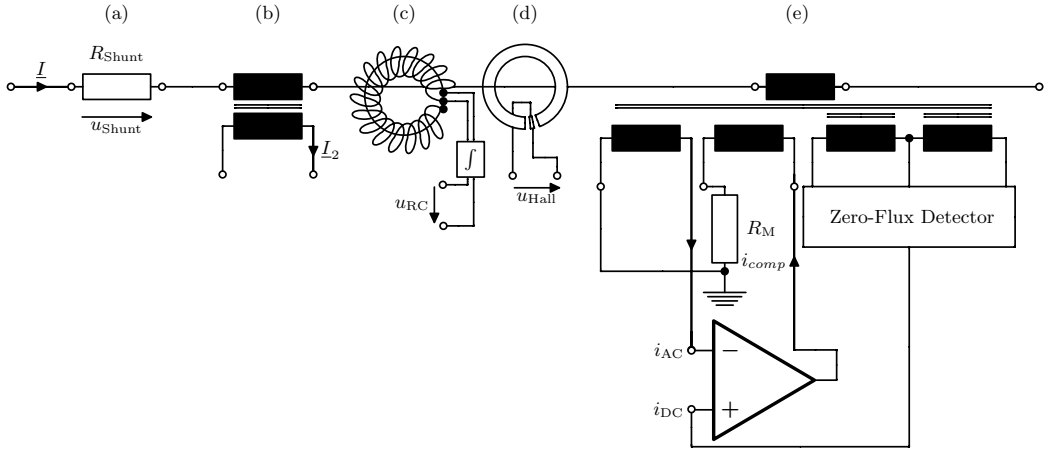

Fig. 5.9: Current Measurement Devices

have high sensitivity, considerable wide dynamic range and resistance to electromagnetic interference [149, 167]. Due to the possibility of DC measurability the systems are interesting for High Voltage Direct Current (HVDC) transmissions.

The FOCS are not investigated on their transfer behaviour in this work due to they are used and designed for high voltage applications. They are considered in the comparison of the measurement devices 5.2.4 due to the principle of measurement can also be applicable in the medium voltage range.

Shunts Measuring resistors with a low resistance are used for measuring impulse currents. They are included in the current path of the circuit, see figure 5.9(a). The resistor should provide very low inductance to have a proportional relation to the measured current.

$$u_{\text{Shunt}} = R_{\text{Shunt}} \cdot i \tag{5.19}$$

The shunt should have a resistive characteristic over the frequency range to be measured, which means a linear scale factor in the measuring range. Further, the rate of electrical power is low due to the low resistance, which is usually between 50 mΩ and 50 µΩ [152]. The main reason for the inappropriate use of shunts for the power measurement is the self-heating. Especially for a high current measurement, the heat dissipation is the limiting factor for a scale factor deviation. The permitted limiting load integral is usually given for an impulse measurement shunts, which defines the range of load the shunt is reversible. The withstand against the influence on the output voltage of a shunt due to interference voltages, and undesirable ground loops is a further reason for the unsuitability. However, applications for a precise high current measurement with shunts is shown in[171], but a phase deviation can be expected for a three phase power measurement due to a separated used ADCs.

The coaxial measuring shunts are used as the reference for the calibration of impulse current measurement devices. They are constructed with low inductance and not influenced by the magnetic field of the current to measure. They are used in section 5.2.2 for the determination of the transfer behaviour of current measurement devices.

Rogowski Coils The Rogowski coil is a toroidal coil without a magnetic core, see figure 5.9(c). It is used for the measurement of alternating and impulse currents, because of its wide bandwidth. Depending on the design low currents with a rise time in the nanosecond range or high currents with typical grid frequency can be measured. They are usually designed ring-shaped and flexible with a possibility to open. It allows a fast placing around the conductor. If the closing mechanism is designed precise, the reproducibility of current measurements is better than 0.1 %.

The measurement uncertainty of the coils is dependent on the position [172]. For reproducible measurements especially with flexible Rogowski coils a centric position of the current conductor is recommended. Proper positioning of primary conductor should be defined by the manufacturer in the installation instructions [173].

The output voltage of a Rogowski coil has to be integrated to determine the desired time curve of the current. For this purpose passive or electronic integrative circuits or numerical integration methods are used, which contribute measuring uncertainty in addition to the Rogowski coil. Numerical integration methods are also possible with the corresponding effort.

A further development is very broadband current measuring coils with iron or ferrite core[174], known as pearson current transformer. They are not focused due to the minimum reachable uncertainty of 1 %.

Printed Circuit Boards (PCB) designs of Rogowski coils are further constructed and used in current measurement applications. The reproducibility of this designs is commonly maximum 1 %. The flexible low-frequency Rogowski coils of Power Electronic Measurements (PEM) device is used in section 5.2.4, which is designed for the measurement of currents with low frequency.

Inductive Current Transformers The inductive current transformers are used for the reducing of high currents to a measurable value of usually 5 A or 1 A, see figure 5.9(b). The scale factor between primary current and secondary current is described by the number of turns ratio between both windings.

$$SF_{\mathrm{CT}} = \frac{i_2}{i_1} = \frac{w_1}{w_2} \tag{5.20}$$

The secondary current is proportional to the primary current when ideal conditions are given. The equivalent circuit model of a current transformer is identical to the voltage transformer, see figure 5.2. The difference is the load on the secondary side, which defines the operation of the transformer form and ratio $w_2 > w_1$. The burden has a low impedance when a current is to measure. Ideal is a value of $Z_{\mathrm{B}} \to 0$ [157]. Estimating a winding ratio of one the equivalent circuit has a voltage drop on R_2, $L_{2\sigma}$ and Z_{B}, which leads to a flux in the iron core and a magnetisation current $\underline{I}_{12} + \underline{I}_{FE}$. This current is not flowing through the burden and represents the error of the current transformer. If the operating point of the current transformer is in the linear range of the hysteresis characteristic, the error will be small, if the transformer is saturated, the error increases. The current deviation is shown in the vector diagram in figure 5.10, which is valid for a stationary condition for one frequency. Further, errors due to external magnetic or

scatter fields is possible. However, the dimensioned current transformer for an operating frequency leads to deviations for the measurement of harmonic frequencies. There are investigations in hysteresis and eddy currents compensation in current transformers[61], which is realised with effort in the digital signal elaboration and detailed information about the used current transformer.

$$\delta_{\mathrm{ICT}} = \frac{\underline{I}_2 - \underline{I}_1^{'}}{\underline{I}_1^{'}} \tag{5.21}$$

$$\delta_{\varphi\mathrm{CT}} = \mid \varphi_{\mathrm{I}_2} - \varphi_{\mathrm{I}_1'} \mid \tag{5.22}$$

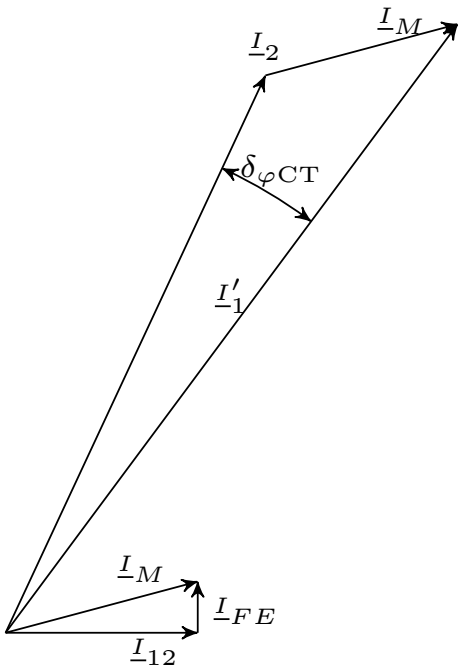

Fig. 5.10: Vector Diagram of Current Transformer

According to these factors, inductive current transformers are classified into accuracy classes. These accuracy classes are defined in the standard IEC 61869-2 [175] dependent on the rated burden and a defined rated current range. An accuracy class of 0.2 defines a maximum deviation of 0.2 % and a limit of maximum 10 minutes phase deviation. The 10 minutes deviation corresponds to 0.167°, which is valid for a rated frequency of 50 Hz. With increasing frequency, the deviation is rising, too. The burden impedance can influence the accuracy of the current transformer[158]. The power factor of the burden must be as high as possible, which means the impedance does not increase with

the frequency and a resulting increase of the magnetisation current is avoided. As far as possible, it is advisable to short-circuit the output of the current transformer and to measure the output current with a precise current measuring clamp [162]. An inductive current transformer is used for the transfer behaviour determination in section 5.2.2.

Current Transducer with Hall Sensor Current transducer using the hall effect, which is based on the moving of charge carriers in the magnetic field due to the Lorentz force. The Hall plate in the air gap of the iron core generates a voltage which is proportional to the current flowing through the conductor, see figure 5.9(d). The fundamental principle of a current sensor based on the Hall effect is explained in more detail in [152, 176]. These current transducers can measure direct, alternating and impulse currents up to 20 kA with a bandwidth up to 25 kHz. The measurement uncertainties can achieve several percents, which makes them suitable and necessary for the control of electrical converter drives.

Higher demands can be satisfied with an implemented compensation winding to the magnetic core, which is known as the zero-flux principle. The zero-flux principle ensures a measurement uncertainty of rated 0.1 % and bandwidths up to 200 kHz are achieved. Only the Zero-Flux Transformer with an electronic Zero-Flux Detector have a higher performance in bandwidth and uncertainty, see in the next paragraph.

Current clamps are well known as current measurement devices using these principles, easy handling and predestinated for measurement outside of the laboratories or start-up of new drive applications.

This current measurement principle is not used for the transfer behaviour determination but included in the comparison of the current measurement devices in section 5.2.4.

Zero-Flux Transformers The zero-flux transformer can measure alternating, impulse and direct currents, figure 5.9(e). They are based on the principle of the current transformer with additional auxiliary windings for compensation purpose. An electronic module with a zero-flux detector measures the DC component and the measured AC signal is given to an operational amplifier, which is connected to the compensation winding. The compensation winding and the supplied current, which is a scaled model of the primary current, causes a flux to reach zero flux in the iron core. The compensation principle is already known from the hall sensor based current transducer, but with an accurate DC current detection. The advantage of the zero-flux is the resolution, which has a relative uncertainty of a few parts per million [176]. Depending on the design of the electronic Zero-Flux Detector, bandwidths from DC up to 500 kHz with a maximum current of 5 kA. The bandwidth of 10 kHz can be reached with maximum 25 kA. This current transformer is particularly suitable for the precise calibration of other current measuring systems [152].

This current measurement principle is not used for the transfer behaviour determination but included in the comparison of the current measurement devices in section 5.2.4 with specifications from data sheets. The zero-flux transformer is not usable for impulse current measurements.

5.2.2 Investigations on Transfer Behaviour of Current Transformers

The transfer behaviour of current transformers is analysed in several publications especially for the usability of grid applications[163, 164, 177, 178]. The impulse current method is used to analyse the transfer behaviour of current measurement devices, which was already applied and described using an impulse voltage in section 5.1.3. The transfer behaviour is analysed in this thesis by several measurements with an impulse current.

A rectangular impulse current is used to analyse the frequency range up to 200 Hz, and an exponential impulse current (8/20) is used for frequencies up to 20 kHz. The department of High-Voltage engineering at the TU Berlin has two installations, which can be used to generate these current forms. The transfer behaviour determination shows significant results for active power measurement in the low-frequency range. The

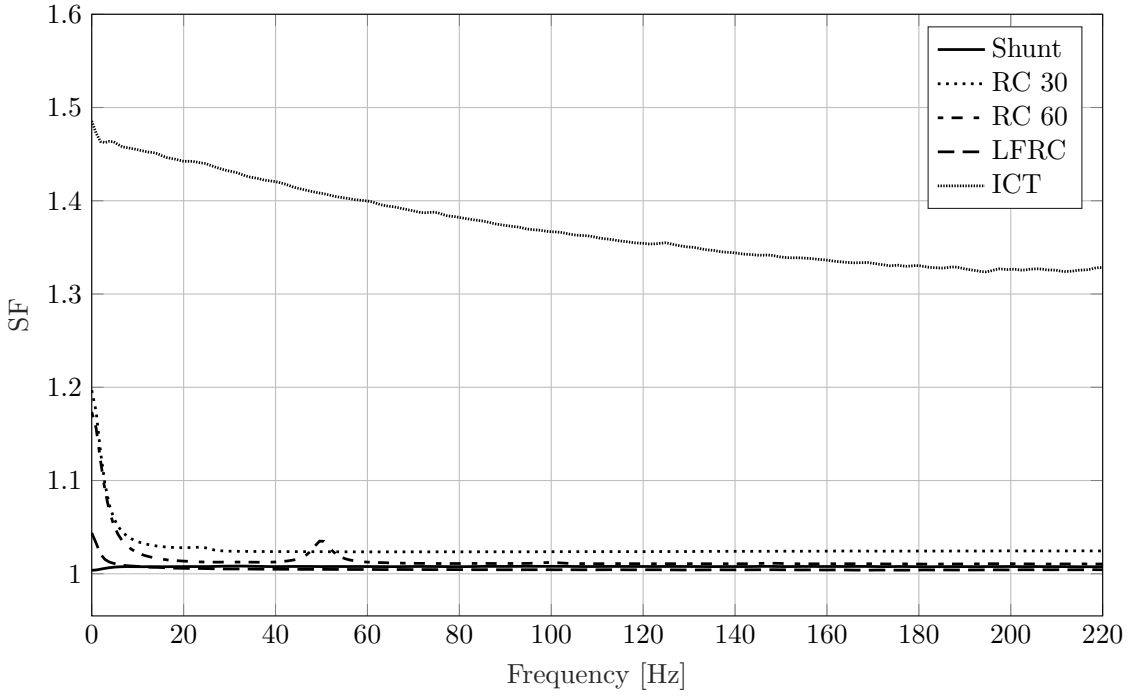

Fig. 5.11: Scale Factor Determination of Current Measurement Devices: Shunt, Rogowski Coil 30 (RC 30),Rogowski Coil 60 (RC 60), Low Frequency Rogowski Coil (LFRC), Inductive Current Transformer (ICT)

frequency behaviour of the individual measurement devices from DC up to 200 Hz is shown in figure 5.11. The scale factor of a Shunt, two Rogowski Coils (RC 30, RC 60), a Low-Frequency Rogowski Coil (LFRC) and a Current Transformer (CT) are shown. The scale factor of the current transformer shows a deviation to the others measurement devices, which is reasoned by the selected burden. The dependence of the burden on

the current transformers is also shown in [158] and is visible in the measurements. The scale factor of the current transformer is changing with the frequency, which makes them only usable for a defined frequency range. However with an error in accuracy due to the non-linear scale factor. The shunt shows a linear scale factor in the frequency range, which is a characteristic behaviour of low inductive impulse measurement shunt. They are used as the reference to the other analysed measurement devices.

The scale factor of the Rogowski Coils has deviations for DC and the low frequencies, which is a known characteristic of the coils. The low-frequency Rogowski coil, which is designed with better performance for low current measurements, shows fewer deviations in the scale factor than the other coils. The Rogowski Coil RC 60 shows a small deviation in the scale factor for 50 Hz, which can be reasoned by a coupling of current carrying parts of the measurement setup.

The phase deviations in figure 5.12 show a typical characteristic of the current transformers, which makes them unsuitable for a harmonic active power measurement. The deviation is increasing the frequency height. The phase deviation of Rogowski coils shows the same behaviour as for the determined scale factor in the low-frequency range next to DC. The shunt has an expected linear phase behaviour for all analysed frequencies. The deviations of 1° for 50 Hz makes the Rogowski Coils unsuitable for a precise active power measurement. The deviation of the current transformer can be compensated with the selection of a correct burden. However, a deviation besides the frequencies of 50 Hz can be expected. The phase deviation has essential influence on the active power determination, which is shown in chapter 6.4.

The scale factor determination of the investigated measurement devices has an uncertainty $\delta_{\text{Calibration}}$ of less than 1 % for each frequency in the considered range from DC to 200 Hz. However if only one scale factor should be given for the entire frequency range, which is usually expected for measurement devices, the deviations of the scale factors have to be added to the uncertainty $\delta_{\text{Calibration}}$. This fact would lead to an uncertainty higher than 1 % for the Rogowski Coils and the current transformer, which can be seen in figure 5.11. Further, the Rogowski Coil RC 60 has a higher uncertainty $\delta_{\text{Calibration}} > 1\,\%$ for 50 Hz due to the coupling of current carrying parts of the measurement setup, as already named before.

5.2.3 Transfer Behaviour of Current Transformers

The frequency ranges of the typical used current measurement devices for medium or high voltage are shown in figure 5.13. The figures show a rough overview of the usable frequency range, which based on the information of the IEC 61869-103 [162] and additional information of the investigations described in this section. Especially the low-frequency Rogowski coil of Power Electronic Measurement is a new invention in reducing the above shown scale factor and phase deviations. The figure does not take into account the main features of the measurement devices, such as size, material, technical design of the active part or the sensor, temperature and voltage coefficients. However, the figure gives an overview, due to the fact the limit values depend on a variety of parameters, within the same technology of measurement device. The specification dependent technologies are marked as an arrow line without a block.

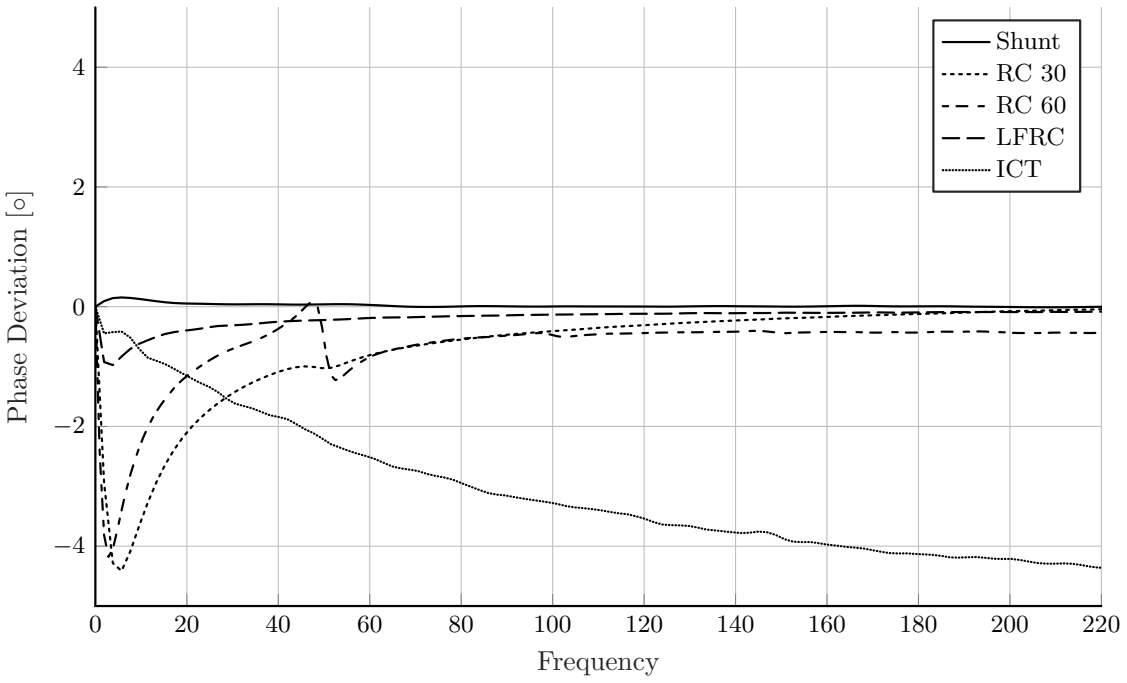

Fig. 5.12: Phase Deviation of Current Measurement Devices: Shunt, Rogowski Coil 30 (RC 30),Rogowski Coil 60 (RC 60), Low Frequency Rogowski Coil (LFRC), Inductive Current Transformer (ICT)

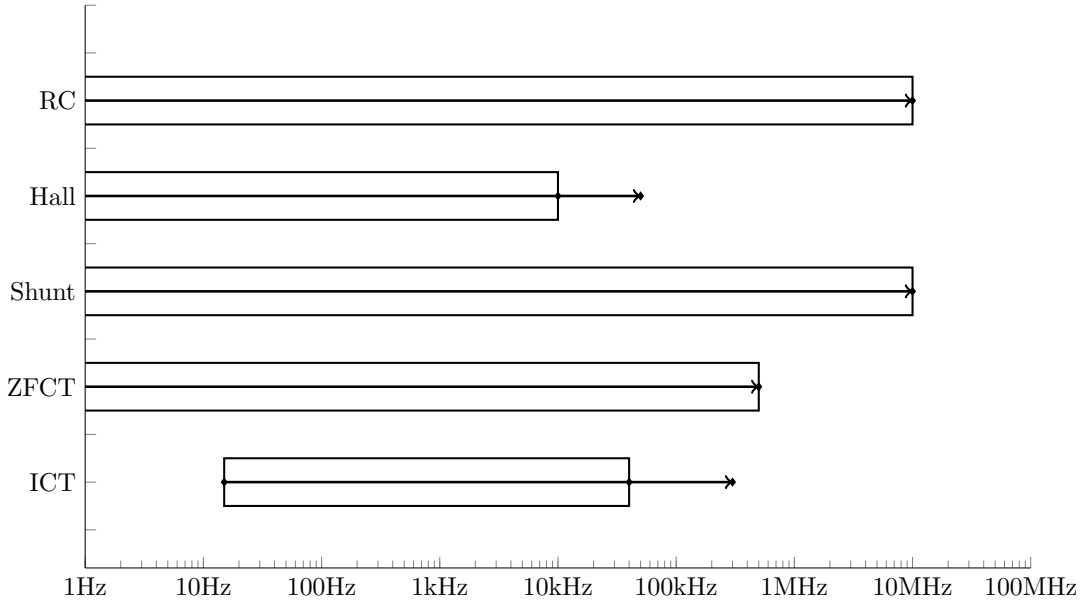

Fig. 5.13: Current Measurement Devices - Frequency Range: Rogowski Coil (RC), Hall Sensors (Hall), Measurement Resistor (Shunt), Zero-Flux Current Transformer (ZFCT) and Inductive Current Transformer (ICT)

The Rogowski coil and the shunt cover the largest frequency range, but for shunts only small currents are measurable with high frequencies. The frequency limit of an inductive current transformer is from 15 Hz to one-digit kHz range, which is the smallest one of all current measurement devices. Dependent on the voltage level the current transformer increases in size and the frequency range decreases. The zero flux and hall sensor based current transformers also have a large frequency range and the possibility to measure high currents. These current transformers are well suitable for control purposes and power measurement of converter operated drives especial due to their low measurement uncertainty.

5.2.4 Comparison of Current Measurement Devices

The classification is based on the articles [162–164, 177, 179, 180] and complemented with results of the investigations in this work. The standard IEC 61869-103 has shown a comparison of current transformer transfer behaviour and accuracy used in the medium or high voltage range.

The comparison of the devices is made with different properties derived for the conditions to a converter operated medium voltage motor. The properties are the same as explained in section 5.1.5. However, the Electrical Analysis Unit for current measurement devices has a higher possibility to influence the current measurement result than the voltage measurement devices.

– The Electrical Analysis Unit criteria qualify the influence of the conditioning of the secondary output of the measurement device to a signal measurable for an ADC. An Electrical Analysis Unit means the required integration circuit for a Rogowski coil, which can be responsible for phase deviation. There are Rogowski coils designed for low frequencies, which is realised due to the integration circuit. The Hall Effect and Zero Flux transducers need a power supply and an electronic circuit for the flux compensation. These electronic circuits are usually increasing the performance of the current transformer principles.

The above named properties are evaluated with the following gradings:

- Excellent ++
- Satisfactory +
- Poor -
- unsatisfactory - -

The comparison in table 5.2 showed the Zero Flux transformer as the best current measurement device. However the Hall Effect transducer or Rogowski Coil are usable for a current and power measurement. It is possible to fix a Rogowski Coil centric around a motor cable to decrease the measurement uncertainty and thus a active power would be possible with sufficient chosen measurement time to get confident mean values.

Tab. 5.2: Comparison of Current Measurement Devices

Properties	Dividers		Transformers/Transducers			
	Rogowski Coil	Shunt	Inductive	Hall Effect	Zero Flux	Fiber-Optic
Frequency Range	+	++	- -	+	++	+
	0.5Hz-75MHz	DC-10MHz	15Hz-13kHz	DC-10kHz	DC-500kHz	DC-6kHz
Uncertainty 50 Hz/> 50 Hz	- -/- -	++/+	++/- -	++/-	++/++	++/+
Weight & Size	++	- -	- -	- -	- -	+
Electrical Analysis Unit	+	++	-	+	+	+
EMC	-	- -	++	++	++	++
Galvanic Isolation	++	- -	++	++	++	++
Sum	6 + & 5 -	7 + & 6 -	6 + & 7 -	8 + & 3 -	11 + & 2 -	12 + & 0 -

6 Measurements on Medium Voltage Drives

The chapter is written to summarise the results of several measurements with different test and measurement setups. The measurement setups have a typical structure of active power measurement systems for medium voltage drives, shown in figure 2.3. They are used for active power measurements on commonly used converter drives in the industry. The possibilities and individual aspects of power measurement with the use of additional current or voltage measurement devices are analysed and show the possibility to handle the transducer uncertainty for a medium voltage test bench design.

6.1 Test and Measurement Setups

The measurement setups are used for their comparison by the active power measurement with two different Test Setups. The detail information about the used machines is listed in the appendix 9.4.

Measurement Setup 1 (MS1) The measurement setup MS1 is a setup with current and voltage transformers, which are suitable for a measurement at 50 Hz. The Aron circuit is used to determine the active power, see figure 2.1. A Data Acquisition (DAQ) board with several ADCs is used for the sampling and quantisation with a sample rate of 20 kHz. The signals are conditioned by precision shunts and isolation amplifiers. The selected transformers are designed for a rated frequency of 50 Hz. Thus the MS1 is specified for measurements with sinusoidal signals up to 100 Hz. The 100 Hz is already measured with a small deviation, which is in the accuracy class of the transformers with 0.2 %. The MS1 is not able to measure DC components.

Measurement Setup 2 (MS2) The measurement setup MS2 consists of zero-flux current transformers and compensated voltage dividers. The respective signals of the three-phase system are recorded directly by a power meter. The voltage dividers and the zero-flux transformers are frequency-independent up to their specified maximum frequency. The voltage dividers can measure frequencies up to 300 kHz with the phase deviations of $\leq 2.5^\circ$ and the scale factor deviations of $\pm 2\,\%$. The Zero-Flux transformers have a small phase deviation and measurement uncertainty within the linear range of the transformer. The transformers have a bandwidth of DC to 80 kHz (-3 dB) with a measurement uncertainty of a few parts per million. The system measures the active power in all the three phases and can measure DC components, see figure 6.1. The power meter operates with a sampling rate of 1.21 MS/s.

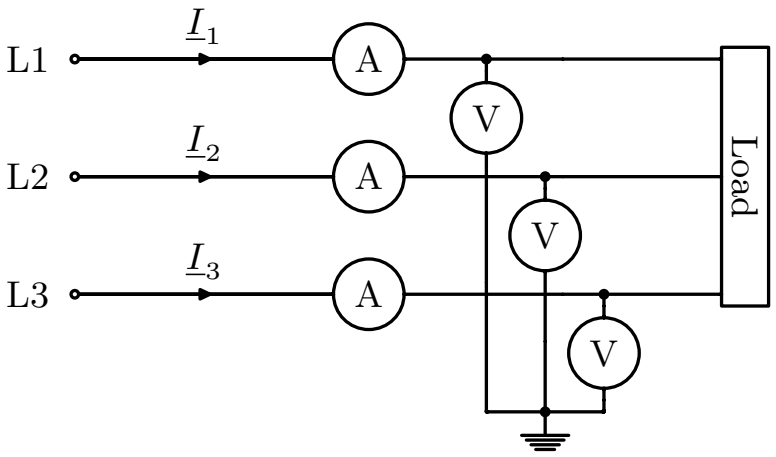

Fig. 6.1: Three Phase Power Measurement - Circuit

Test Setup 1 (TS1) The TS1 has a 3L-NPC-VSC converter [181], which is feeding an induction motor. This motor is mechanically coupled to a Load machine with less rated power than the induction motor. The load machine is used to test the induction motor at partial load. The voltage form is shown in figure 2.2.

Test Setup 2 (TS2) The TS2 has an M2C converter [107], which is a multilevel technology of converters with an almost sinusoidal output voltage used for medium voltage drives. The converter is feeding an induction motor. This motor was mechanically coupled via a torque sensor to a load. The load has the same rated power than the induction motor to apply full-load tests. The output voltage and current waveforms are shown in the appendix 9.4.1.

6.2 Comparison of Active Power Measurement Setups

The focus of this section is the comparison between typically used measurement systems for medium voltage drives. The results described in this section are based on measurements with the converter operated induction motor (TS1).

Measurement Circuit The active power measurement of a three phase drive with the Aron circuit[1] or the three-phase circuit[2] can be seen as identical if no harmonic active power of the third order and multiple is included. The three phase measurement has only the advantage of the possibility to measure DC components. The sum of all phase currents in a three phase system has to be zero, which is the condition for the

[1]The Aron circuit is also known as the Two Wattmeters Method
[2]The three-phase circuit also known as the Three Wattmeters Method

usability of the Aron circuit. The start point of motors is always not connected to the supplying inverter, which describes the equation 6.1.

$$0 = I_1 + I_2 + I_3 \tag{6.1}$$

The third harmonic or its multiple is in general not expectable, as they are compensating each other in a symmetrical three phase system. But in converter drive applications asymmetrical conditions can occur, and the condition in equation 6.1 is not fulfilled. The asymmetrical conditions can be arising with parasitic capacitances or unsymmetric converter supply voltage, which the DC currents in all three phases have shown in the section 6.3. Therefore the three phase active power measurements is recommended for motors supplied with converters, which was already shown for small drives[182].

The measurement uncertainty of the systems to compare was determined for two operation points with load and two without load. The four different operation points are shown in table 6.1. The operation point No-Load 2 is examined with reduced stator voltage, which is usually done in a No-Load test for the separation of windage losses[3] and iron losses. A warm-up of the machine under test is a precondition, which is done until an approximately constant operating temperature is reached. In general, the measurement is started with the first load point. The active power is measured with the MS1 and MS2, which record the values for several cycles.

A cycle is defined by the time an active power value P is calculated, which is a mean value of the power oscillation. Furthermore, the root mean square values of voltage U_{RMS} and current I_{RMS}, the phase angle φ, the base frequency f_0 and other computable values from the digital signals are determined. The cycle time of 0.4 s is chosen for both measurement systems. The cycle time corresponds exactly to 24 periods of the fundamental frequency of 60 Hz. Therefore the determined quantities are averaged over the number of periods in one cycle, which already reduces the variation of the determined quantity.

The MS2 records more than 1000 cycles during the recording in one operating point. The MS1 records more than 500 values in the same recording, which takes about 400 seconds. The lower number of cycles for the MS1 results from the slightly larger computation time of its measuring program.

The evaluation of the measurement uncertainty is already sufficient with 10 periods at 50 Hz for a measured value, where a statement on the probability distribution is possible. A standard deviation is determined from the measured values of P, which is described in GUM Type A. The method described according to GUM Type A is used for the measurement uncertainty evaluation of an input quantity, see section 3. The Type A evaluation was used to compare the measured output quantity with the theoretically calculated uncertainty Type B, see figure 6.8.

The determined standard deviation of the individual measured quantities are used to calculate a normal distribution to represent an ideal distribution around the mean value [126], like the grey curve in figure 6.2. Furthermore, the figure shows the probability of the occurring measured values. The measured values are sorted into 150 W ranges

[3] Includes friction losses

by the histogram display. A normal distribution of the measured values can be seen, which fits perfectly to the calculated. The equation for the normal distribution is given in equation 6.2, with the standard deviation σ and expected value μ.

$$f(x) = \frac{1}{\sqrt{2\pi} \cdot \sigma} \cdot e^{\left(\frac{1}{2} \cdot \left(\frac{x-\mu}{\sigma}\right)^2\right)} \tag{6.2}$$

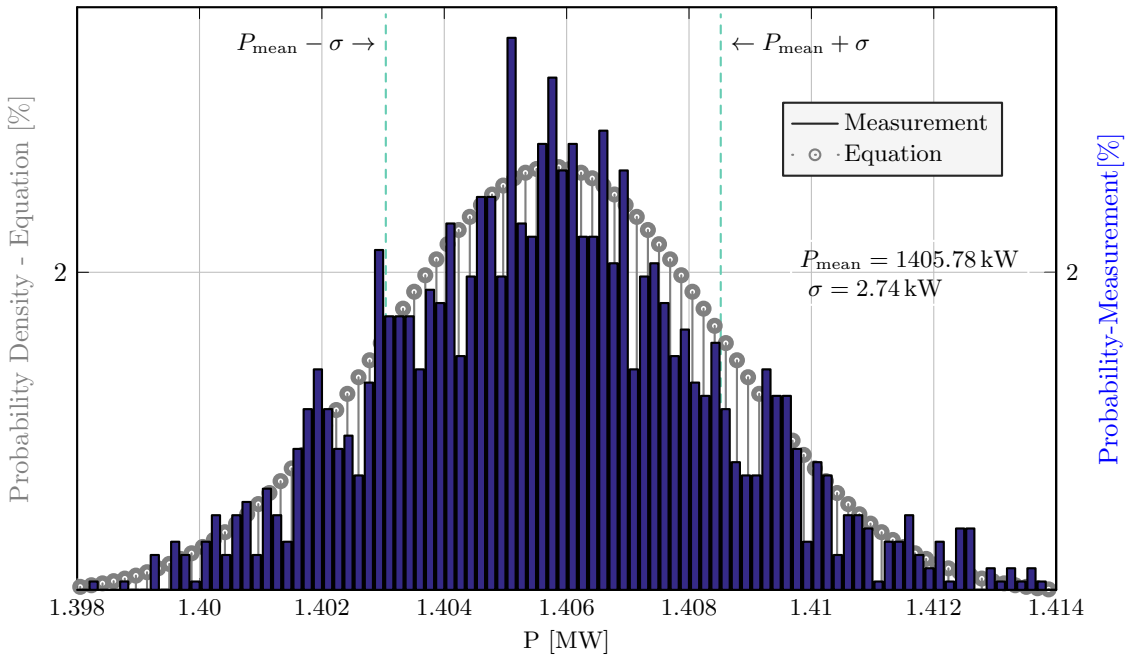

Fig. 6.2: Histogram MS1 - Load 1

The histogram shows the probability of the measured values of more than 1000 cycles. The ordinate axis gives the probability density of the measured values and the values determined by the equation 3.12 of the normal distribution in chapter 3.4. The measured values are with 76 % in the limit of plus/minus σ to P_{mean}.

Measurement Uncertainty and Deviation The comparison between the measurement system MS1 and MS2 is made with the determined standard deviations of the measurements. In the table 6.1 the results are given. The comparable quantities are the active power P and the extended measurement uncertainty $\delta_{95\%}$. The relative numbers are related to the corresponding measurement values. The measurement uncertainties of the MS1 are significant compared to MS2, which are larger than 1 % except the last operation point. The measurement uncertainty of the phase determination is the critical quantity, which contributes the main part to the MS1 total measurement uncertainty. Especially the low sampling rate is a bottleneck of the measurement system MS1. The analysis in section 6.4 indicates the fact of an increased phase angle error.

Tab. 6.1: Measurement Values and Uncertainty MS1 & MS2 with TS1

	MS1 P	MS1 $\delta_{95\%}$	MS2 P	MS2 $\delta_{95\%}$
Load 1	1390.6 kW	±15.6 kW (1.1 %)	1405.8 kW	±5.5 kW (0.4 %)
Load 2	776.8 kW	±16.2 kW (2.1 %)	784.5 kW	±3.5 kW (0.4 %)
No-Load 1	229.9 kW	±14.0 kW (5.8 %)	234.8 kW	±1.9 kW (0.8 %)
No-Load 2	222.1 kW	± 0.6 kW (0.3 %)	224.4 kW	±0.3 kW (0.1 %)

A further difference between the considered measurement systems is the deviation between both, which are shown in table 6.2.

Tab. 6.2: Deviation of the Mean Value MS1 and MS2 with TS1

	Absolute	in %
Load 1	15.2 kW	1.1
Load 2	7.7 kW	1.0
No-Load 1	4.9 kW	2.1
No-Load 2	2.3 kW	1

The relative quantities are referred to the measurement values of MS2. The significant difference is larger than 1 %, which is a result of the harmonic active power measurement. The figure 6.3 shows the harmonic components P_H with the order five, seven and eleven of the power oscillation. The sum of them is less than 1 %. In the table 6.3 active power components are given, which are determined for Load and No-Load.

Tab. 6.3: Harmonic Active Power MS2 with TS1

	P_{SUM}	P_1	P_{H}	$P_{\mathrm{H}}/P_{\mathrm{SUM}}$ [%]
Load 1	1405.8 kW	1388.97 kW	12.183 kW	0.865
No-Load 1	234.8 kW	233.17 kW	1.662 kW	0.71

Therefore the measurement system MS1 is not suitable for a harmonic active power measurement. A measurement deviation due to the used voltage and current transform-

ers can be a further uncertainty contribution of the MS1. The scale factor deviation of the measurement transformers increases for frequency ranges above 50 Hz, which is shown in section 5.2.2 and 5.1.3. However, the different scale factor in the considered frequency can be used in a recording device for a correct determination of the individual oscillations. This combination in a power measurement system would lead to more computations effort with the frequency components. An example of such a solution was given by Cataliotti [183] using a Rogowski Coil for a power measurement setup.

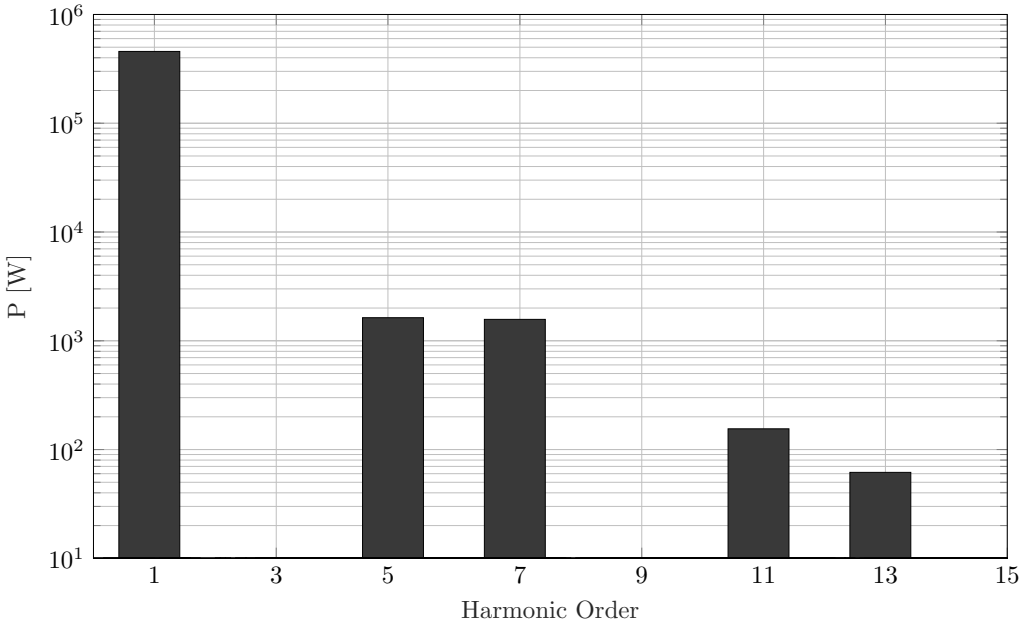

Fig. 6.3: Harmonic Active Power

The MS1 and MS2 are used for measurements with the TS2. The TS2 has no harmonic active power to measure due to the almost sinusoidal voltage form, see the appendix 9.4.1. However, it is possible to measure on TS2 a converter drive with 12 MW. The different operation points and measurement results are shown in the table 6.4.

The results for the measurement uncertainty of MS1 are higher than for the MS2. Due to the low sample rate of the MS1, which leads to a high phase angle error. The mean values have less deviation, which is listed in table 6.5.

The drive has no harmonic active power, and a deviation is given due to an offset between both measurement systems. The uncertainties reach values less than 0.1 %, which increases for the operation point with no load. The section 6.4 shows the influence of a phase angle error with a higher phase angle. The higher phase angle leads to a higher part of the total measurement uncertainty due to the phase angle error. The comparison of the TS2 measurement uncertainties between Type B and Typ A, as well the measurement uncertainty budgets, are shown in the appendix 9.4.1.

Tab. 6.4: Measurement Values and Uncertainty MS1 & MS2 with TS2

	MS1 P	MS1 $\delta_{95\%}$	MS2 P	MS2 $\delta_{95\%}$
Load 1	11 249.6 kW	±100.8 kW (0.9 %)	11 220.3 kW	±3.2 kW (0.03 %)
Load 2	9282.9 kW	±96.3 kW (1.0 %)	9252.4 kW	±2.7 kW (0.03 %)
Load 3	6215.6 kW	±43.1 kW (0.7 %)	6185.7 kW	±3.2 kW (0.05 %)
Load 4	3083.2 kW	± 97.7 kW (3.2 %)	3059.9 kW	±2.0 kW (0.06 %)
No-Load 1	203.9 kW	± 33.12 kW (16.2 %)	184.0 kW	±1.7 kW (0.90 %)

Tab. 6.5: Deviation of the Mean Value MS1 and MS2 with TS2

	Absolute	in %
Load 1	29.4 kW	0.3
Load 2	30.5 kW	0.3
Load 3	29.9 kW	0.5
Load 4	23.3 kW	0.8
No-Load 1	19.9 kW	10.8

6.3 Measurement of DC Components

The measurement system MS2 can measure DC components of the active power. Furthermore, the measuring circuit of the two systems are different and have to be taken into account. The Aron circuit is used by the MS1 and a three-phase circuit is used by the MS2. The latter one measures the phase voltages to the ground potential. The measurements of the phase voltage contain DC components.[4]

The measurement has shown the identical DC voltage values per cycle in all three phases, which means a shifting of the ground potential. DC components of the current have been measured in the phases of the machine, which can influence the determined active power. Eighty cycles of DC active power in all phases is shown in Figure 6.4, measured with TS1. Values of almost 6 kW have been measured. The sum of all three DC components shows a compensation, which results in an average value of 177 W for all the considered cycles. Therefore, there is no influence of DC components on the active power [5], however additional compensating processes are acting in the machine. In one phase the currents reach almost 7 % of the RMS value, where an influence on the magnetic circuit can be expected. However, saturation of the magnetic core has to be avoided. [113, 184, 185]

[4] A DC signal has always the same amplitude per definition. So in measurements a DC signal is defined during a time interval, which is one cycle in this work.

[5] Further investigations are necessary to analyse the DC components concerning common mode voltages.

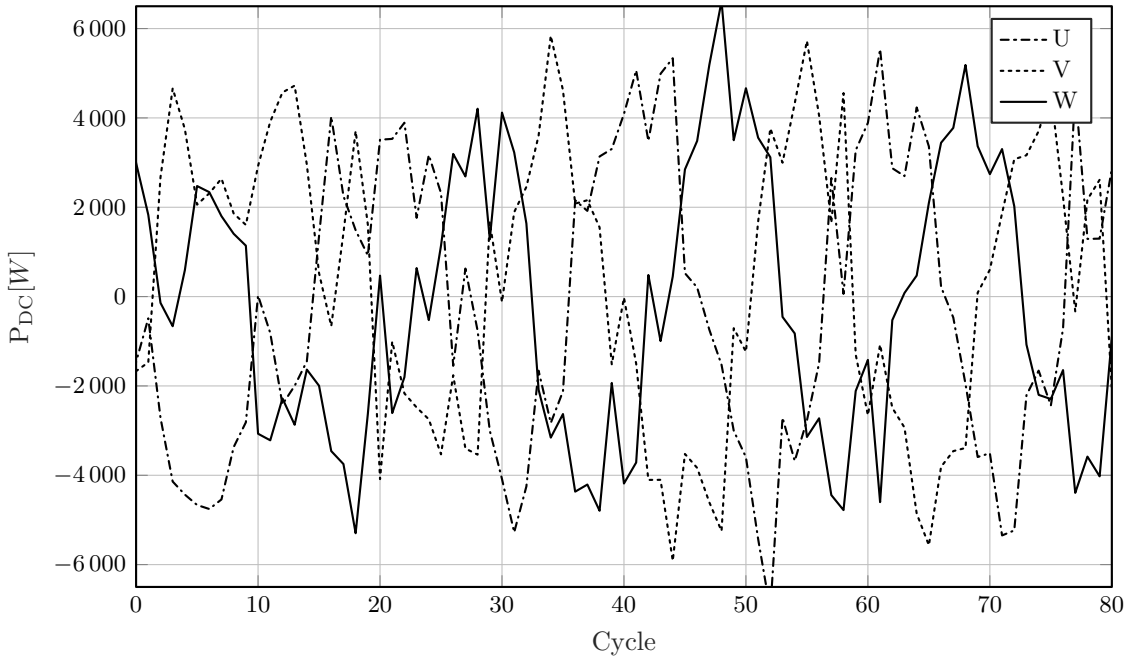

Fig. 6.4: DC Power in the Three Phases (Cycle = 10 Periods of Base Frequency)

6.4 Phase Angle Uncertainty

The influence of the measured input quantities on the total measurement uncertainty $\delta_{P_{Total}}$ of active power is analysed in this section with a calculated uncertainty analysis. The measurement result of TS2 should show the uncertainty behaviour of the input quantities. The uncertainty of the phase angle δ_φ is analysed to show the relation of each uncertainty part. The sensitive factors have an essential impact due to their angle dependence, see equations 3.4 to 3.6. The operation point Load 1 of the TS2 is used, where a phase angle of 25.79° is measured.

An uncertainty limit for the active power δ_P of 0.3 % is drawn in figure 6.5. The limit is chosen due to the defined uncertainty limits for voltage and current measurement devices in the standard IEC 60034-2-1, which is given with 0.2 %. The equation 6.3 is used for an estimation with relative uncertainties δ_g, which is applicable for the uncertainty determination of simple measurements. This means the sensitive factors of the error propagation is equal to one, see in section 3.2.

$$\delta_P = \sqrt{\sum_{g=1}^{N} (\delta_g)^2} \tag{6.3}$$

The further uncertainty condition of 0.2 % is defined in IEC 60034-2-1 with a power factor PF = 1, which is the fulfilled with $\cos\varphi = 1$ for sinusoidal signals. The figure 6.5 shows the set of curves below 0.2 % for a phase angle of 1°.

The set of curves in figure 6.5 show different phase angle errors δ_φ from 0.0336° to 0.9°. The higher the uncertainty δ_φ is, the limit of 0.3 % is exceeded with a small phase angle φ. An operation point typical for a induction motor no load test can be challenging for a measurement system.

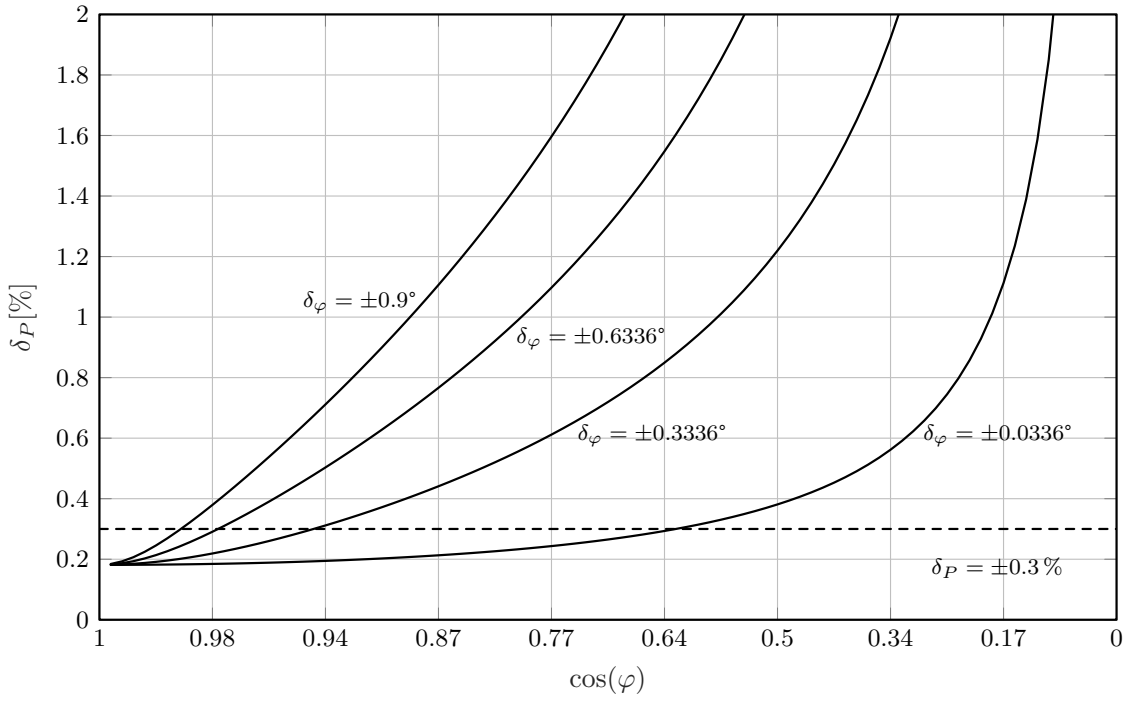

Fig. 6.5: Uncertainty of the Phase Angle

The differences in the uncertainty parts of the total measurement uncertainty $\delta_{\mathrm{P_{Total}}}$ are dependent on the phase angle error, see figure 6.6. The set of curves are given with the phase angle, voltage and current uncertainty. The higher the phase angle uncertainty δ_φ is, and the phase angle increases φ, the more the uncertainty part of the phase angle uncertainty is dominating the total measurement uncertainty.

The MS2 phase angle uncertainty 0.0336° has the lowest and shows the minor influence on the total measurement uncertainty. For its reduction, the uncertainty part of the voltage or current measurement has to be reduced. The MS1[6] has a $\delta_\varphi \approx 1°$, which is the main contribution for the total measurement uncertainty.

[6]The detailed uncertainty budget for the MS1 and TS2 is given in the appendix 9.4.1

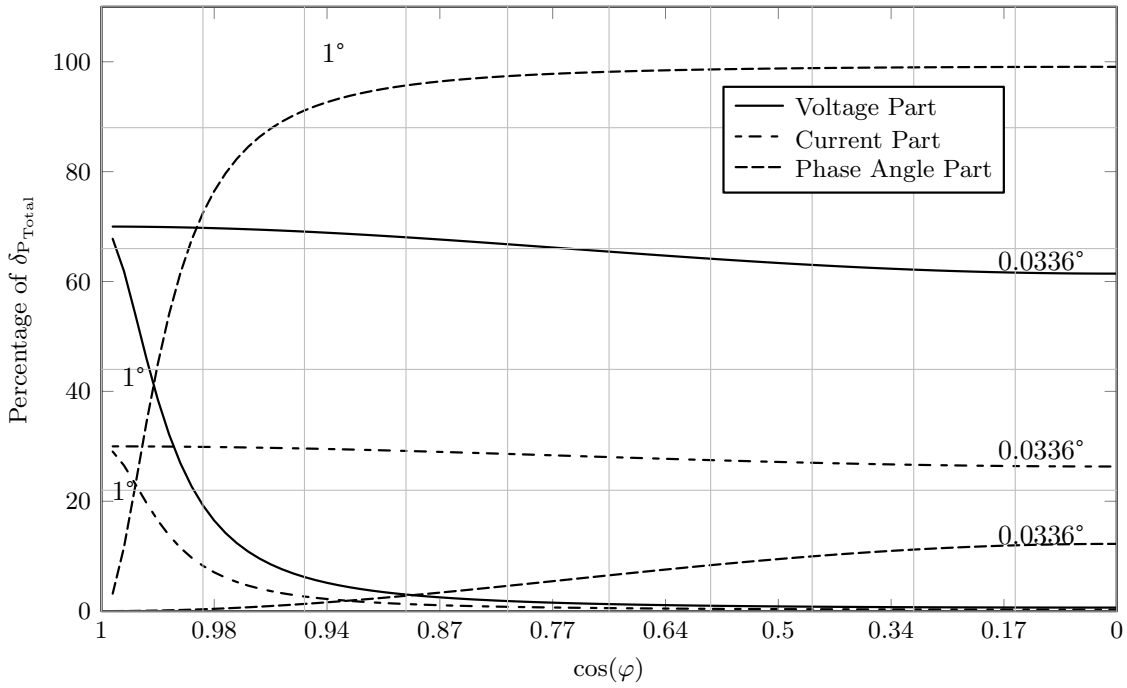

Fig. 6.6: Uncertainty Parts of the Total Measurement Uncertainty $\delta_{\mathrm{P_{Total}}}$

6.5 Fundamental and Harmonics Ratio of Active Power

The harmonic ratio $P_{\mathrm{Harmonic}}/P_{\mathrm{Total}}$ is important for the uncertainty parts of the total active power $\delta_{\mathrm{P_{Total}}}$, which has a base frequency part or a higher harmonic part. Based on the equation 4.19 in section 4.2.2 the ratio of harmonics to the base frequency is analysed. The DC component of the active power is neglected, so the equation for the total active power P_{Total} is given with the base frequency component P_1 and a higher harmonic component P_{Harmonic}.

$$P_{\mathrm{Total}} = P_1 + P_{\mathrm{Harmonic}} \tag{6.4}$$

$$P_{\mathrm{Harmonic}} = \sum_{h=2}^{\frac{N}{2}} P_h \tag{6.5}$$

The uncertainty of the higher harmonics is in general larger than the uncertainty of the base frequency, which is usually defined for measurement devices in a defined frequency range. As an exemplary analysis the uncertainty of the higher harmonics is assumed with 0.54 % and the uncertainty of the base frequency with 0.11 % of the measured active power. Dependent on the harmonic ratio $P_{\mathrm{Harmonic}}/P_{\mathrm{Total}}$ from 0 % to 100 %, the uncertainty parts change their contribution to the total uncertainty of active power measurement, see in figure 6.7. The part of the harmonic active power

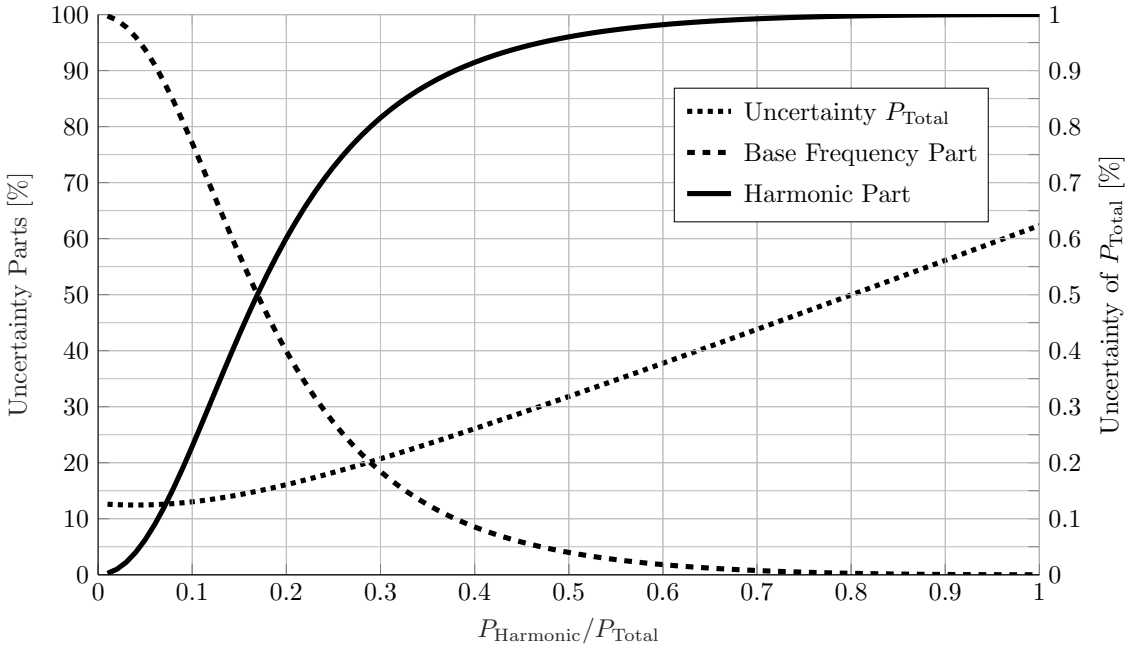

Fig. 6.7: Uncertainty of the Harmonic Active Power Ratio

P_{Harmonic} increases. The ratio $P_{\mathrm{Harmonic}}/P_{\mathrm{Total}}$ of 18 % is the turning point in the case of the power measurement with the TS2 is assumed with a measured electrical power of 11 220.3 kW.

Using the measurements described in section 6.2, the harmonics active power of converter drives is expected or to be low. The standard IEC 60034-1 defines the maximum THD values for voltage or current between 2 % and 3 %, which is far below the 18 % uncertainty analysis. Despite an uncertainty of 100 % for the harmonics, the base frequency part is dominating, due to the ratio between the base frequency and harmonics. It can be summarised, that the uncertainty of the harmonic active power is irrelevant for the total measurement uncertainty $\delta_{\mathrm{P_{Total}}}$. However, the measurements in section 4.2.2 has shown a deviation between MS1 and MS2. So the conclusion is the ability to measure harmonic active power is necessary to calculate the exact active power value. The uncertainty parts of the harmonics active power are covered by the base frequency part.

6.6 Results of Comparison

The measurement systems MS1 and MS2 has shown differences in the determined measurement values and uncertainties. The consideration of all components of the measurement setup about possible uncertainty sources shows the fundamental influences on a measurement of the active power. The measurement transformers and dividers should have a frequency independent scale factor at least in the frequency range where harmonic active power is expected. If a device has a nonlinear scale factor, it is possible to deposit this scale factor in the digital measurement device. However the effort of

measurement algorithm implementation increases. The transformers or dividers have a limited frequency or a limited bandwidth in which a frequency independent behaviour can be expected.

The measurement uncertainty of a used measurement system influences the active power measurement. Especially the uncertainty of a phase determination with a phase angle near 80° or 90° can have a significant impact. To have a sufficient accuracy of a phase angle determination, a high level of sample rate is necessary to determine the zero crossings correctly. Therefore an averaging with some periods can be advantageous.

A further advantage of a high sampling rate is fast evaluation of quantities for applied measurement in a test bench area. Accurate measurements results can be reached in less time. If a No-Load test ist examined, this could be feasible due to a fast experimental procedure, which is required by the standard IEC 60034-2-1.

The measurement range of a measuring card or a power analyser may be not sufficiently used dependent on the operation point. The No-Load test requires a reduction of the stator voltage. There are small active powers to measure with a phase angle between 70° and 90°. The uncertainty of a phase determination can have a significant influence on the active power measurement, which is visible on the equations 3.3 and 3.6, as well shown in section 6.4.

If a used current transformer for a load test is used for a no-load test, the uncertainty of the transformer can be higher due to the small use of the measurement range. However, this fact is dependent on the transformer type. The used zero-flux current transformers have a higher uncertainty as certified when the current to measure is below 2 % of the rated current.

A measurement uncertainty comparison of the MS1 and MS2 is done with the methods of GUM Typ A and Typ B, see in figure 3.1. The latter one is based on defined equations and collected data in calibration protocols, only. The figure 6.8 shows the values determined with both methods for the operation point Load 1 of TS1. The calculated measurement uncertainties Type B cover the measured uncertainties values Type A partially. The influence of the converter control has to be considered in the measurement model (Type B), which is only possible with a determination of a standard deviation. The influence of the converter control is shown in chapter 3.1, where figure 3.3 shows an active power variation of ±2.5 kW in 1000 cycles per phase. With the equation 3.11 a value of ±4.33 kW can be added to the measurement uncertainty of the total active power. The Type B determination with the uncertainty of the control cover the Type A determination. The dashed error bar in figure 6.8 shows the calculated uncertainty with 5.48 kW for MS2 and 15.7 kW for MS1, which includes the induces uncertainty of the drive control.

However a sufficient averaging would lead to a measurement value with a high probability, near to the true value. Future standards should define a minimum number of periods to record for the determination of an active power value or further necessary quantities. Furthermore, a number of minimum averages can be useful, which was already shown for low voltage drives [102]. With the figures 3.3 an average value of minimum 80 cycles can give a active power value with a higher probability. The cycle time of 0.4 s is used of MS2 in the TS1, which means a minimum recording of 40 s is necessary to reach the

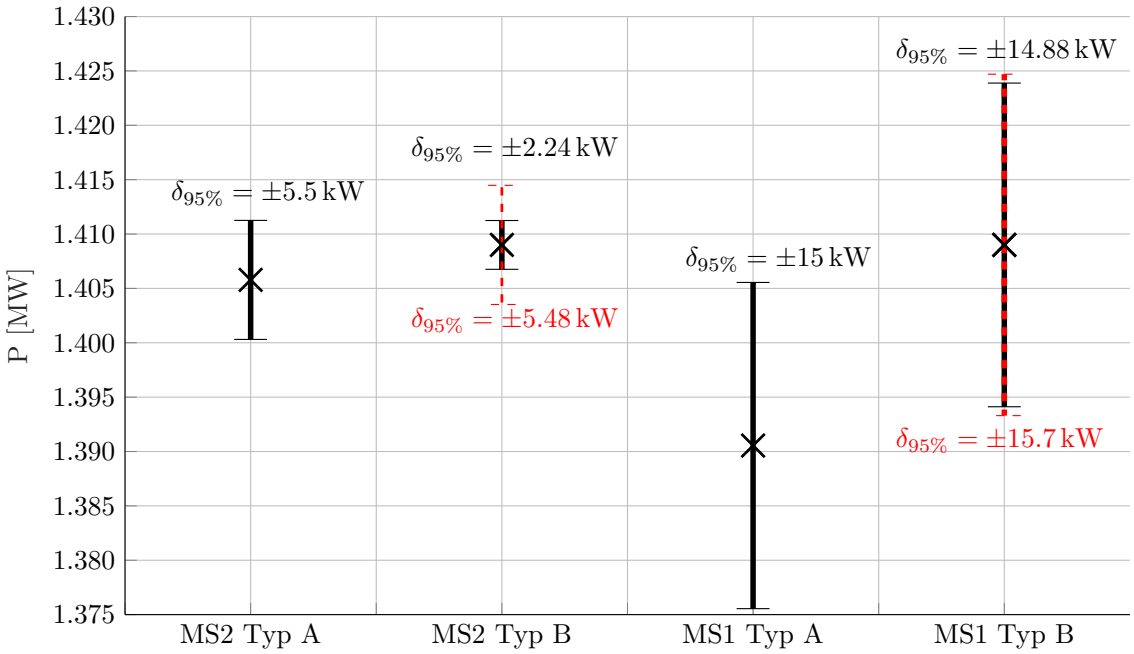

Fig. 6.8: Comparison of Measurement Uncertainty GUM Typ A and GUM Typ B for Load 1 (Red Dashed Error Bar: Includes the Uncertainty of the Drive Control)

minimum average value for the active power with the minimum of 80 cycles. Dependent on the drive control, measurement setup and base frequency, few measuring time is necessary and recorded cycles respectively.

The less used measurement range of a current or voltage input channels of the measurement devices induces a higher uncertainty, which has been already shown for smaller drives in [23]. For the individual operation points has to be checked if the measurement ranges of a measuring card or power analyser are entirely used. It can be advantageous to change an operation point to better utilise the measurement range.

The used voltage divider can be replaced by dividers with fewer uncertainties, which are used for calibration purpose. However, this would increase the costs for a measurement setup. An uncertainty determination can qualify the measured value with a high probability. The determination with the Type B method can optimise the measurement setup selection before the implementation.

7 Uncertainty Limits of Power Measurement

Determination of medium voltage (MV) motors efficiency is subjected to the uncertainty of the electrical power measurement. The commonly used methods for determination of synchronous and induction motors efficiency are analysed in this respect. As in this chapter shown, a measurement uncertainty analysis must get obligatory, to have efficiency values with a high probability.

7.1 Determination of Efficiency

The test methods are different for induction machines and synchronous machines. The figure 7.1 shows test methods common used for MV machines, which are defined in IEC 60034-2-1 and IEC 60034-2-2. The latter on describes methods for large drives when a full-load test is not possible. A full-load test is usually not possible due to the

Induction Machine	2-1-1C	Summation of losses with additional load losses from assigned allowance and calculated losses
	2-1-1D	Dual supply back-to-back-test
Synchronous Machine	2-1-2C	Summation of separate losses without a full load test
	2-1-2D	Dual supply back-to-back-test

Fig. 7.1: In Appliance with IEC 60034-2-1 Test Methods for the Determination of Efficiency of MV Machines; Induction Machines and Synchronous Machines

non-availability of a suitable load machine in the test field. However, if two identical machines are available, a back-to-back test (2-1-1D and 2-1-2D) or a direct method (2-1-1A and 2-1-2A) are possible.

Direct Method - 2-1-1A & 2-1-2A Some facts on the usability of the direct test method are summarised, which are 2-1-1A for induction and 2-1-2A for synchronous machines. In chapter 6, a torque measurement has been done with the Test Setup 2 (TS2). The uncertainty of the output power measurement is dominated by the torque transducer, which leads to uncertainties higher than $\pm 10\,\mathrm{kW}$[1] for the output power. The speed measurement has a relative uncertainty of $0.03\,\%$, where the relative torque measurement uncertainty has a value of $0.3\,\%$. All measured operation points with TS2 show higher uncertainties than the specified value in the data sheets. The output power measurement is the dominating uncertainty part, which also has a high uncertainty contribution compared to the indirect test methods shown in the appendix 9.5 – 9.7. In general, the determination of the efficiency with a full-load test and an output power measurement with torque transducer is an exception in the area of MV machines.

7.1.1 Induction Motors

The sum of the total losses P_L is subtracted from the rated electric power P_1 and set into its relation.

$$\eta = \frac{P_1 - P_\mathrm{L}}{P_1} \tag{7.1}$$

The equation for the total losses of induction machines is given.

$$P_\mathrm{L} = P_\mathrm{Cu1} + P_\mathrm{Cu2} + P_\mathrm{C} + P_\mathrm{LL} \tag{7.2}$$

The indirect method is based on the summation of the individual determined losses. These losses are for an induction machine:

- Stator copper losses P_Cu1,
- Rotor copper losses P_Cu2,
- Stray load losses P_LL,
- Constant losses P_C, seperated in windage losses P_FW and iron losses P_FE.

These losses should be determined with a load test, a load-curve test, a no-load test and a resistance measurement. The standard IEC 60034-2-3 requests a further load-curve test and no-load test with converter supply, where the following additional losses are determined

- Load-dependent additional harmonic losses $P_\mathrm{LL,H}$,
- Constant additional harmonic losses $P_\mathrm{C,H}$.

[1] The uncertainty is based on the uncertainty for the torque measurement, which is given in the data sheet.

In general, the load test is an exception for tests with MV machines. The machines are individually manufactured. Thus, it is difficult to find a corresponding load machine with the same rated power, the same shaft height and sufficient capacity of the test field supply. The summation of the losses with the corresponding equations for the determination of induction motor efficiency is described in appendix 9.7.

Usually, a no-load test and resistance measurement are the possible tests to apply, which leads to the following summary and suggestions for the determination of the efficiency of converter operated MV drives. The equations for the individual determination of the losses are described in the appendix 9.7.

- The stator copper losses P_{Cu1} can be calculated with the measured resistance and the given rated current of the calculation data.
- The rotor copper losses P_{Cu2} are calculated with the rated slip and the calculated stator copper losses P_{Cu1}, as well the measured constant iron losses P_{FE} are subtracted.
- The stray load losses are calculated with a factor 0.5 % of the rated power, which is prescribed by the the standard IEC 60034-2-1.
- The constant losses can be determined by the measurement of the no load losses.
- The additional load losses $P_{\mathrm{LL,H}}$ due to converter supply should be covered by a constant factor, as defined for the stray load losses. The article [14] showed the characteristic of load-dependent parts of the additional load and the stray load losses. There are shown the differences between converter supply and sinusoidal supply. However, a definition of a constant factor can lead to higher assumed losses, but the worst case of losses can be covered. Especially when a load test and the determination of the load-dependent losses is usually not possible.
- The additional constant losses $P_{\mathrm{C,H}}$ are determinable due to the no-load test with a converter supply of the induction machine.

The test methods which are based on a short circuit test are not realisable, because a locked rotor test could typically not be done with converters. The converters are not dimensioned for operation with a short circuit current of approximately five times higher rated current.

7.1.2 Synchronous Machines

The indirect method 2-1-2C for synchronous machines has the advantage to determine the efficiency without a load test, which is the main difference to the indirect method 2-1-1C for the induction machines. However, a short circuit test is requested, which is not applicable to a converter.

The equation for the total losses of synchronous machines is given.

$$P_{\mathrm{L,SM}} = P_{\mathrm{Cu1}} + P_{\mathrm{E}} + P_{\mathrm{C}} + P_{\mathrm{LL}} \tag{7.3}$$

Compared to the induction motor, the losses of the excitation system P_{E} have to be measured.

These synchronous machine losses are given.

- Stator copper losses P_{Cu1},
- Stray load losses P_{LL},
- Constant losses P_{C}, separated in windage losses P_{FW} and iron losses P_{FE}.
- Excitation losses P_{E},

Due to a converter supply, the following losses can be expected.

- Load-dependent additional harmonic losses $P_{\mathrm{LL,H}}$,
- Constant additional harmonic losses $P_{\mathrm{C,H}}$.

The summary and suggestion of the individual losses determination can be given.

- The stator copper losses P_{Cu1} can be determined with the measured resistance and the measured rated current in a short circuit test, with a sinusoidal source instead of a converter.
- The stray load losses P_{LL} can be determined with a short circuit test, with a sinusoidal supply. A determination of the $P_{\mathrm{LL,H}}$ is only possible with a load or partial load test. Two measured load points are necessary to extrapolate a load curve for the stray load losses determination.
- The determination of the $P_{\mathrm{C,H}}$ is possible with a no-load test under sinusoidal and converter supply.
- The excitation losses P_{E} can measured with standard low voltage equipment.

7.1.3 Back-To-Back - 2-1-1D & 2-1-2D

The back to back test is usable for all machine types. The test is favoured when two identical machines are available or manufactured. Both machines are coupled, one is operating as a generator and the other as a motor. The efficiency η is determined with the half of the total losses, the mean of the input power of generator P_1 and motor P_2.

$$\eta = 1 - \frac{P_{\mathrm{L}}}{\frac{P_1+P_2}{2} + P_{1E}} \tag{7.4}$$

The total losses P_{L} and the input power of the excitation systems $P_{1\mathrm{E}}$ must be added. The $P_{1\mathrm{E}}$ is only necessary for the determination of synchronous machines efficiency. For

the efficiency calculation of induction machines, the variable is not necessary for the equations 7.4 and 7.5.

$$P_{\mathrm{L}} = \frac{1}{2} \cdot (P_1 - P_2) + P_{1E} \tag{7.5}$$

The input power of the excitation systems $P_{1\mathrm{E}}$ is given with, $P_{1\mathrm{E,M}}$ for the motor and $P_{1E,G}$ for the generator.

$$P_{1E} = \frac{1}{2} \cdot \left(P_{1E,M} + P_{1E,G}\right) \tag{7.6}$$

The uncertainty of the back to back test is dependent on two measurements systems for MV drives, one for the load machine and one for the Device Under Test (DUT). The uncertainty analysis is recommended for a measurement system selection for both used machines.

7.1.4 Uncertainty Comparison of Methods for the Determination of Efficiency

The choice of the indirect method for the determination of MV drives efficiency is due to the feasibility of the tests. A full-load test requires, in any case, a higher installation effort compared to a no-load test.

An uncertainty analysis is done with the typical test methods for induction machines. The data of test setup TS2 with the corresponding measurement system MS2 is used and summarised in appendix 9.4. Especially for the test setup TS2 a torque measurement is done, which makes an uncertainty analysis possible of the direct method for determination of efficiency.

The detailed uncertainty budgets for the efficiency test methods are given in the appendix 9.5 to 9.7. The comparison in table 7.1 shows all analysed test methods. Two methods are a good solution for a determination of efficiency with low uncertainty, but the direct method has a higher uncertainty compared to the other possible methods. However, the indirect methods have the most calculated values, where no uncertainty contribution is assumed.

Tab. 7.1: Measurement Uncertainty of Induction Motor Test Methods

Method	Expanded Uncertainty
2-1-1A Direct	±0.23 %
2-1-1D Back-To-Back	±0.02 %
Indirect without Load Test	±0.03 %

The uncertainty analysis for the synchronous machine is not done, due to the missing of real measurement data for comparison in this work. However, the indirect method for the synchronous machine is almost the same as for the induction machine. The losses of the excitation system have to be measured which can be measured with low voltage measurement equipment. The uncertainty can be expected as very low, in the same amount of the uncertainty for the two better methods of the induction machine, see table 7.1.

Conclusion of the Analysis The analysis in chapter 6 and in this section shows the possibility to qualify the uncertainty of the measurements done on MV drives with TS1 and TS2. The indirect test method has a low uncertainty, which is important for the determination of efficiency. As well, the tolerance limits 10 % of $\cdot(1-\eta)$ can be applicable:

- Despite only a no-load test is possible for a DUT; uncertainty can be calculated for the realisable test.
- The measurement system can be chosen individual, which efforts a measurement system with high performance,
- The classification of the uncertainty can lead to a confident result with a high probability of the determined efficiency

Efficiency Classes The uncertainty analysis section 7.1 shows the possibility to fulfil the tolerance limits of IEC 60034-1. In table 7.2 the tolerance limits for high power drives are given. The uncertainty class for electrical measurement quantities must have 0.2 % of the displayed value, see IEC 60034-2-1. If the tolerance limits $(1-\eta)$ should be applied to MV motors the requested uncertainty class of 0.2 % is not sufficient. The uncertainty limits given in IEC 60034-2-1 have to be adapted to the tolerance limits $(1-\eta)$ for the high power motors. The basic for a classification of the drives should be an uncertainty value which is based on uncertainty analysis. The uncertainty classes should be defined dependent on the uncertainty limits. However, an uncertainty analysis requires a careful determination of an efficiency value.

Tab. 7.2: Tolerance Limits for High Power Machines

η	$10\,\%(1-\eta)$
96 %	0.4 %
97 %	0.3 %
98 %	0.2 %
99 %	0.1 %

The standard IEC 60034-2-2 defines special methods for the determination of large drives efficiency. A notice to the section 7.1.2 in IEC 60034-2-2 advises calculating a mean value of several measurements in one operation point. The advice is important with the investigated measurements on the large drives in this thesis. It increases the probability of a determined efficiency value. This issue is encouraged by the results in chapter 6, where the influence of the control circuit of large converter drives is shown. This confirms the necessity of a definition of obligatory uncertainty analysis in IEC 60034-2-2.

7.2 Limits of Measurement Transformers, Dividers and Power Analysers

The results of the analysed measurement systems are used to show possible limits of the individual measurement components. The used system MS2 has a high performance for active power measurements in the MV range. The measurements in section 6.2 have uncertainties for the active power values with 0.03 %, which can be higher if the used measurement range has a nonlinear scale factor. The test on machines can be applied with measurement transformers despite the measurement range is not optimised used. Especially the no-load test is applied after the load test, where the transformers or measurement devices are not changed.

In general, the uncertainty limits on the market available measurement devices are dominated by Resistive Capacitive Dividers and Zero-Flux Current Transformers. Despite the low uncertainty of the used measurement system MS2, there are dividers which have a smaller uncertainty. As well there are zero-flux current transformers, which can have a better performance with a lower measurement range. The voltage divider and the current transformer are also usable for the harmonic measurement due to the low measurement uncertainty over a wide frequency range, see chapter 5.

Uncertainty for η below 0.2 % is also possible with inductive voltage and current transformers for 50 Hz when a sinusoidal supply voltage is applied. Measurement with the TS2 and MS1 has shown in some operation points an uncertainty better than 1 %. However, the signal conditioning and the used measurement device induces the most uncertainty of MS1.

The data acquisition and processing has an impact on the active power determination, which is primarily caused due to the signal conditioning and its different measurement ranges. The used measurement devices have different measurement ranges which have been chosen individual on the test setup and its requirements for the applied tests. The different measurement ranges allow the testing of machines of different rated power categories. The ADC and signal processing has limits dependent on the maximum frequency to measure and the expected uncertainty, which is shown with equation 4.35. MV drives have maximum expectable frequencies up to 20 kHz in the supply voltages. Nowadays, power analysers have sample frequencies f_S above 1 MHz, which is more than sufficient for the active power measurement on MV drives. An analysis with sample frequencies f_S below 1 MHz can have good measurement results with low uncertainty.

A further characteristic of a measurement devices is the memory depth, besides the required sample frequency. It is necessary to calculate a mean value out of several base frequencies, which can be problematic, if a chosen measurement device has not enough memory depth.

Harmonic power measurement has increased requirements, which is a limit for the individual used measurement components.

- Less uncertainty in the harmonic measurement range
- Higher sample rate f_S for a correct determination of higher harmonics
- In general high efficiencies can be expected for high power drives. The same applies for the uncertainty of a high power drive measurement system. High accuracy or a low measurement setup uncertainty must be applied for high power drives.
- An low uncertainty is necessary due to the losses components which are in the tenth percent range.

7.3 Limits for Medium Voltage Drives and Tests

The discussion about the determination of efficiency of motors in several articles and the proposals in the relevant IEC working groups have shown the importance of the tolerance limits. Doppelbauer summarised in the article [22] some facts of the discussions and analysed the methods for the determination of small motors[1] efficiency.

The standard IEC 60034-1 describes the tolerance limits for the determination of efficiency with 10 % of $(1 - \eta)$ for motors above 150 kW rated power, e.g. a motor with $\eta = 98\,\%$ has a tolerance of 0.2 %. The tolerance limit is higher for small machines in the low voltage supply, which are motors common manufactured in a mass production. In general, half of the tolerance defined in IEC 60034-1 is for variations of material and process during mass production, while the other half is available for measurement uncertainty [22]. High power motors primarily would need a defined tolerance limit for the measurement uncertainty of the whole test setup. The measurement uncertainty can be different dependent on the examined test methods.

With the introducing of the efficiency classes, the discussion to reduce the tolerance limits seems as not realisable. The current IEC 60034-1 allows a tolerance with 10 % of $(1 - \eta)$ for motors above 150 kW rated power, which was questionable with the results in [22]. There are higher uncertainties determined with an increased rated power of the machines, which is shown in the section before. The defined tolerance limit defined in IEC 60034-1 expects a very low uncertainty for high power motors, which is a challenging task. This is only realisable with the indirect test methods and a measurement uncertainty analysis, which was shown in this thesis.

The characteristic of converter-fed MV drives and the tests methods which are necessary, represent conditions for a determination of efficiency with low uncertainty. In the

[1] Tests with 10 different motors with rated power between 0.37 kW and 315 kW

chapters 3 and 6 the control of the drive applications is identified as essential uncertainty contribution. The used current measurement devices for the control loop of a converter have uncertainties.

Converter fed drives have the possibility to change its switching frequency, which can result in different additional losses. The investigations of [23, 186] with small drives have shown the importance of losses determination, which is induced by harmonics.

The THD values for the supply voltage are a limit for the harmonic content. The investigation in section 6.5 shows that the harmonic active power uncertainty does not affect the total measurement uncertainty when the drive is compliant with the THD limits, given in IEC 60034-1. The further impact has the phase angle φ shown in section 6.4, which is essential for the test methods. Usually, the indirect determination of efficiency is applied for large drives, which requires a no-load test. The phase angle uncertainty has an impact on the total measurement uncertainty. The no-load test is usually the only possible test to apply, see the explanations in the section 7.1. The following limits are given:

- The confident measurement results are given with some periods to record, a defined sample rate f_S and an uncertainty specification based on measurements or calculations.
- A uncertainty based on measurements GUM Typ A is more reliable compared to an uncertainty calculation with GUM Typ B. The influence on the uncertainty due to the control of the drive requires a mean value calculated from several measurement cycles for confident results.
- An proposal for the harmonic analysis is already given in the standards IEC 61000-4-7 [145] and Institute of Electrical and Electronics Engineers (IEEE) Std 519 [187] with a defined number of periods for a value determination.
- The question of the additional losses due to the converter supply can be estimated with the constant factor defined in IEC 60034-2-1, which is usually the worst case and should include the possible losses. The determination of the losses is often a research issue, when no torque measurement is possible.

7.4 Guideline of Measurement Setup Selection

The measurement system for the active power measurement of MV drives has to fulfil several requirements. They are a result of the investigations of this thesis and summarised in the following list.

- The measurement system has to be chosen individually dependent on the test methods, which can require a higher system performance. Different measurement devices corresponding the test method to examine should be considered for their use.
- The classification of the measurement setup uncertainty with the guidelines of GUM is recommended for a determination of machine quantities with high probability.

- An uncertainty limit defines with 10 % of $(1-\eta)$ for the determination of efficiency should be reached.
- An active power value should be an average value of a number of cycles. The values can also be used for the specification of a standard deviation. A measurement of several values allows the identification of additional uncertainty sources, e.g. control of the drive application.
- The guidelines of GUM should be used to identify the main uncertainty parts in a measurement setup and to give the possibility of an improvement.
- The cycle time and sample frequency f_S should be chosen to calculate an active power value with high confidence, see section 4.3.
- Three phase active power measurements is recommended for machines operated with converters.

8 Conclusion

The thesis showed the measurement uncertainty of the active power measurement to be used for the determination of efficiency of MV motors. The results are summarised in the following main points.

- Methods and guidelines to handle the uncertainty of measurement setups used for the determination of the efficiency of converter supplied medium-voltage drives are given. The uncertainty analysis methods are applied to typical medium voltage drives to identify the main factors of influence when the electrical active power is measured. Different converter types with their typical voltage forms are used for the supply of induction machines. The analysis with the drives and the used measurement setups demonstrate the essential determination of all influences on a measurement, to characterise or rather quantify them in order to obtain a meaningful result.
- The influence of the drive control on the active power measurement is shown. The measurement of medium voltage drives requires a correct consideration of the measurement results to account for the application control influence. The drive application and the used control circuit can influence the active power measurement, which should not be underrated.
- Guideline for an active power measurement is given. The signal conditioning, digitalising of signal forms, the mean value determination or the selected sample frequency has a significant influence on the uncertainty. The results have shown that the determination of mean values with several individual measurements lead to confident results and an uncertainty specification, which leads to trustable efficiency values with a high probability, too.
- The knowledge of the transfer behaviour is essential for the correct determination of harmonics in the voltage and current signals. The important issue of a measurement system is the ability to measure the correct harmonic active power, which can also influence the determined total active power. The typically used voltage and current measurement devices in the medium voltage range are analysed with their transfer behaviour. Especially a transformer or divider with low uncertainty is preferred, due to the wide measuring range where a measurement of small amplitudes in no load case must be possible.
- Advises for further standard definitions are given. If the energy efficiency classes are introduced for medium voltage drives, a specification of uncertainty should be obligatory to provide with an efficiency value. The indirect method for the determination of efficiency and the Back-To-Back test have the lowest uncertainty. The load dependent additional harmonic losses have been calculated if a load test is not possible. Otherwise, a partial load test will be necessary for the synchronous

machines to extrapolate the load dependent losses. The choice of measurement devices is dependent on the test methods, especially if the indirect method for determination of the efficiency is used. The possibility to test a machine with rated load is usually not realisable with medium voltage drives with high power and parts of a loss determination are based on calculations.

For a future classification of large drives with efficiency classes, the requirements for a measurement uncertainty have to be adapted in the corresponding standards for the determination of the efficiency. Instructions for the measurement uncertainty determination of a measurement setup must be included. It is obvious if determined motor efficiencies should be compliant with the limits of future energy efficiency classes and comparable results should be generated.

The presented uncertainty methods for the active power measurement are usable for the implementation of a measurement setup for small machines, too.

Further Work

The following investigations can be made with the basic results of this thesis:

- The uncertainty analysis of active power of the harmonics. In the grid the harmonics are of interest.
- Implement and analyse a measurement system which can have several scale factors of the used measurement devices in a specified frequency range. There will be a measurement system necessary, which transfers the measured voltage and current signals in the frequency range.

9 Appendix

9.1 Uncertainty of Harmonics

The equations for the harmonic components of voltage 4.17 is used to do an uncertainty calculation for voltage harmonics dependent on the sampled data. The uncertainty calculation for current harmonics is not derived as it is based on the same principle of the voltage harmonics. They are used in section 4.3 on the sampled voltage and current signals to calculate the uncertainty of the harmonic active power.

9.1.1 Alternating Component

The equation 9.1 is the model equation with the voltage sample u_n, number of samples N and the harmonic order h. The voltage samples u_1 to u_N are the input quantities for the model equation:

$$\hat{U}_h = \frac{2}{N} \cdot \left| \sum_{n=1}^{N} u_n \cdot e^{-j \cdot \frac{2\pi}{N} \cdot h \cdot (n-1)} \right| := f_{U_h}(u_1,...,u_N) \tag{9.1}$$

The equation separated in real and imaginary part.

$$\hat{U}_h = \frac{2}{N} \cdot \sqrt{\left[\underbrace{\sum_{n=1}^{N} u_n \cdot \cos\left(\frac{2\pi}{N} \cdot h \cdot (n-1) \right)}_{\Re} \right]^2 + \left[\underbrace{\sum_{n=1}^{N} u_n \cdot \sin\left(\frac{2\pi}{N} \cdot h \cdot (n-1) \right)}_{\Im} \right]^2} \tag{9.2}$$

The uncertainty of the harmonic components is given with δ_u, the same uncertainty of all voltage samples,

$$\delta^2_{\hat{U},h} = \sum_{m=1}^{N} \left(c_{m,h} \cdot \delta_{u_m} \right)^2 = \delta^2_u \cdot \left(\sum_{m=1}^{N} c_{m,h} \right)^2 \tag{9.3}$$

with the sensitive coefficient

$$c_{m,h} = \frac{\partial f_{U_h}}{\partial u_m} = \frac{2}{N} \cdot \frac{\Re \cdot \sum_{m=1}^{N} \cos\left(\frac{2\pi}{N} \cdot h \cdot (m-1)\right) + \Im \cdot \sum_{m=1}^{N} \sin\left(\frac{2\pi}{N} \cdot h \cdot (m-1)\right)}{\sqrt{\Re^2 + \Im^2}} \tag{9.4}$$

which can be used in equation 9.3. This leads to the following equation and results in the equation for the harmonic uncertainty.

$$\delta^2_{\hat{U}_h} = \frac{4 \cdot \delta_u^2}{N^2 \cdot (\Re^2 + \Im^2)} \cdot \sum_{m=1}^{N} \left(\Re \cdot \cos\left(\frac{2\pi}{N} \cdot h \cdot (m-1)\right) + \Im \cdot \sin\left(\frac{2\pi}{N} \cdot h \cdot (m-1)\right)\right)^2 \tag{9.5}$$

$$\sum_{m=1}^{N} \sin\left(\frac{2\pi}{N} \cdot h \cdot (m-1)\right) = \sum_{m=1}^{N} \cos\left(\frac{2\pi}{N} \cdot h \cdot (m-1)\right) = \frac{N}{2} \tag{9.6}$$

$$\delta^2_{\hat{U}_h} = \frac{2 \cdot \delta_u^2}{N} \qquad \rightarrow \qquad \delta_{\hat{U}_h} = \sqrt{\frac{2 \cdot \delta_u^2}{N}} \tag{9.7}$$

9.1.2 DC Component

The determination of the dc component of voltage, current and power is given by the mean of the samples, see equation 4.21. The rules of GUM lead to the following equation for the voltage uncertainty of the dc component.

$$\delta_{U_0} = \sqrt{\frac{\delta_u^2}{N}} \tag{9.8}$$

The difference to equation 9.7 is the factor two.

9.1.3 Uncertainty of the Phase

The phase of the harmonics is determined with the imaginary and real components of the Fourier coefficient, see equation 9.2, which is used as model equation for the uncertainty determination.

$$\varphi_h := f_{\varphi_h}(u_1,...,u_N) = \begin{cases} \arctan\left(\frac{\Im}{\Re}\right) & \text{for } \Re > 0 \\ \pi + \arctan\left(\frac{\Im}{\Re}\right) & \text{for } \Re < 0 \end{cases} \tag{9.9}$$

The uncertainty of each sample point δ_{u} are the same for all samples, which leads to a simple calculation. For an general measured sample the variable m is introduced.

$$\delta_{\varphi_h} = \sqrt{\delta_{\mathrm{u}}^2 \cdot (c_{1,h}^2 + ... + c_{N,h}^2)} = \sqrt{\delta_{\mathrm{u}}^2 \cdot \sum_{m=1}^{N} c_{m,h}^2} \tag{9.10}$$

The equation 9.10 has the following sensitive coefficients defined.

$$c_{m,h} = \frac{\partial f_{\varphi_h}}{\partial u_m} \tag{9.11}$$

$$c_{m,h}^2 = \frac{\left(\frac{\partial \Im}{\partial u_m}\right)^2 \cdot \Re^2 + \left(\frac{\partial \Re}{\partial u_m}\right)^2 \cdot \Im^2}{\left(\Re^2 + \Im^2\right)^2} - \frac{2 \cdot \Re \cdot \Im \cdot \left(\frac{\partial \Re}{\partial u_m}\right) \cdot \left(\frac{\partial \Im}{\partial u_m}\right)}{\left(\Re^2 + \Im^2\right)^2} \tag{9.12}$$

With the use of the following relation.

$$\frac{\partial}{\partial x}\left(\arctan\frac{-h}{g}\right) = -\frac{\frac{\partial h}{\partial x} \cdot g - \frac{\partial g}{\partial x} \cdot h}{h^2 + g^2} \tag{9.13}$$

The sensitive coefficient with the consideration of equation 9.6,

$$\sum_{m=1}^{N}\left(\frac{\partial \Im}{\partial u_m}\right)^2 = \frac{1}{N^2}\sum_{m=1}^{N}\sin^2\left(\frac{2\pi}{N} \cdot h \cdot (m-1)\right) = \frac{1}{2N} \quad {}^{1} \tag{9.14}$$

$$\sum_{m=1}^{N}\left(\frac{\partial \Re}{\partial u_m}\right)^2 = \frac{1}{N^2}\sum_{m=1}^{N}\cos^2\left(\frac{2\pi}{N} \cdot h \cdot (m-1)\right) = \frac{1}{2N} \tag{9.15}$$

$$\tag{9.16}$$

$$\begin{aligned}&\sum_{m=1}^{N} 2 \cdot \Re \cdot \Im \cdot \left(\frac{\partial \Re}{\partial u_m}\right) \cdot \left(\frac{\partial \Im}{\partial u_m}\right) \\ &= \frac{-2}{N^2} \cdot \Re \cdot \Im \cdot \sum_{m=1}^{N} \cos\left(\frac{2\pi}{N} \cdot h \cdot (m-1)\right) \sin\left(\frac{2\pi}{N} \cdot h \cdot (m-1)\right) = 0\end{aligned} \tag{9.17}$$

which leads to a simplified form.

$$\sum_{m=1}^{N} c_{m,h}^2 = \sum_{m=1}^{N} \frac{2}{N \cdot \hat{U}_h^2} \tag{9.18}$$

Thus, the uncertainty of the harmonic phase component is given.

$$\delta_{\varphi_h} = \sqrt{\delta_{\mathrm{u}}^2 \cdot \frac{2}{N} \cdot \sum_{m=1}^{N} \frac{1}{\hat{U}_h^2}} \tag{9.19}$$

9.2 Sample Frequency for Higher Frequency Signals

The equation 4.35 provides a sample frequency f_S dependent on the focused uncertainty δ_{AP}, the cycle time T_{cycle}, the period time of voltage base frequency t_0 and the maximum frequency expected f_{max} in the power signal. The figure shows the sample frequency for f_{max} of 50 kHz with t_0=0.02 s and T_{cycle}=0.2 s.

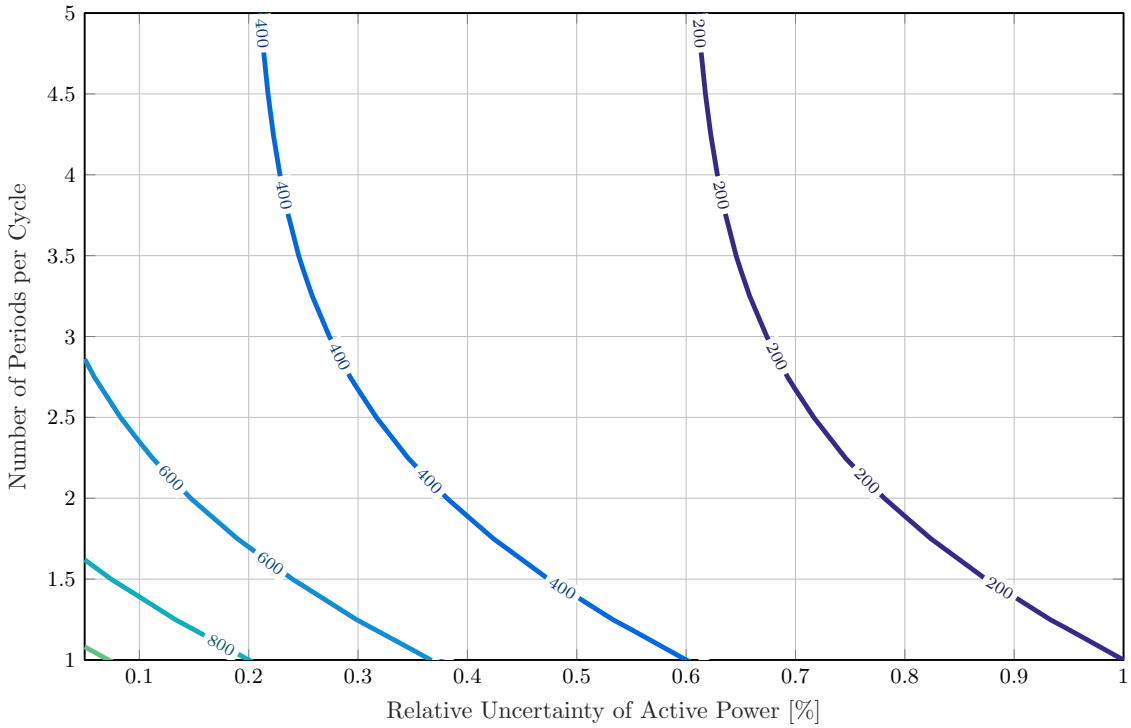

Fig. 9.1: Sample Frequency in kHz for f_{max}=50 kHz

9.3 Determination of Measurement Device Transfer Behaviour

In figure 9.2 the circuit to generate the step response with voltage transformer, which is the device under test, and the reference divider is shown.

Fig. 9.2: Frequency Behaviour Measurement of Voltage Transformer

9.4 Measurement Applications and Motors

The specifications of the machines under test is described in the tables 9.1 for the Test Setup 1 (TS1), and Test Setup 2 (TS2) in table 9.2. The Motor of TS1 was operated with a three level Neutral-Point Clamped Voltage Source Converter (3L-NPC-VSC) and the TS2 with a Modular Multi-Point Converter (M2C).

Tab. 9.1: Motor Data Test Setup 1 (TS1) and 3L-NPC-VSC

	Value
Rated Power P_N	16 000 kW
Rated Voltage U_N	6600 V
Rated Current I_N	1560 A
Rated Speed n	1493.5 rpm
$\cos_\varphi$	0.92

Tab. 9.2: Motor Data Test Setup 2 (TS2) and M2C Converter

	Value
Rated Power P_N	12 000 kW
Rated Voltage U_N	6600 V
Rated Current I_N	1193 A
Rated Speed n	1481 rpm
$\cos_\varphi$	0.91
η	96.85 %

9.4.1 Voltages, Currents and Uncertainties of the Test Setup 2

The typical voltage form of a M2C converter is show in the figure 9.3 with the corresponding harmonics in the figure 9.5. The converter topology has several voltage steps which allows generate an almost sinusoidal form. The harmonics are measurable in the range of 5 kHz which are producing no measurable active power component.

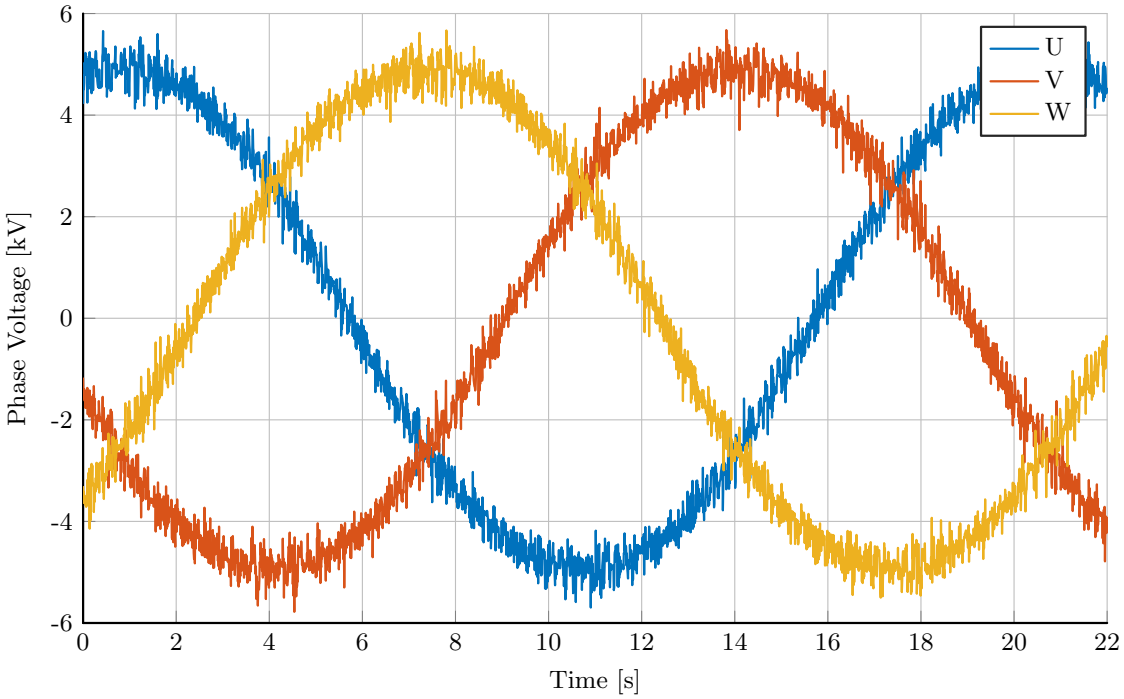

Fig. 9.3: Line Voltages of a M2C Multilevel-Converter

The budget for measurement uncertainty for both measurement setups is given in the tables 9.3 and 9.4.

The measurement values in the table 9.5 are influences by the converter control, which is visible in the high measurement uncertainties. This fact is already shown in the figures 3.3 and 3.4 in chapter 3. However standard deviation are calculated for the active power, the phase angle, the root mean square value of voltages and currents. The voltage and current uncertainty is given with a coverage factor of $k = 2$ in table 9.5.

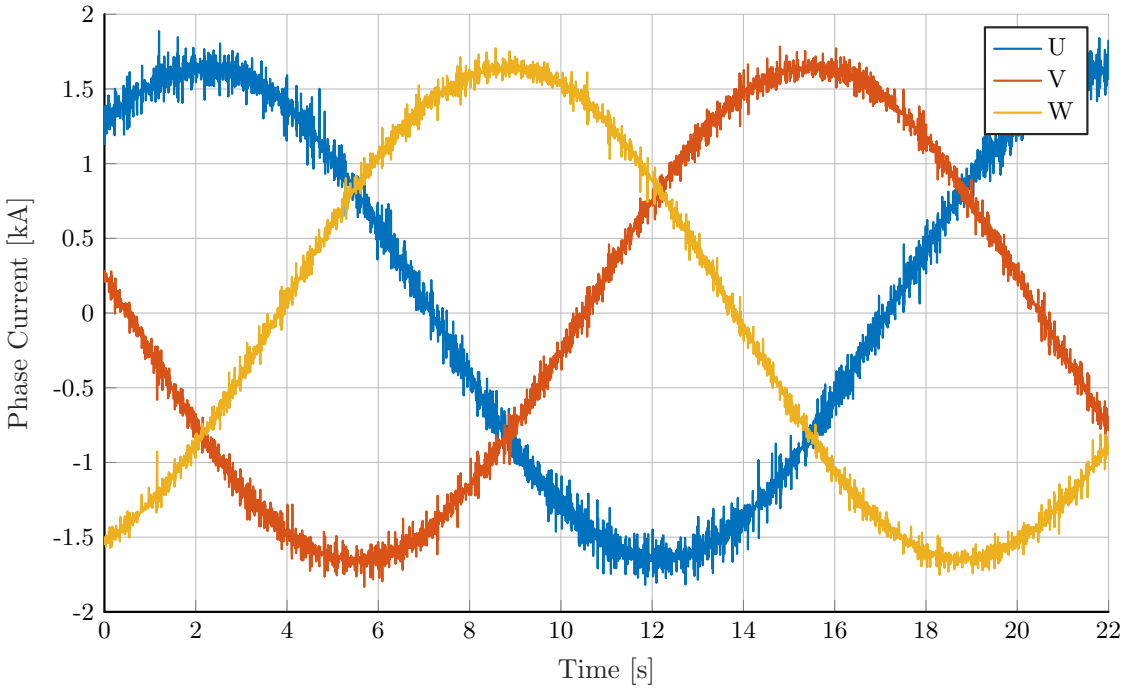

Fig. 9.4: Phase Currents of a M2C Multilevel-Converter

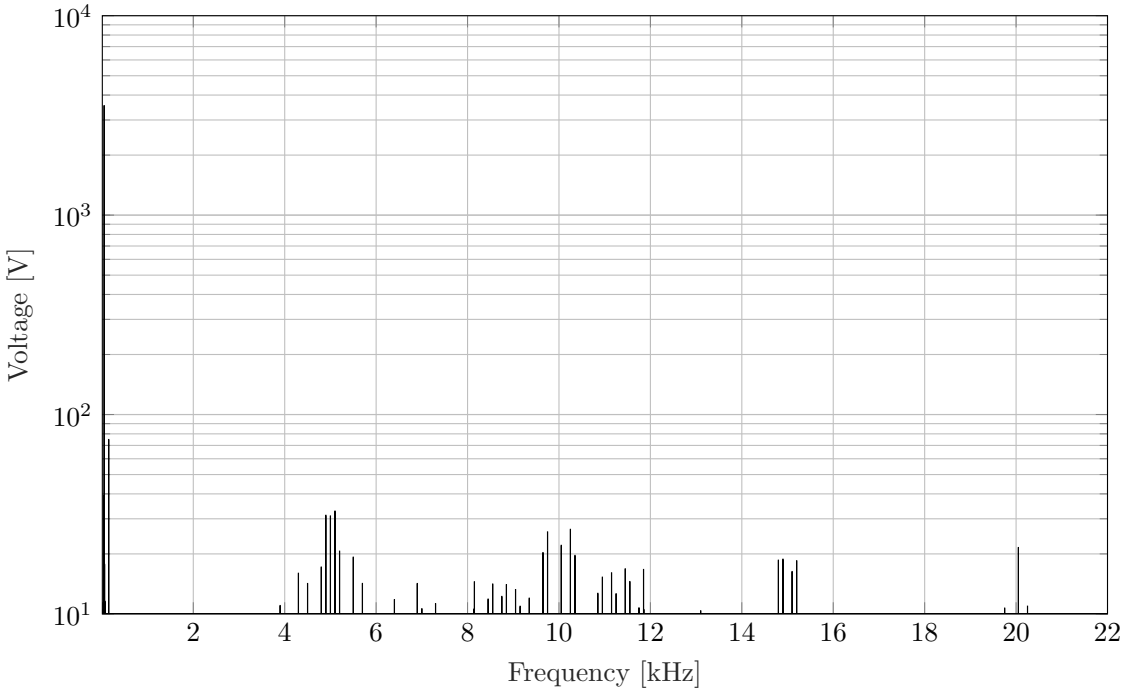

Fig. 9.5: Voltage Spectrum of a M2C Multilevel-Converter

Tab. 9.3: Measurement Uncertainty Budget - one Phase - MS2 with TS2

Quantity	Value	$\delta(U,I,\varphi)$	Probability distribution	$c(U,I,\varphi)$	Uncertainty	Total MU Part
U	3547 V	5.6923 V	Rectangle	1060.5 A	3485.4 W	66.50 %
I	1177 A	1.2905 A	Rectangle	3197.1 V	2382.1 W	31.06 %
φ	25.66°	0.0336°	Rectangle	1.807 MW	0.7 W	2.44 %

Measured Quantity	P
Value	3761.7 kW
Expanded Measurement Uncertainty $\delta_{95\%}$	± 8.5 kW
Coverage factor k	2

Tab. 9.4: Measurement Uncertainty Budget - one Phase - MS1 with TS2

Quantity	Value	$\delta(U,I,\varphi)$	Probability distribution	$c(U,I,\varphi)$	Uncertainty	Total MU Part
U	3547 V	6.132 V	Rectangle	1060.5 A	3754.6 W	3.22 %
I	1177 A	3.2928 A	Rectangle	3197.1 V	6078.0 W	8.44 %
φ	25.66°	1.08°	Rectangle	1.807 MW	19 670 W	88.35 %

Measured Quantity	P
Value	3761.7 kW
Expanded Measurement Uncertainty $\delta_{95\%}$	± 41.854 kW
Coverage factor k	2

Tab. 9.5: Measurement Values and Uncertainty MS2 with TS2

	$\varphi_{50\text{Hz}}$	$\delta_{\varphi,95\%}$	$U_{\text{Phase,TRMS}}$	$\delta_{U,95\%}$	$I_{\text{Phase,TRMS}}$	$\delta_{I,95\%}$
Load 1	25.791°	±0.228°	3545 V	±11.4 V	1178.58 A	±4.06 A
Load 2	24.700°	±0.312°	3606 V	±7.0 V	946.48 A	±1.68 A
Load 3	26.468°	±0.363°	3691 V	±8.0 V	628.30 A	±1.14 A
Load 4	36.365°	± 0.276°	3599 V	±2.2 V	357.86 A	±0.24 A
No-Load 1	84.092°	± 0.486°	3502 V	±10.0 V	189.33 A	±0.48 A

9.5 Uncertainty Type B - Direct Method for Determination of Efficiency

The equation for determination of the efficiency is the model equation for the uncertainty analysis.

$$\eta_{\mathrm{Direct}} = \frac{P_{\mathrm{m}}}{P_1} \tag{9.20}$$

The uncertainty for the efficiency η_{Direct} is a calculated with the uncertainty of the input power $\delta_{\mathrm{P_1}}$ and the output power $\delta_{\mathrm{P_m}}$. The latter one is calculated with a speed and torque measurement, where the torque measurement is the dominating part.

$$\delta_{\eta_{\mathrm{Direct}}} = k \cdot \sqrt{\left(\frac{\partial \eta_{\mathrm{Direct}}}{\partial P_1} \cdot \delta_{\mathrm{P_1}}\right)^2 + \left(\frac{\partial \eta_{\mathrm{Direct}}}{\partial P_m} \cdot \delta_{\mathrm{P_m}}\right)^2} \tag{9.21}$$

The sensitive coefficients are derived from the model equation.

$$\frac{\partial \eta_{\mathrm{Direct}}}{\partial P_1} = -\frac{P_{\mathrm{m}}}{P_1^2} \qquad \frac{\partial \eta_{\mathrm{Direct}}}{\partial P_{\mathrm{m}}} = \frac{1}{P_1} \tag{9.22}$$

The uncertainties are assumed with a normal distribution, which means a coverage factor of $k = 2$. The uncertainty budget is given in the table 9.6.

Tab. 9.6: Measurement Uncertainty Budget - Direct η with Output Power Measurement and Rated Load

Input Quantity	Value	δ	Probability Distribution	Sensitive Coefficient	Uncertainty	Total MU Part
P_1	11 220 kW	3.2 kW	Normal	3.1 $\mathrm{nW^{-1}}$	5.0 μW	1.5 %
P_{m}	10 880 kW	25.2 kW	Normal	89.0 $\mathrm{nW^{-1}}$	1.1 mW	98.5 %
$\delta_{\eta_{\mathrm{Direct}}}$	96.97 %				0.23 %	

9.6 Uncertainty Type B - Back to Back

The equation for determination of the efficiency is the model equation for the uncertainty analysis.

$$\eta_{\mathrm{BtB}} = 1 - \frac{P_{\mathrm{L}} \cdot 2}{P_1 + P_2} \tag{9.23}$$

The uncertainty for the efficiency η_{BtB} is a calculated with the uncertainty of the input power δ_{P_1}, the output power δ_{P_2} and the total losses $\delta_{\mathrm{P}_\mathrm{L}}$. The total losses P_{L} are calculated with the following equation.

$$P_{\mathrm{L}} = \frac{1}{2} \cdot (P_1 - P_2) \tag{9.24}$$

The P_1 is the measured input power and P_2 is the measured output power. The uncertainty for the total losses $\delta_{\mathrm{P}_\mathrm{L}}$ can be determined with the following equation.

$$\delta_{\mathrm{P}_\mathrm{L}} = k \cdot \sqrt{\left(\frac{\partial \mathrm{P}_\mathrm{L}}{\partial P_1} \cdot \delta_{\mathrm{P}_1}\right)^2 + \left(\frac{\partial \mathrm{P}_\mathrm{L}}{\partial P_2} \cdot \delta_{\mathrm{P}_2}\right)^2} \tag{9.25}$$

The sensitive coefficients are derived from equation for the total losses 9.24.

$$\frac{\partial \mathrm{P}_\mathrm{L}}{\partial P_1} = \frac{1}{2} \qquad\qquad \frac{\partial \mathrm{P}_\mathrm{L}}{\partial P_\mathrm{L}} = -\frac{1}{2} \tag{9.26}$$

The uncertainty budget for $\delta_{\mathrm{P}_\mathrm{L}}$ is given in the table 9.7.

Tab. 9.7: Measurement Uncertainty Budget - Back to Back $\delta_{\mathrm{P}_\mathrm{L}}$ with $k = 2$

Input Quantity	Value	δ	Probability Distribution	Sensitive Coeff.	Uncertainty	Total MU Part
P_1	11 220 kW	3.2 kW	Normal	0.5	0.8 kW	50 %
P_2	10 540 kW	3.2 kW	Normal	−0.5	0.8 kW	50 %
$\delta_{\mathrm{P}_\mathrm{L}}$	340 kW				2.3 kW	

The uncertainty for the efficiency $\delta_{\eta_{\mathrm{BtB}}}$ can be determined with the following equation.

$$\delta_{\eta_{\mathrm{BtB}}} = k \cdot \sqrt{\left(\frac{\partial \eta_{\mathrm{BtB}}}{\partial P_1} \cdot \delta_{\mathrm{P}_1}\right)^2 + \left(\frac{\partial \eta_{\mathrm{BtB}}}{\partial P_2} \cdot \delta_{\mathrm{P}_2}\right)^2 + \left(\frac{\partial \eta_{\mathrm{BtB}}}{\partial P_L} \cdot \delta_{\mathrm{P}_\mathrm{L}}\right)^2} \tag{9.27}$$

The sensitive coefficients are derived from the model equation 9.23.

$$\frac{\partial \eta_{\mathrm{BtB}}}{\partial P_1} = \frac{\partial \eta_{\mathrm{BtB}}}{\partial P_2} = \frac{2 \cdot P_{\mathrm{L}}}{(P_1 + P_2)^2} \qquad \frac{\partial \eta_{\mathrm{BtB}}}{\partial P_{\mathrm{L}}} = \frac{2}{P_1 + P_2} \tag{9.28}$$

The uncertainties are assumed with a normal distribution, which means a coverage factor of $k = 2$. The uncertainty budget for $\delta_{\eta_{\mathrm{BtB}}}$ is given in the table 9.8.

Tab. 9.8: Measurement Uncertainty Budget - Back to Back η with $k = 2$

Input Quantity	Value	δ	Probability Distrib.	Sensitive Coeff.	Uncertainty	Total MU Part
P_1	11 220 kW	3.2 kW	Normal	$1.4\,\mathrm{nW}^{-1}$	$2.3\,\mu$W	0.0 %
P_2	10 540 kW	3.2 kW	Normal	$1.4\,\mathrm{nW}^{-1}$	$2.3\,\mu$W	0.0 %
P_{L}	340 kW	2.3 kW	Normal	$-92\,\mathrm{nW}^{-1}$	$-110\,\mu$W	99.9 %
$\delta_{\eta_{\mathrm{BtB}}}$					0.02 %	

9.7 Uncertainty Type B - Indirect Method for Determination of Induction Motor Efficiency

The equation for determination of the efficiency is the model equation for the uncertainty analysis. The method here is not considering the temperature correction of the individual losses. Only the uncertainty of the indirect determination of the efficiency is analysed.

$$\eta_{\mathrm{ID}} = \frac{P_1 - P_{\mathrm{L}}}{P_1} \tag{9.29}$$

The uncertainty for the efficiency η_{ID} is a calculated with the uncertainty of the input power $\delta_{\mathrm{P_1}}$ and the determined losses $\delta_{\mathrm{P_L}}$

$$\delta_\eta = k \cdot \sqrt{\left(\frac{\partial \eta_{\mathrm{ID}}}{\partial P_1} \cdot \delta_{\mathrm{P_1}}\right)^2 + \left(\frac{\partial \eta_{\mathrm{ID}}}{\partial P_{\mathrm{L}}} \cdot \delta_{\mathrm{P_L}}\right)^2} \tag{9.30}$$

The sensitive coefficients are derived from the model equation.

$$\frac{\partial \eta}{\partial P_1} = -\frac{1}{P_1} \qquad\qquad \frac{\partial \eta}{\partial P_{\mathrm{L}}} = \frac{P_{\mathrm{L}}}{{P_1}^2} \tag{9.31}$$

The uncertainties are assumed with a normal distribution, which means a coverage factor of $k = 2$.

Total Losses P_{L} The total losses are a summation of the individual losses.

$$P_{\mathrm{L}} = P_{\mathrm{Cu1}} + P_{\mathrm{Cu2}} + P_{\mathrm{C}} + P_{\mathrm{LL}} \tag{9.32}$$

The sensitive coefficients are equal to one due to the summation.

$$\delta_{\mathrm{P_L}} = k \cdot \sqrt{(\delta_{\mathrm{P_{Cu1}}})^2 + (\delta_{\mathrm{P_{Cu2}}})^2 + (\delta_{\mathrm{P_C}})^2 + (\delta_{\mathrm{P_{LL}}})^2} \tag{9.33}$$

Stator Copper Losses P_{Cu1} The stator copper losses are calculated with the phase current I_{N} in rated point and the stator phase resistance R.

$$P_{\mathrm{Cu1}} = \frac{3}{2} \cdot I_{\mathrm{N}}^2 \cdot R \tag{9.34}$$

The uncertainty is calculated with the uncertainty of the current measurement $\delta_{\mathrm{I_N}}$ and the phase resistance measurement δ_R.

$$\delta_{\mathrm{P_{Cu1}}} = k \cdot \sqrt{\left(\frac{\partial P_{\mathrm{Cu1}}}{\partial I_{\mathrm{N}}} \cdot \delta_{\mathrm{I_N}}\right)^2 + \left(\frac{\partial P_{\mathrm{Cu1}}}{\partial R} \cdot \delta_R\right)^2} \tag{9.35}$$

$$\frac{\partial P_{\mathrm{Cu1}}}{\partial I_{\mathrm{N}}} = 3 \cdot I_{\mathrm{N}} \cdot R \qquad \frac{\partial P_{\mathrm{Cu1}}}{\partial R} = \frac{3}{2} \cdot I_{\mathrm{N}}^2 \tag{9.36}$$

Constant Losses P_{C} The constant losses are calculated with the subtraction of the stator copper losses P_{Cu1} from the measured active power in no load operation P_0

$$P_{\mathrm{C}} = P_0 - P_{\mathrm{Cu1}} \tag{9.37}$$

The sensitive coefficients are equal to one due to the summation, which leads to a geometric sum of the individual uncertainties.

$$\delta_{\mathrm{P_C}} = k \cdot \sqrt{(\delta_{\mathrm{P_0}})^2 + (\delta_{\mathrm{P_{Cu1}}})^2} \tag{9.38}$$

The constant losses are divided in the friction and windage losses P_{FW} and iron losses P_{FE}. The uncertainty of both components is not considered separately. They can be assumed with the uncertainty of the constant losses $\delta_{\mathrm{P_C}}$ due to the determination with one measurement, the no-load test, which is already shown by Aarniovuori in [23].

$$P_{\mathrm{C}} = P_{\mathrm{FW}} + P_{\mathrm{FE}} \tag{9.39}$$

Rotor Copper Losses P_{Cu2} The rotor copper losses are calculated with the stator copper losses P_{Cu1}, the iron losses P_{FE}, the electrical power P_1 and the slip s. The slip is determined in previous works with minor influence due to the less uncertainty of the speed measurement. Further, the rotor copper losses are calculated values for large motors dependent on available and desired the test setup.

$$P_{\mathrm{Cu2}} = (P_1 - P_{\mathrm{Cu1}} - P_{\mathrm{FE}}) \cdot s \tag{9.40}$$

The sensitive coefficients are equal to one due to the summation, which leads to a geometric sum of the individual uncertainties.

$$\delta_{\mathrm{P_{Cu2}}} = k \cdot \sqrt{(\delta_{\mathrm{P_1}})^2 + (\delta_{\mathrm{P_{Cu1}}})^2 + (\delta_{\mathrm{P_C}})^2} \tag{9.41}$$

Stray-Load Losses P_{LL} The stray load losses are calculated with a multiplication of a constant factor with the determined electrical active power in the rated point P_1. If an output measurement is not possible, the constant factor is the best solution for the determination of the stray-load losses of the large motors.

$$P_{\mathrm{LL}} = 0.005 * P_1 \tag{9.42}$$

If a full load-test is not possible, the stray-load losses are dependent on the quadratic of the measured current I to the rated current I_{N}.

$$P_{\mathrm{LL}} = 0.005 * P_1 \cdot \left(\frac{I}{I_{\mathrm{N}}}\right)^2 \tag{9.43}$$

The sensitive coefficient is given by the constant factor and the uncertainty of the stray load losses $\delta_{\mathrm{P_{LL}}}$.

$$\delta_{\mathrm{P_{LL}}} = k \cdot \sqrt{\left(\frac{\partial P_{\mathrm{LL}}}{\partial P_1} \cdot \delta_{\mathrm{P_1}}\right)^2} \qquad \frac{\partial P_{\mathrm{LL}}}{\partial P_1} = 0.005 \tag{9.44}$$

Tab. 9.9: Measurement Uncertainty Budget Induction Machine - Indirect η without Full-Load Test

Input Quantity	Value	δ	Probability Distribution	Sensitive Coefficient	Uncertainty	Total MU Part
P_1	11 220 kW	0 kW	Normal	3.1 $\mathrm{nW^{-1}}$	0 mW	0 %
P_{Cu1}	48 237 kW	1.05 kW	Normal	1 $\mathrm{W^{-1}}$	0.10 mW	10.5 %
P_{Cu2}	157 160 kW	2.28 kW	Normal	1 $\mathrm{W^{-1}}$	0.20 mW	50 %
P_{C}	124 830 kW	2.03 kW	Normal	1 $\mathrm{W^{-1}}$	0.18 mW	39.5 %
P_{LL}	61 962 kW	0 kW	Normal	1 $\mathrm{W^{-1}}$	0 mW	0 %
$\delta_{\eta_{\mathrm{ID}}}$	96.505 %				0.0288 %	

The uncertainties for the active power measurement P_1, the rated current for the stator copper losses calculation and the stray load losses P_{LL} are zero, due to they are calculated value.

10 Bibliography

[1] A. T. de Almeida, F. J. T. E. Ferreira, and G. Baoming.
"Beyond Induction Motors 2014; Technology Trends to Move Up Efficiency".
In: *IEEE Transactions on Industry Applications* 50.3 (2014), pp. 2103–2114.
ISSN: 0093-9994. DOI: 10.1109/TIA.2013.2288425.

[2] F. J. T. E. Ferreira and A. T. de Almeida.
"Reducing Energy Costs in Electric-Motor-Driven Systems: Savings Through Output Power Reduction and Energy Regeneration".
In: *IEEE Industry Applications Magazine* 24.1 (2018), pp. 84–97.
ISSN: 1077-2618. DOI: 10.1109/MIAS.2016.2600685.

[3] "Rotating electrical machines - Part 30-1: Efficiency classes of line operated AC motors (IE code)". In: *IEC 60034-30-1:2014* (2014), pp. 1–50.

[4] "Rotating electrical machines - Part 30-2: Efficiency classes of variable speed AC motors (IE-code)". In: *IEC TS 60034-30-2:2016* (2016), pp. 1–22.

[5] "Rotating electrical machines - Part 2-1: Standard methods for determining losses and efficiency from tests (excluding machines for traction vehicles)".
In: *IEC 60034-2-1:2014 (Revision of IEC 60034-2-1:2007)* (2014), pp. 1–186.

[6] "IEEE Standard Test Procedure for Polyphase Induction Motors and Generators".
In: *IEEE Std 112-2004 (Revision of IEEE Std 112-1996)* (2004), pp. 1–179.
DOI: 10.1109/IEEESTD.2004.95394.

[7] "IEEE Guide for Test Procedures for Synchronous Machines Part I Acceptance and Performance Testing Part II Test Procedures and Parameter Determination for Dynamic Analysis".
In: *IEEE Std 115-2009 (Revision of IEEE Std 115-1995)* (2010), pp. 1–219.
DOI: 10.1109/IEEESTD.2010.5464495.

[8] "Rotating electrical machines - Part 2-3: Specific test methods for determining losses and efficiency of converter-fed AC motors".
In: *IEC TS 60034-2-3:2013* (2013), pp. 1–44.

[9] "Ecodesign For Power Drive Systems, Motor Starters, Power Electronics And Their Driven Applications - Part 2: Energy Efficiency Indicators For Power Drive Systems And Motor Starters". In: *EN 50598-2:2014* (2014), pp. 1–138.

[10] "Ecodesign For Power Drive Systems, Motor Starters, Power Electronics And Their Driven Applications - Part 1: General Requirements For Setting Energy Efficiency Standards For Power Driven Equipment Using The Extended Product Approach (EPA), And Semi Analytic Model (SAM)".
In: *EN 50598-1:2014* (2014), pp. 1–26.

[11] "Ecodesign For Power Drive Systems, Motor Starters, Power Electronics And Their Driven Applications - Part 3: Quantitative Eco Design Approach Through Life Cycle Assessment Including Product Category Rules And The Content Of Environmental Declarations".
In: *EN 50598-3:2015* (2015), pp. 1–50.

[12] I.P. Tsoumas, H. Tischmacher, and P. Kollensperger. "The European Standard EN 50598-2: Efficiency classes of converters and drive systems". In: *Electrical Machines (ICEM), 2014 International Conference on* (2014), pp. 929–935. DOI: 10.1109/ICELMACH.2014.6960292.

[13] "Adjustable speed electrical power drive systems - Part 4: General requirements - Rating specifications for a.c. power drive systems above 1 000 V a.c. and not exceeding 35 kV". In: *IEC 61800-4:2002* (2012), pp. 1–219.

[14] H. Karkkainen, L. Aarniovuori, M. Niemela, and J. Pyrhonen. "Converter-Fed Induction Motor Efficiency: Practical Applicability of IEC Methods".
In: *IEEE Industrial Electronics Magazine* 11.2 (2017), pp. 45–57.
ISSN: 1932-4529. DOI: 10.1109/MIE.2017.2693421.

[15] E.B. Agamloh. "Power and Efficiency Measurement of Motor-Variable Frequency Drive Systems". In: *Pulp and Paper Industry Conference (PPIC), 2015 61st IEEE* (2015), pp. 1–8. ISSN: 0190-2172.
DOI: 10.1109/PPIC.2015.7165864.

[16] R. Antonello, F. Tinazzi, and M. Zigliotto. "Energy efficiency measurements in IM: The non-trivial application of the norm IEC 60034-2-3:2013".
In: *Electrical Machines Design, Control and Diagnosis (WEMDCD), 2015 IEEE Workshop on* (2015), pp. 248–253.
DOI: 10.1109/WEMDCD.2015.7194537.

[17] F. J. T. E. Ferreira, G. Baoming, and A. T. de Almeida.
"Reliability and operation of high-efficiency induction motors".
In: *2015 IEEE/IAS 51st Industrial Commercial Power Systems Technical Conference (I CPS)* (2015), pp. 1–13. ISSN: 2158-4893.
DOI: 10.1109/ICPS.2015.7266412.

[18] A. Möhle. "Determination of motor efficiency on the basis of IEC 60034-2-1 Round-Robin testing for the improvement of the standard".
In: *Motor Summit, Zürich, Switzerland* (2010), pp. 38–39.

[19] H. Karmaker, G.A. Knierim, Mantak Ho, and B. Palle. "Methodologies for Testing a 2 MW Permanent Magnet Wind Turbine Generator".
In: *Power and Energy Society General Meeting, 2011 IEEE* (2011), pp. 1–5.
ISSN: 1944-9925. DOI: 10.1109/PES.2011.6039715.

[20] H. Auinger.
"Determination and designation of the efficiency of electrical machines".
In: *Power Engineering Journal* 13.1 (1999), pp. 15–23. ISSN: 0950-3366.
DOI: 10.1049/pe:19990106.

[21] L. Aarniovuori, P. Rasilo, M. Niemelä, and J. J. Pyrhönen.
"Analysis of 37-kW Converter-Fed Induction Motor Losses".
In: *IEEE Transactions on Industrial Electronics* 63.9 (2016), pp. 5357–5365.
ISSN: 0278-0046. DOI: 10.1109/TIE.2016.2555278.

[22] M. Doppelbauer. "Measurement Uncertainty of Direct And Indirect Efficiency Testing of Induction Machines". In: *Energy Efficiency in Motor Driven Systems, 2015. EEMODS'2015. 9th International Conference on* (2015).

[23] L. Aarniovuori, J. Kolehmainen, A. Kosonen, M. Niemela, and J. Pyrhonen. "Uncertainty in Motor Efficiency Measurements". In: *Electrical Machines (ICEM), 2014 International Conference on* (2014), pp. 323–329. DOI: 10.1109/ICELMACH.2014.6960200.

[24] Johannes Teigelköter, Andreas Stock, Thomas Kowalski, Stefan Staudt, Klaus Lang, and Dirk Eberlein. "Highly dynamic power measurement on the electrical power train of electrical drives". In: *ETG Kongress 2013* (2013).

[25] Christian Lehrmann, Uwe Dreger, and Frank Lienesch. "Wirkungsgradbestimmung an (explosiongeschützten) elektrischen Maschinen - eine Übersicht unter den Aspekten der Messunsicherheit". In: *ETG Kongress 2011* (2011).

[26] Paul Braun and Fluri Rolf. "Elektrische Leistungsmessung für einen Kompressorprüfstand". In: *etz Elektrotechnik und Automation* 132.8 (2011), pp. 40–47.

[27] Christian Lehrmann, Uwe Dreger, and Frank Lienesch. "Wirkungsgradbestimmung an elektrischen Maschinen, gegenüberstellung und Optimierung verschiedener Verfahren". In: *electrosuisse and VSE* (Nov. 2010), pp. 37–43.

[28] David Lindenthaler and Georg Brasseur. "AC power measurements of electric drives: a method incorporating calorimetry and DC measurements only". In: *e & i Elektrotechnik und Informationstechnik* 134.2 (2017), pp. 197–202. ISSN: 1613-7620. DOI: 10.1007/s00502-017-0488-0.

[29] L. Aarniovuori, H. Kärkkäinen, A. Kosonen, J. Pyrhönen, Z. Liu, and W. Cao. "Overview of calorimetric systems used in loss determination of electric motors and drives". In: *IECON 2017 - 43rd Annual Conference of the IEEE Industrial Electronics Society* (2017), pp. 2110–2115. DOI: 10.1109/IECON.2017.8216354.

[30] E. B. Agamloh. "A Comparison of direct and indirect measurement of induction motor efficiency". In: *2009 IEEE International Electric Machines and Drives Conference* (2009), pp. 36–42. DOI: 10.1109/IEMDC.2009.5075180.

[31] Erik Sperling and Peter Schegner. "A possibility to measure power quality with RC-divider". In: *Electricity Distribution (CIRED 2013), 22nd International Conference and Exhibition on* (2013), pp. 1–4. DOI: 10.1049/cp.2013.0602.

[32] A. Cataliotti, V. Cosentino, and S. Nuccio. "The Measurement of Reactive Energy in Polluted Distribution Power Systems: An Analysis of the Performance of Commercial Static Meters". In: *Power Delivery, IEEE Transactions on* 23.3 (2008), pp. 1296–1301. ISSN: 0885-8977. DOI: 10.1109/TPWRD.2008.919239.

[33] E. So. "Harmonic Measurements: Current and Voltage Transducers". In: *Power Engineering Society General Meeting, 2003, IEEE* 1 (2003), –98 Vol. 1. DOI: 10.1109/PES.2003.1267138.

[34] S. Svensson. "Power Measurement Techniques for Nonsinusoidal Conditions: The Significance of Harmonics for the Measurement of Power and Other AC Quantities". PhD thesis. 1999. ISBN: 9789171977601.

[35] E. So and B. Djokic. "A New Current-Comparator-Based High-Voltage Low-Power-Factor Wattmeter". In: *IEEE Transactions on Instrumentation and Measurement* 48.2 (1999), pp. 434–438. ISSN: 0018-9456. DOI: 10.1109/19.769619.

[36] M. Kaczmarek and S. Jama. "Accuracy of inductive voltage transformer in the presence of voltage high harmonics". In: *2014 ICHVE International Conference on High Voltage Engineering and Application* (2014), pp. 1–4. DOI: 10.1109/ICHVE.2014.7035462.

[37] M. Freiburg, M. Krüger, F. Predl, and J. Frank. "Messung und Modellierung des Magnetisierungsverhaltens induktiver Spannungswand-ler im Kontext eines neuen, modellbasierten Vor-Ort-Genauigkeitsnachweises". In: *Diagnostik Elektrischer Betriebsmittel* (2014).

[38] M. Klatt, J. Meyer, M. Elst, and P. Schegner. "Frequency Responses of MV voltage transformers in the range of 50 Hz to 10 kHz". In: *Harmonics and Quality of Power (ICHQP), 2010 14th International Conference on* (2010), pp. 1–6. DOI: 10.1109/ICHQP.2010.5625484.

[39] S. Zhao, H.Y. Li, Crossley P, and F. Ghassemi. "Testing and modelling of voltage transformer for high order harmonic measurement". In: *Electric Utility Deregulation and Restructuring and Power Technologies (DRPT), 2011 4th International Conference on* (2011), pp. 229–233. DOI: 10.1109/DRPT.2011.5993894.

[40] J. Meyer, R. Stiegler, M. Klatt, M. Elst, and E. Sperling. "Accuracy of Harmonic Voltage Measurement in the Frequency Range up to 5 kHz using conventional Instrument Transformers". In: *International Conference on Electrical Distribution, 2011 CIRED 21th International Conference on* 0917 (2011), pp. 1–4.

[41] R. Stiegler, J. Meyer, and P. Schegner. "Portable measurement system for the frequency response of voltage transformers". In: *Harmonics and Quality of Power (ICHQP), 2012 IEEE 15th International Conference on* (2012), pp. 745–750. ISSN: 1540-6008. DOI: 10.1109/ICHQP.2012.6381233.

[42] T. Pfajfar, J. Meyer, P. Schegner, and I. Papic. "Influence of instrument transformers on harmonic distortion assessment". In: *Power and Energy Society General Meeting, 2012 IEEE* (2012), pp. 1–6. ISSN: 1944-9925. DOI: 10.1109/PESGM.2012.6345309.

[43] K. Draxler, R. Prochazka, J. Hlavaček, M. Knenicky, and R. Styblikova. "Use of a Nanocrystalline Core for a Precise Non-invasive AC Current Measurement". In: *2016 Conference on Precision Electromagnetic Measurements (CPEM 2016)* (2016), pp. 1–2. DOI: 10.1109/CPEM.2016.7540492.

[44] C. Buchhagen, C. Reese, L. Hofmann, and H. Daumling. "Calculation of the Frequency Response of Inductive Medium Voltage Transformers". In: *Energy Conference and Exhibition (ENERGYCON), 2012 IEEE International* (2012), pp. 794–799. DOI: 10.1109/EnergyCon.2012.6348259.

[45] C. Buchhagen, M. Fischer, L. Hofmann, and H. Daumling. "Metrological determination of the frequency response of inductive voltage transformers up to 20 kHz". In: *Power and Energy Society General Meeting (PES), 2013 IEEE* (2013), pp. 1–5. ISSN: 1944-9925. DOI: 10.1109/PESMG.2013.6672835.

[46] C. Buchhagen, L. Hofmann, and H. Daumling. "Compensation of the first natural frequency of inductive medium voltage transformers". In: *Power System Technology (POWERCON), 2012 IEEE International Conference on* (2012), pp. 1–6. DOI: 10.1109/PowerCon.2012.6401406.

[47] C. Buchhagen, A. Pawellek, L. Hofmann, and H. Daumling. "Analysis of an inductive medium voltage transformer with compensated first natural frequency". In: *Power and Energy Society General Meeting (PES), 2013 IEEE* (2013), pp. 1–5. ISSN: 1944-9925. DOI: 10.1109/PESMG.2013.6672839.

[48] G. Crotti, D. Gallo, D. Giordano, C. Landi, M. Luiso, and M. Modarres. "Frequency Response of MV Voltage Transformer Under Actual Waveforms". In: *IEEE Transactions on Instrumentation and Measurement* 66.6 (2017), pp. 1146–1154. ISSN: 0018-9456. DOI: 10.1109/TIM.2017.2652638.

[49] M. Faifer, R. Ottoboni, S. Toscani, C. Cherbaucich, M. Gentili, and P. Mazza. "A medium voltage signal generator for the testing of voltage measurement transducers". In: *Instrumentation and Measurement Technology Conference (I2MTC), 2013 IEEE International* (2013), pp. 194–199. ISSN: 1091-5281. DOI: 10.1109/I2MTC.2013.6555408.

[50] A. Brandolini, M. Faifer, and R. Ottoboni. "A Simple Method for the Calibration of Traditional and Electronic Measurement Current and Voltage Transformers". In: *Instrumentation and Measurement, IEEE Transactions on* 58.5 (2009), pp. 1345–1353. ISSN: 0018-9456. DOI: 10.1109/TIM.2008.2009184.

[51] Hédio Tatizawa, Erasmo Silveira Neto, Geraldo Francisco Burani, Antonio A.C. Arruda, Kleiber T. Soletto, and Nelson M. Matsuo. *Calibration of High Voltage Transducer for Power Quality Measurements in Electric Networks*. Ed. by Andreas Eberhard. 2011, pp. 237–254. DOI: 10.5772/595.

[52] G. Crotti, D. Giordano, and A. Sardi. "Development of a RC medium voltage divider for on-site use". In: *Precision Electromagnetic Measurements (CPEM), 2010 Conference on* (2010), pp. 655–656. DOI: 10.1109/CPEM.2010.5544525.

[53] G. Crotti, D. Giordano, D. Bartalesi, C. Cherbaucich, and P. Mazza. "Set-up of calibration systems for inductive and electronic measurement transformers". In: *Applied Measurements for Power Systems (AMPS), 2013 IEEE International Workshop on* (2013), pp. 24–28. DOI: 10.1109/AMPS.2013.6656220.

[54] G. Crotti, D. Gallo, D. Giordano, C. Landi, and M. Luiso. "Medium Voltage Divider Coupled With an Analog Optical Transmission System". In: *Instrumentation and Measurement, IEEE Transactions on* 63.10 (2014), pp. 2349–2357. ISSN: 0018-9456. DOI: 10.1109/TIM.2014.2317294.

[55] E. Mohns, P. Räther, and H. Badura. "An AC Power Standard for Loss Measurement Systems for Testing Power Transformers". In: *IEEE Transactions on Instrumentation and Measurement* 66.9 (2017), pp. 2225–2232. ISSN: 0018-9456. DOI: 10.1109/TIM.2017.2698678.

[56] G. Aristoy, A. Santos, and D. Slomovitz. "Testing Methods for Measuring the Effects of Stray Capacitances on High-Voltage Current Transformers". In: *Instrumentation and Measurement, IEEE Transactions on* 64.8 (2015), pp. 2200–2207. ISSN: 0018-9456. DOI: 10.1109/TIM.2015.2393395.

[57] A. Cataliotti, D. Di Cara, A.E. Emanuel, and S. Nuccio. "Improvement of Hall Effect Current Transducer Metrological Performances in the Presence of Harmonic Distortion". In: *Instrumentation and Measurement, IEEE Transactions on* 59.5 (2010), pp. 1091–1097. ISSN: 0018-9456. DOI: 10.1109/TIM.2009.2038308.

[58] A. Cataliotti, D. Di Cara, A.E. Emanuel, and S. Nuccio. "A Novel Approach to Current Transformer Characterization in the Presence of Har-monic Distortion". In: *Instrumentation and Measurement, IEEE Transactions on* 58.5 (2009), pp. 1446–1453. ISSN: 0018-9456. DOI: 10.1109/TIM.2008.2009419.

[59] A. Cataliotti, D. Di Cara, P.A. Di Franco, A.E. Emanuel, and S. Nuccio. "Frequency response of Measurement Current Transformers". In: *Instrumentation and Measurement Technology Conference Proceedings, 2008. IMTC 2008. IEEE* (2008), pp. 1254–1258. ISSN: 1091-5281. DOI: 10.1109/IMTC.2008.4547234.

[60] A. E. Emanuel and J. A. Orr. "Current Harmonics Measurement by Means of Current Transformers". In: *IEEE Transactions on Power Delivery* 22.3 (2007), pp. 1318–1325. ISSN: 0885-8977. DOI: 10.1109/TPWRD.2007.900108.

[61] N. Locci and C. Muscas. "Hysteresis and eddy currents compensation in current transformers". In: *Power Delivery, IEEE Transactions on* 16.2 (2001), pp. 154–159. ISSN: 0885-8977. DOI: 10.1109/61.915475.

[62] Fernando Garnacho, Abderrahim Khamlichi, and Jorge Rovira. "The Design and Characterization of a Prototype Wideband Voltage Sensor Based on a Resistive Divider". In: *Sensors* 17.11 (2017).

[63] Dipl.-Ing. Georg Monien. "Die Beeinflussung der Messabweichung von Feldsonden und Stromzangen durch reale Umgebungsbedingungen". PhD thesis. 2003.

[64] M. Faifer and R. Ottoboni. "An Electronic Current Transformer Based on Rogowski Coil". In: *Instrumentation and Measurement Technology Conference Proceedings, 2008. IMTC 2008. IEEE* (2008), pp. 1554–1559. ISSN: 1091-5281. DOI: 10.1109/IMTC.2008.4547290.

[65] Dipl.-Ing. Stephan Kloska. "Untersuchungen zum Einsatz von miniaturisierter konventioneller Stromwandler und Rogowskispulen in der Mittelspannungstechnik unter besonderer Berücksichtigung der EMV". PhD thesis. 1995.

[66] M. Kaczmarek. "Development and application of the differential voltage to single-ended voltage converter to determine the composite error of voltage transformers and dividers for transformation of sinusoidal and distorted voltages". English. In: *Measurement* 101.Complete (2017), pp. 53–61. DOI: 10.1016/j.measurement.2017.01.021.

[67] M. Kaczmarek. "Accuracy of Current Transformer with Current Errors at Harmonics Equal to the Limiting Values Defined in IEC 60044-8 Standard for Transformation of Distorted Primary Current". In: *2015 Modern Electric Power Systems (MEPS)* (2015), pp. 1–4. DOI: 10.1109/MEPS.2015.7477205.

[68] M. Kaczmarek. "Operation of Inductive Protective Current Transformer in Condition of Distorted Current Transformation".
In: *2015 Modern Electric Power Systems (MEPS)* (2015), pp. 1–4.
DOI: 10.1109/MEPS.2015.7477206.

[69] A. Brandolini, M. Faifer, and R. Ottoboni.
"A Novel and Simple Method for VT and CT Calibration".
In: *Instrumentation and Measurement Technology Conference Proceedings, 2008. IMTC 2008. IEEE* (2008), pp. 1879–1884. ISSN: 1091-5281.
DOI: 10.1109/IMTC.2008.4547352.

[70] A-R A M Makky, H. Abo-Zied, F.N. Abdelbar, and P. Mutschler.
"Design of the instrument current transformer for high frequency high power applications". In: *Power System Conference, 2008. MEPCON 2008. 12th International Middle-East* (2008), pp. 230–233.
DOI: 10.1109/MEPCON.2008.4562343.

[71] F. Du, Z. Liu, W. Chen, Y. Zhuo, and M. Anheuser. "A Novel Combined Alternate Current Sensor for Variable-Frequency Scenario".
In: *2017 IEEE International Workshop on Applied Measurements for Power Systems (AMPS)* (2017), pp. 1–5. DOI: 10.1109/AMPS.2017.8078342.

[72] M. Klatt, J. Meyer, and P. Schegner. "Comparison of measurement methods for the frequency range of 2 kHz to 150 kHz". In: *2014 16th International Conference on Harmonics and Quality of Power (ICHQP)* (2014), pp. 818–822.
ISSN: 1540-6008. DOI: 10.1109/ICHQP.2014.6842791.

[73] D. Williamson. *Discrete-time Signal Processing: An Algebraic Approach.* Advanced Textbooks in Control and Signal Processing. Springer London, 2012.
ISBN: 9781447105411.

[74] D. Lindenthaler. "Signal-bandwidth evaluation for electric power calculation in PWM driven motors". In: *29th Conference on Precision Electromagnetic Measurements (CPEM 2014)* (2014), pp. 626–627. ISSN: 0589-1485.
DOI: 10.1109/CPEM.2014.6898541.

[75] D. Lindenthaler and G. Brasseur. "Signal-Bandwidth Evaluation for Power Measurements in Electric Automotive Drives". In: *IEEE Transactions on Instrumentation and Measurement* 64.6 (2015), pp. 1336–1343.
ISSN: 0018-9456. DOI: 10.1109/TIM.2015.2419052.

[76] D Lindenthaler and H Zangl. "Evaluation of Uncertainty in AC Power Calculation with Asynchronously Sampled Data".
In: *Journal of Physics: Conference Series* 450.1 (2013), p. 012043.

[77] F. Avallone, C. De Capua, and C. Landi. "Measurement station performance optimization for testing on high efficiency variable speed drives".
In: *Quality Measurement: The Indispensable Bridge between Theory and Reality (No Measurements? No Science! Joint Conference - 1996: IEEE Instrumentation and Measurement Technology Conference and IMEKO Tec* 2 (1996), 1098–1103 vol.2. DOI: 10.1109/IMTC.1996.507334.

[78] P. Arpaia, F. Avallone, A. Baccigalupi, and C. DeCapua. "Real-Time Algorithms for Active Power Measurements on PWM-Based Electric Drives".
In: *Instrumentation and Measurement Technology Conference, 1995. IMTC/95. Proceedings. Integrating Intelligent Instrumentation and Control., IEEE* (1995), pp. 680–. DOI: 10.1109/IMTC.1995.515404.

[79] G. Betta, C. Liguori, and A. Pietrosanto. "Structured approach to estimate the measurement uncertainty in digital signal elaboration algorithms". In: *Science, Measurement and Technology, IEE Proceedings* - 146.1 (1999), pp. 21–26. ISSN: 1350-2344. DOI: 10.1049/ip-smt:19990001.

[80] Giovanni Betta, Consolatina Liguori, and Antonio Pietrosanto. "Propagation of uncertainty in a discrete Fourier transform algorithm". In: *Measurement* 4 (), pp. 231 –239. ISSN: 0263-2241. DOI: http://dx.doi.org/10.1016/S0263-2241(99)00068-8.

[81] R. Langella and A. Testa. "The effects of integration intervals on recursive rms and powers measurement in the presence of non-sinusoidal conditions". In: *2010 IEEE International Workshop on Applied Measurements for Power Systems* (2010), pp. 47–52. DOI: 10.1109/AMPS.2010.5609518.

[82] R. Langella and A. Testa. "The effects of the smoothing of the results on the measurement accuracy of RMS and powers in systems under nonsinusoidal conditions". In: *2008 13th International Conference on Harmonics and Quality of Power* (2008), pp. 1–6. ISSN: 1540-6008. DOI: 10.1109/ICHQP.2008.4668822.

[83] N. M. Natalinova, O. V. Galtseva, and E. A. Moldovanova. "Express evaluation of measurement uncertainty digital power meter in LabVIEW". In: *2016 Third International Conference on Electrical, Electronics, Computer Engineering and their Applications (EECEA)* (2016), pp. 52–56. DOI: 10.1109/EECEA.2016.7470765.

[84] J. Kolanko, Z. Leonowicz, L. Ładniak, P. Musz, J. Dudzik, P. Modzel, and Z. Wierzbicki. "AC power and energy measurements based on physical definitions". In: *2015 IEEE 15th International Conference on Environment and Electrical Engineering (EEEIC)* (2015), pp. 1620–1624. DOI: 10.1109/EEEIC.2015.7165414.

[85] A. Cataliotti, D. Di Cara, A.E. Emanuel, and S. Nuccio. "Current Transformers Effects on the Measurement of Harmonic Active Power in LV and MV Networks". In: *Power Delivery, IEEE Transactions on* 26.1 (2011), pp. 360–368. ISSN: 0885-8977. DOI: 10.1109/TPWRD.2010.2079336.

[86] A. Bernieri, L. Ferrigno, M. Laracca, and C. Landi. "Efficiency of active electrical power consumption in the presence of harmonic pollution: a sensitive analysis". In: *Instrumentation and Measurement Technology Conference (I2MTC), 2010 IEEE* (2010), pp. 1447–1452. ISSN: 1091-5281. DOI: 10.1109/IMTC.2010.5487994.

[87] A. Cataliotti, D. Di Cara, A. E. Emanuel, and S. Nuccio. "Influence of Current Transformers on the Measurement of Harmonic Active Power". In: *Exploring New Frontiers of Instrumentation and Methods for Electrical and Electronic Measurements, 2008. 16th IMEKO TC4 Symposium* (2008).

[88] H.E. Jordan, R.C. Zowarka, T.J. Hotz, and J.R. Uglum. "Induction Motor Performance Testing With an Inverter Power Supply: Part 1". In: *Magnetics, IEEE Transactions on* 43.1 (2007), pp. 242–245. ISSN: 0018-9464. DOI: 10.1109/TMAG.2006.887671.

[89] R.C. Zowarka, T.J. Hotz, J.R. Uglum, and H.E. Jordan. “Induction Motor Performance Testing With an Inverter Power Supply: Part 2”. In: *Magnetics, IEEE Transactions on* 43.1 (2007), pp. 275–278. ISSN: 0018-9464. DOI: 10.1109/TMAG.2006.887599.

[90] F. Holzmann. *Leistungsmessung bei dreiphasigen Stromrichterantrieben.* Forschungsberichte des Landes Nordrhein-Westfalen. VS Verlag für Sozialwissenschaften, 2013. ISBN: 9783322884473.

[91] C. Bassi, M. Filippo, D. Giulivo, and A. Tessarolo. “Experimental Assessment of Medium-Voltage Induction Motor Performance Under Multilevel PWM Inverter Supply”. In: *Power Electronics, Electrical Drives, Automation and Motion (SPEEDAM), 2012 International Symposium on* (2012), pp. 253–258. DOI: 10.1109/SPEEDAM.2012.6264451.

[92] A. Tessarolo, G. Zocco, and C. Tonello. “Design and testing of a 45-MW 100-Hz quadruple-star synchronous motor for a Liquefied Natural Gas turbo-compressor drive”. In: *Industry Applications, IEEE Transactions on* 47.3 (2011), pp. 1210–1219. ISSN: 0093-9994. DOI: 10.1109/TIA.2011.2126036.

[93] S. Schröder, Pierluigi Tenca, T. Geyer, P. Soldi, L.J. Garces, R. Zhang, T. Toma, and P. Bordignon. “Modular High-Power Shunt-Interleaved Drive System: A Realization up to 35 MW for Oil and Gas Applications”. In: *Industry Applications, IEEE Transactions on* 46.2 (2010), pp. 821–830. ISSN: 0093-9994. DOI: 10.1109/TIA.2010.2041084.

[94] F. Endrejat and B. van Blerk. “Large medium voltage drives -efficiency, energy savings and availability”. In: *PCIC Europe 2010 Conference Record* (2010), pp. 1–8. ISSN: 2151-7665.

[95] H. Walter, A. Moehle, and M. Bade. “Asynchronous Solid Rotors as High-Speed Drives in the Megawatt Range”. In: *2007 IEEE Petroleum and Chemical Industry Technical Conference* (2007), pp. 1–8. ISSN: 0090-3507. DOI: 10.1109/PCICON.2007.4365799.

[96] A. Antonopoulos, G. Moree, J. Soulard, L. Angquist, and H.-P. Nee. “Experimental evaluation of the impact of harmonics on induction motors fed by modular multilevel converters”. In: *Electrical Machines (ICEM), 2014 International Conference on* (2014), pp. 768–775. DOI: 10.1109/ICELMACH.2014.6960268.

[97] D. Buzzini and M. Zago. “Testing Large ASDS”. In: *Industry Applications, IEEE Transactions on* 49.4 (2013), pp. 1873–1882. ISSN: 0093-9994. DOI: 10.1109/TIA.2013.2255851.

[98] A. Tessarolo, C. Bassi, and D. Giulivo. “Performance of a high-power induction motor supplied by two in-phase voltage-source inverters”. In: *EUROCON - International Conference on Computer as a Tool (EUROCON), 2011 IEEE* (2011), pp. 1–4. DOI: 10.1109/EUROCON.2011.5929415.

[99] Christian Jäckle. “Measuring Frequency Converters, Which Accuracy can you expect?” In: *ZES Zimmer, Application Note 109* (2013).

[100] Antonio Cataliotti, Valentina Cosentino, Dario Di Cara, Alessandro Lipari, and Salvatore Nuccio.
"A DAQ-based sampling wattmeter for IEEE Std. 1459-2010 powers measurements. Uncertainty evaluation in nonsinusoidal conditions".
In: *Measurement* 61.0 (2015), pp. 27 –38. ISSN: 0263-2241.
DOI: http://dx.doi.org/10.1016/j.measurement.2014.10.033.

[101] A.J. Schwab and W. Kürner. *Elektromagnetische Verträglichkeit.*
VDI-Buch, Springer Berlin Heidelberg, 2010. ISBN: 9783642166105.
DOI: 10.1007/978-3-642-16610-5.

[102] R. Lampl and F. Healy.
"Power analysis of converter drives-digital transient torque measurement".
In: *Power Electronics and Variable Speed Drives, 1998. Seventh International Conference on (Conf. Publ. No. 456)* (1998), pp. 579–585. ISSN: 0537-9989.
DOI: 10.1049/cp:19980590.

[103] Spielbauer, Hans-Kilian. "Ein Verfahren zur Leistungsmessung an Stromrichtern mit Wechselanteilen hoher Frequenz in Strom und Spannung".
PhD thesis. 1990.

[104] O. Drubel.
Converter Applications and Their Influence on Large Electrical Machines.
Lecture Notes in Electrical Engineering Series.
Springer London, Limited, 2013. ISBN: 9783642362811.

[105] Dipl.-Ing. Sven Tschirley. "Automatisierte messtechnische Charakterisierung von 10kV Integrierten Gate-kommutierten Thyristoren (IGCTs)".
PhD thesis. 2007.

[106] J. Rodriguez, S. Bernet, B. Wu, J. O. Pontt, and S. Kouro. "Multilevel Voltage-Source-Converter Topologies for Industrial Medium-Voltage Drives".
In: *IEEE Transactions on Industrial Electronics* 54.6 (2007), pp. 2930–2945.
ISSN: 0278-0046. DOI: 10.1109/TIE.2007.907044.

[107] S. Rohner. *Untersuchung des Modularen Mehrpunktstromrichters M2C für Mittelspannungsanwendungen.* Verlag Dr. Hut, 2011. ISBN: 9783868539332.

[108] R. D. Klug and N. Klaassen.
"High power medium voltage drives - innovations, portfolio, trends".
In: *2005 European Conference on Power Electronics and Applications* (2005), 10 pp.–P.10. DOI: 10.1109/EPE.2005.219669.

[109] R. Vargas, J. Rodriguez, C. A. Rojas, and M. Rivera.
"Predictive Control of an Induction Machine Fed by a Matrix Converter With Increased Efficiency and Reduced Common-Mode Voltage".
In: *IEEE Transactions on Energy Conversion* 29.2 (2014), pp. 473–485.
ISSN: 0885-8969. DOI: 10.1109/TEC.2014.2299594.

[110] B. Wu, J. Pontt, J. Rodriguez, S. Bernet, and S. Kouro.
"Current-Source Converter and Cycloconverter Topologies for Industrial Medium-Voltage Drives".
In: *IEEE Transactions on Industrial Electronics* 55.7 (2008), pp. 2786–2797.
ISSN: 0278-0046. DOI: 10.1109/TIE.2008.924175.

[111] J. Kang, E. Yamamoto, M. Ikeda, and E. Watanabe. "Medium-Voltage Matrix Converter Design Using Cascaded Single-Phase Power Cell Modules".
In: *IEEE Transactions on Industrial Electronics* 58.11 (2011), pp. 5007–5013.
ISSN: 0278-0046. DOI: 10.1109/TIE.2011.2148679.

[112] A.K. Abdelsalam, M.I. Masoud, M.S. Hamad, and B.W. Williams. "Improved Sensorless Operation of a CSI-Based Induction Motor Drive: Long Feeder Case".
In: *Power Electronics, IEEE Transactions on* 28.8 (2013), pp. 4001–4012. ISSN: 0885-8993. DOI: 10.1109/TPEL.2012.2230648.

[113] F. Jenni and D. Wüest. *Steuerverfahren für selbstgeführte Stromrichter.* vdf Hochschulverlag AG and B.G. Teubner Verlag, 1995.

[114] S. Madhusoodhanan, K. Mainali, A. Tripathi, K. Vechalapu, and S. Bhattacharya. "Medium voltage (>2.3 kV) high frequency three-phase two-level converter design and demonstration using 10 kV SiC MOSFETs for high speed motor drive applications". In: *2016 IEEE Applied Power Electronics Conference and Exposition (APEC)* (2016), pp. 1497–1504. DOI: 10.1109/APEC.2016.7468066.

[115] M. Glinka. *Modulares Mehrpunkt-Umrichtersystem - ein neuartiges Konzept am Beispiel der elektrischen Traktion.* Forschungsberichte Leistungselektronik und Steuerungen. Shaker Verlag, 2011. ISBN: 9783844001051.

[116] M. Galek. *M2C-Converter auf Basis von MOS-Transistoren für Niederspannungsnetze.* Forschungsberichte Leistungselektronik und Steuerungen. 2016. ISBN: 9783844048704.

[117] S. M. Goetz, A. V. Peterchev, and T. Weyh. "Modular Multilevel Converter With Series and Parallel Module Connectivity: Topology and Control".
In: *IEEE Transactions on Power Electronics* 30.1 (2015), pp. 203–215. ISSN: 0885-8993. DOI: 10.1109/TPEL.2014.2310225.

[118] L. M. Tolbert, Fang Zheng Peng, and T. G. Habetler. "Multilevel converters for large electric drives".
In: *IEEE Transactions on Industry Applications* 35.1 (1999), pp. 36–44. ISSN: 0093-9994. DOI: 10.1109/28.740843.

[119] C. Newton, M. Sumner, and T. Alexander. "Multi-level converters: a real solution to high voltage drives?"
In: *IEE Colloquium on Update on New Power Electronic Techniques (Digest No: 1997/091)* (1997), pp. 3/1–3/5. DOI: 10.1049/ic:19970529.

[120] V. N. Ferreira, G. A. Mendonça, A. V. Rocha, R. S. Resende, and B. J. Cardoso Filho. "Medium voltage IGBT-based converters in mine hoist systems".
In: *2016 IEEE Industry Applications Society Annual Meeting* (2016), pp. 1–8. DOI: 10.1109/IAS.2016.7731919.

[121] *PLECS - The Simulation Platform for Power Electronic Systems - User Manual.* Version 4.0. Plexim GmbH. 2016.

[122] Redzo Muratovic, Thomas Mallits, and Ernst Schmautzer. "Berechnung der wechselseitigen ohmschen und induktiven Beeinflussung durch Höchs-tspannungs-Kabelsysteme".
In: *e&i Elektrotechnik und Informationstechnik* 131.8 (2014), pp. 329–335. DOI: 10.1007/s00502-014-0269-y.

[123] H. Prassler. “Kettenleiter-Netzmodell für das elektromagnetische Feld in den Nuten elektrischer Maschinen”.
In: *Archiv für Elektrotechnik* 56.4 (1974), pp. 212–216. ISSN: 1432-0487. DOI: 10.1007/BF01496738.

[124] D. Schröder. *Elektrische Antriebe - Grundlagen: Mit durchgerechneten Übungs- und Prüfungsaufgaben*. Springer-Lehrbuch. Springer Berlin Heidelberg, 2017. ISBN: 9783642304712.

[125] D. Schröder.
Leistungselektronische Schaltungen: Funktion, Auslegung und Anwendung.
Springer-Lehrbuch. Springer Berlin Heidelberg, 2012. ISBN: 9783642301049.

[126] ISO/IEC. *Guide 98-3: Uncertainty of measurement – Part 3: Guide to the expression of uncertainty in measurement (GUM:1995)*. Tech. rep.
Geneve, 2008.

[127] Seung-Ho Song, Jong-Woo Choi, and Seung-Ki Sul.
“Current measurements in digitally controlled AC drives”.
In: *Industry Applications Magazine, IEEE* 6.4 (2000), pp. 51–62.
ISSN: 1077-2618. DOI: 10.1109/2943.847916.

[128] D.W. Clarke. “Designing phase-locked loops for instrumentation applications”.
In: *Measurement* 32.3 (2002), pp. 205 –227. ISSN: 0263-2241.

[129] F.M. Gardner. *Phaselock Techniques*. Wiley, 2005. ISBN: 9780471732686.

[130] “Instrument transformers –Part 8: Electronic current transformers”.
In: *IEC 60044-8:2002* (2002).

[131] A. Heimbrock and H.O. Seinsch. “Neue Erkenntnisse über Oberschwingungsverluste in umrichtergespeisten Käfigläufern”.
In: *e & i Elektrotechnik und Informationstechnik* 7/8 (2005), pp. 274–282.

[132] H. Neudorfer, E. Schmidt, and F. Müllner.
“Analytische Berechnung und messtechnischer Vergleich von Zusatzverlusten stromrichtergespeister Asynchron-Traktionsmaschinen”. German.
In: *e & i Elektrotechnik und Informationstechnik* 128.5 (2011), pp. 142–150.
ISSN: 0932-383X. DOI: 10.1007/s00502-011-0824-8.

[133] R. Lerch. *Elektrische Messtechnik: Analoge, Digitale Und Computergestutzte Verfahren, 6., Bearb. Aufl. 2013*. Springer-Lehrbuch.
Springer Berlin Heidelberg, 2012. ISBN: 9783642226083.

[134] J. Zitzelsberger. *Optimierte Raumzeigermodulation zur Verringerung gleichtaktbedingter Lagerströme*. Berichte aus der Elektrotechnik. Shaker, 2007.
ISBN: 9783832266462.

[135] “IEEE Standard for Terminology and Test Methods for Analog-to-Digital Converters”.
In: *IEEE Std 1241-2010 (Revision of IEEE Std 1241-2000)* (2011), pp. 1–139.
DOI: 10.1109/IEEESTD.2011.5692956.

[136] A. Cataliotti, V. Cosentino, D. Di Cara, A. Lipari, S. Nuccio, and C. Spataro.
“Development of a high-accuracy PC-based wattmeter with commercial data acquisition boards”. In: *Instrumentation and Measurement Technology Conference (I2MTC), 2011 IEEE* (2011), pp. 1–5. ISSN: 1091-5281.
DOI: 10.1109/IMTC.2011.5944271.

[137] G. Cipriani, R. Miceli, and C. Spataro. “Uncertainty evaluation in the measurements for the electric power quality analysis”.
In: *2013 International Conference on Renewable Energy Research and Applications (ICRERA)* (2013), pp. 1151–1156.
DOI: 10.1109/ICRERA.2013.6749926.

[138] Salvatore Nuccio and Ciro Spataro. *Figures of Merit for Analog-to-Digital Converters: The Optimal Set for the Uncertainty Evaluation.* 2008.

[139] Salvatore Nuccio and Ciro Spataro.
“A Monte Carlo method for the auto-evaluation of the uncertainties in analog-to-digital conversion-based measurements”.
In: *COMPEL - The international journal for computation and mathematics in electrical and electronic engineering* 23.1 (2004), pp. 148–158.
DOI: 10.1108/03321640410507617.
eprint: http://dx.doi.org/10.1108/03321640410507617.

[140] Emilio Ghiani, N. Locci, and C. Muscas.
“Auto-evaluation of the uncertainty in virtual instruments”.
In: *Instrumentation and Measurement, IEEE Transactions on* 53.3 (2004), pp. 672–677. ISSN: 0018-9456. DOI: 10.1109/TIM.2004.827080.

[141] Ciro Spataro.
ADC Based Measurements: a Common Basis for the Uncertainty Estimation. 2010.

[142] A. Cataliotti, V. Cosentino, D. Di Cara, A. Lipari, S. Nuccio, and C. Spataro.
“A PC-Based Wattmeter for Accurate Measurements in Sinusoidal and Distorted Conditions: Setup and Experimental Characterization”.
In: *Instrumentation and Measurement, IEEE Transactions on* 61.5 (2012), pp. 1426–1434. ISSN: 0018-9456. DOI: 10.1109/TIM.2011.2178679.

[143] A.E. Emanuel. *Power Definitions and the Physical Mechanism of Power Flow.* Wiley - IEEE. Wiley, 2011. ISBN: 9781119957287.

[144] T. Butz. *Fourier Transformation for Pedestrians.*
Undergraduate Lecture Notes in Physics.
Springer International Publishing, 2015. ISBN: 9783319169859.

[145] “Electromagnetic compatibility (EMC) - Part 4-7: Testing and measurement techniques - General guide on harmonics and interharmonics measurements and instrumentation, for power supply systems and equipment connected thereto”. In: *IEC 61000-4-7:2002+AMD1:2008 CSV* (2009), pp. 1–82.

[146] T. Tarasiuk. “Comparative Study of Various Methods of DFT Calculation in the Wake of IEC Standard 61000-4-7”. In: *IEEE Transactions on Instrumentation and Measurement* 58.10 (2009), pp. 3666–3677.
ISSN: 0018-9456. DOI: 10.1109/TIM.2009.2019308.

[147] “High-voltage test techniques - Part 2: Measuring systems”.
In: *IEC 60060-2:2010* (2010), pp. 1–149.

[148] Rethmeier, Kay. “Neue Auskoppelverfahren und Sensoren zur Vor-Ort-Teilentladungsmessung an Hoch-spannungs-Kabelanlagen”.
PhD thesis. 2006.

[149] K. Bohnert, P. Gabus, H. Brändle, and Aftab Khan.
“Fiber-Optic Current and Voltage Sensors for High-Voltage Substations”.
In: *In Proceedings of the 16th International Conference on Optical Fiber Sensors* (2003), pp. 752–754.

[150] A. Kumada and K. Hidaka.
"Directly High-Voltage Measuring System Based on Pockels Effect".
In: *IEEE Transactions on Power Delivery* 28.3 (2013), pp. 1306–1313.
ISSN: 0885-8977. DOI: 10.1109/TPWRD.2013.2250315.

[151] A. Küchler.
High Voltage Engineering: Fundamentals - Technology - Applications.
VDI-Buch. Springer Berlin Heidelberg, 2017. ISBN: 9783642119934.

[152] K. Schon. *High Impulse Voltage and Current Measurement Techniques: Fundamentals - Measuring Instruments - Measuring Methods*. Springer, 2013.
ISBN: 9783319006048.

[153] T. Harada, Y. Aoshima, T. Okamura, and K. Hiwa.
"Development of a high voltage universal divider". In: *IEEE Transactions on Power Apparatus and Systems* 95.2 (1976), pp. 595–602. ISSN: 0018-9510.
DOI: 10.1109/T-PAS.1976.32140.

[154] G. Müller and B. Ponick. *Grundlagen elektrischer Maschinen*.
Elektrische Maschinen. Wiley-VCH, 2006. ISBN: 9783527405244.

[155] Y. I. Tygai and A. B. Besarab. "The mathematical model of voltage transformers for the study of ferroresonant processes".
In: *2014 IEEE International Conference on Intelligent Energy and Power Systems (IEPS)* (2014), pp. 77–80. DOI: 10.1109/IEPS.2014.6874207.

[156] E. Price. "A tutorial on ferroresonance". In: *2014 67th Annual Conference for Protective Relay Engineers* (2014), pp. 676–704.
DOI: 10.1109/CPRE.2014.6799036.

[157] "Instrument transformers - Part 3: Additional requirements for inductive voltage transformers". In: *IEC 61869-3:2011* (2011).

[158] M. Arzberger, M. Kahmann, and P. Zayer. *Handbuch Elektrizitätsmesstechnik*.
Vde Verlag GmbH, 2017. ISBN: 9783802211607.

[159] M. Brehm, G. Aristoy, L. Trigo, A. Santos, and D. Slomovitz.
"Errors of Capacitive-Voltage-Transformers Used for Harmonic Measurements".
In: *2017 IEEE URUCON* (2017), pp. 1–4.
DOI: 10.1109/URUCON.2017.8171892.

[160] D. Lin, C. Bin, and C. Weigen. "Research on the measurement error of capacitor voltage transformer under various insulation characteristics".
In: *2016 IEEE International Conference on High Voltage Engineering and Application (ICHVE)* (2016), pp. 1–4. DOI: 10.1109/ICHVE.2016.7800796.

[161] H.J. Köster.
Übertragungsverhalten von Hochstrom-Messeinrichtungen für transiente Ströme.
Technischer Bericht: Forschungsgemeinschaft für Elektrische Anlagen und Stromwirt-schaft, year=2000, publisher=FGH.

[162] "Instrument transformers - The use of instrument transformers for power quality measurement". In: *IEC TR 61869-103:2012* (2012), p. 84.

[163] Ruthard Minkner and Edmund O. Schweitzer.
"Low Power Voltage And Current Transducers For Protecting And Measuring Medium And High Voltage Systems". In: (2000).

[164] J. Schmid and K. Kunde. "Application of non conventional voltage and currents sensors in high voltage transmis-sion and distribution systems". In: *Smart Measurements for Future Grids (SMFG), 2011 IEEE International Conference on* (2011), pp. 64–68. DOI: 10.1109/SMFG.2011.6125766.

[165] *ZES Sensors and Accessories - for precision power meters LMG series.* ZES ZIMMER Electronic Systems GmbH. 2014.

[166] K. Schon. *Hochspannungsmesstechnik: Grundlagen – Messgeräte - Messverfahren.* Springer Fachmedien Wiesbaden, 2017. ISBN: 9783658151782.

[167] J. Nedoma, M. Fajkus, and R. Martinek. "Measurement of electric current using optical fibers: A Review". In: *Przegląd Elektrotechniczny* 93.11 (2017), pp. 140–145.

[168] Ricardo M. Silva, Hugo Martins, Ivo Nascimento, José M. Baptista, António Lobo Ribeiro, José L. Santos, Pedro Jorge, and Orlando Frazão. "Optical Current Sensors for High Power Systems: A Review". In: *Applied Sciences* 2.3 (2012), pp. 602–628.

[169] Muhammad Nasir, Adam Dysko, Pawel Niewczas, Campbell Booth, Philip Orr, and G Fusiek. "Development of power system differential protection based on optical current measurement". In: *Power Engineering Conference (UPEC), 2013 48th International Universities'* (2013), pp. 1–4. DOI: 10.1109/UPEC.2013.6714988.

[170] Yang Huayun, Jiang Bo, Jiang Wei, Zhang Jiamin, Jiang Yinxia, and Liu Kun. "The All-digital Electrical Energy Metering System Based on Optical Current and Voltage Transducer". In: *Power and Energy Engineering Conference (APPEEC), 2010 Asia-Pacific* (2010), pp. 1–4. DOI: 10.1109/APPEEC.2010.5448274.

[171] Benjamin Seel and Peter Schneider. "Shuntbasierte Stromsensoren für die Antriebstechnik". In: *18. GMA/ITG-Fachtagung Sensoren und Messsysteme* (2016), pp. 1–5. DOI: 10.5162.

[172] W. F. Ray and C. R. Hewson. "High Performance Rogowski Current Transducers". In: *Conference Record of the 2000 IEEE Industry Applications Conference. Thirty-Fifth IAS Annual Meeting and World Conference on Industrial Applications of Electrical Energy (Cat. No.00CH37129)* 5 (2000), 3083–3090 vol.5. ISSN: 0197-2618. DOI: 10.1109/IAS.2000.882606.

[173] "Practical Aspects of Rogowski Coil Applications to Relaying". In: *Special Report - IEEE Power Engineering Society* (2010).

[174] C. Waters. "Current Transformers Provide Accurate, Isolated Measurements". In: *PCIM* (1986).

[175] "Instrument transformers - Part 2: Additional requirements for current transformers". In: *IEC 61869-2:2012* (2012).

[176] Neergard A. Bezold H. Engelade Th. "Breitbandige Präzisionswandler für Messungen an Umrichtersystemen". In: *Antriebstechnik* 42 (2003), pp. 64–71.

[177] Kerstin Kunde, Holger Däumling, Ralf Huth, Hans-Werner Schlierf, and Joachim Schmid. "Übertragungsverhalten von Messwandlern im kHz-Bereich". In: *etz Elektrotechnik und Automation* 6 (2012), pp. 2–5.

[178] P. Bertolotto, M. Faifer, and R. Ottoboni. "High Voltage Multi-Purpose Current and Voltage Electronic Transformer". In: *Instrumentation and Measurement Technology Conference Proceedings, 2007. IMTC 2007. IEEE* (2007), pp. 1–5. ISSN: 1091-5281. DOI: 10.1109/IMTC.2007.379148.

[179] M. Cerqueira Bastos. "High Precision Current Measurement for Power Converters. High Precision Current Measurement for Power Converters". In: arXiv:1607.01584. arXiv:1607.01584 (2016). 10 pages, contribution to the 2014 CAS - CERN Accelerator School: Power Converters, Baden, Switzerland, 7-14 May 2014, 10 p.

[180] L. Xiang and H. Bei and T. Yue and Y. Tian and Y. Fan. "Characteristic study of electronic voltage transformers' accuracy on harmonics". In: *2016 China International Conference on Electricity Distribution (CICED)* (2016), pp. 1–6. DOI: 10.1109/CICED.2016.7576073.

[181] J. A. Sayago, T. Bruckner, and S. Bernet. "How to Select the System Voltage of MV Drives: A Comparison of Semiconductor Expenses". In: *IEEE Transactions on Industrial Electronics* 55.9 (2008), pp. 3381–3390. ISSN: 0278-0046. DOI: 10.1109/TIE.2008.924032.

[182] "Wirkungsgrad-Messung an 3-phasigen Systemen". In: *Das Test & Messtechnik Magazin, Yokogawa Deutschland GmbH* (2011), pp. 6–7.

[183] Antonio Cataliotti, Valentina Cosentino, Dario Di Cara, Salvatore Nuccio, and Giovanni Tinè. "Rogowski coil current transducer compensation method for harmonic active power error". In: *Measurement* 63 (2015), pp. 240 –251. ISSN: 0263-2241. DOI: http://dx.doi.org/10.1016/j.measurement.2014.12.005.

[184] Daniel Schmitt. "Modular Multilevel Converter M2C für Multiterminal HVDC". PhD thesis. 2012.

[185] Thomas Weidinger. "Untersuchung von Gleichtaktschwingungen in elektrischen Antriebssystemen". PhD thesis. 2009.

[186] L. Aarniovuori, H. Kärkkäinen, M. Niemelä, and J. Pyrhönen. "PWM power distribution and switching frequency analysis in motor drives". In: *IECON 2016 - 42nd Annual Conference of the IEEE Industrial Electronics Society* (2016), pp. 4356–4361. DOI: 10.1109/IECON.2016.7793738.

[187] "IEEE Recommended Practice and Requirements for Harmonic Control in Electric Power Systems". In: *IEEE Std 519-2014 (Revision of IEEE Std 519-1992)* (2014), pp. 1–29. DOI: 10.1109/IEEESTD.2014.6826459.

Schriftenreihe **Elektrische Energietechnik an der TU Berlin**
Hrsg.: Prof. Dr. Sibylle Dieckerhoff, Prof. Dr. Julia Kowal, Prof. Dr. Ronald Plath, Prof. Dr. Uwe Schäfer

ISSN 2367-3761 (print)
ISSN 2367-377X (online)

1: Dinca, Christian: Motor design for maximum material exploitation and magnetization procedure with in-line quality check for mass production. - 2017. - XV, 168 S.
ISBN **978-3-7983-2883-9** (print) EUR **13,00**
ISBN **978-3-7983-2884-6** (online)
DOI 10.14279/depositonce-5630

2: Gkountaras, Aris: Modeling techniques and control strategies for inverter dominated microgrids. - 2017. - 169 S.
ISBN **978-3-7983-2872-3** (print) EUR **12,00**
ISBN **978-3-7983-2873-0** (online)
DOI 10.14279/depositonce-5520

3: Wolz, Christoph: Ein schnelles und genaues Simulationsmodell für permanentmagnet-erregte Kommutatormotoren kleiner Leistung mit Zahnspulen unter Berücksichtigung nichtlinearer Eigenschaften. - 2017. - XXI, 178 S.
ISBN **978-3-7983-2934-8** (print) EUR **14,00**
ISBN **978-3-7983-2935-5** (online)
DOI 10.14279/depositonce-5911

4: noch nicht erschienen

Universitätsverlag der TU Berlin

Test Bench Design for Power Measurement of Inverter-Operated Machines in the Medium Voltage Range

This thesis gives an overview of test bench design for inverter operated Medium Voltage (MV) drives with the focus on the active power measurement. The sources of measurement setup uncertainty are analysed and methods are shown to assess these uncertainties. Further, a possibility is shown to do quantitative uncertainty estimations which are verified with measurements through different measurement setups for MV drives operated with multilevel converters. The influence of measurement transducers, voltage dividers, power meters and data acquisition boards are considered. The digital signal processing is analysed and the possibilities to reduce its uncertainty contribution on an active power measurement is shown. An analysis is made with the conventional measurement devices in the MV-range. The transfer behaviour of the devices and the characteristics of the uncertainty are investigated. Measurements are done on typical medium voltage drives with an uncertainty analysis, which shows the essential aspects of active power measurement. The results show the significance of a measurement setup performance.

ISBN 978-3-7983-3024-5 (print)
ISBN 978-3-7983-3025-2 (online)

ISBN 978-3-7983-3024-5

http://verlag.tu-berlin.de